

# Fast Update Path Oracle on Updated Terrain Surfaces

Yinzhao Yan

The Hong Kong University of  
Science and Technology  
yyanas@cse.ust.hk

Raymond Chi-Wing Wong

The Hong Kong University of  
Science and Technology  
raywong@cse.ust.hk

Christian S. Jensen

Aalborg University  
csj@cs.aau.dk

**Abstract**—The booming of computer graphics technology facilitates the growing use of terrain data. Notably, shortest path querying on a terrain surface is central in a range of applications and has received substantial attention from the database community. Despite this, computing shortest paths on-the-fly on a terrain surface remains very expensive, and all existing oracle-based algorithms are only efficient when the terrain surface is fixed. They rely on large data structures that must be reconstructed from scratch when updates to the terrain surface occur, which is very time-consuming. To advance the state-of-the-art, we propose an efficient  $(1 + \epsilon)$ -approximate shortest path oracle on an updated terrain surface. This oracle is capable of improved performance in terms of the oracle construction time, oracle update time, output size and shortest path query time due to the concise information it maintains about shortest paths between all pairs of points-of-interest stored in the oracle. Our empirical study shows that in realistic settings, when compared to the best-known oracle, our oracle is capable of improvements in oracle construction time and oracle update time of up to 1.3 times and 88 times, and of improvements in output size and shortest path query time of up to 12 times and 3 times.

## I. INTRODUCTION

Calculating shortest paths on terrain surfaces is a topic of widespread interest in both industry and academia [55]. In industry, well-known companies and applications, including Metaverse [8] and Google Earth [4], rely on the ability to find shortest paths on terrain surfaces (e.g., in virtual reality or on Earth) to assist users to reach destinations more quickly. In academia, shortest path querying on terrain surfaces also attracts considerable attention [21], [29], [32], [33], [36], [38], [52], [53], [56], [57]. A terrain surface is represented by a set of *faces*, each of which is captured by a triangle. A face thus consists of three line segments, called *edges*, connected with each other at three *vertices*. Figures 1 (a) and (b) show a real map of Valais, Switzerland [9] with an area of  $20\text{km} \times 20\text{km}$ , and Figures 1 (c) and (d) show Valais terrain surface (consisting of vertices, edges and faces).

### A. Motivation

1) **Updated terrain surface:** The computation of shortest paths on updated terrain surfaces occurs in many scenarios.

(i) **Earthquake:** We aim at finding the shortest rescue paths for life-saving after an earthquake. The death toll of the 7.8 magnitude earthquake on Feb 6, 2023 in Turkey and Syria exceeded 40,000 [12], and more than 69,000 died in

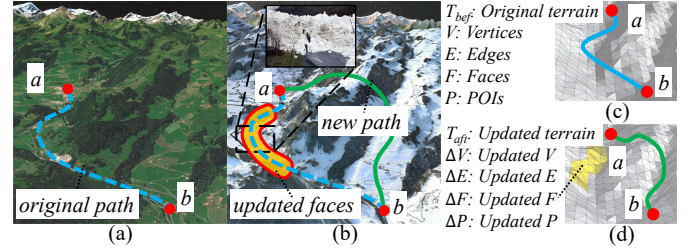


Fig. 1. The real map (a) before and (b) after updates, the terrain surface (c) before and (d) after updates for avalanche in Valais, Switzerland

the 7.9 magnitude earthquake on May 12, 2008 in Sichuan, China [47]. Table I lists 6 earthquakes, data from which we use in experiments. A rescue team can save 3 lives every 15 minutes [37], and we expect that the team can arrive at the sites of the quake as early as possible. In practice, (a) satellites or (b) drones can be used to collect the terrain surface after an earthquake, which takes (a) 10s and USD \$48.72 [42], and (b) 144s  $\approx$  2.4 min and USD \$100 [15] for a  $1\text{km}^2$  region, respectively, which are both time-efficient and cost-efficient.

(ii) **Avalanche:** Earthquakes may cause avalanches. The 4.1 magnitude earthquake on Oct 24, 2016 in Valais [9] caused an avalanche: Figures 1 (a) and (b) (resp. Figures 1 (c) and (d)) shows the original and new shortest paths between  $a$  and  $b$  on a real map (resp. a terrain surface) before and after terrain surface updates, where  $a$  is a village and  $b$  is a hotel. We need to efficiently calculate the new shortest paths for rescuing.

(iii) **Marsquake:** As observed by NASA's InSight lander on May 4, 2022 [34], Mars also experienced a marsquake. In NASA's Mars exploration project [10] (with cost USD 2.5 billion [39]) and the SpaceX Mars project [11] (with cost USD 67 million per launch [3]), Mars rovers should find the shortest escape paths quickly and autonomously in regions affected by marsquakes to avoid damage.

2) **POIs:** Given a set of *Points-Of-Interest* (POI) on a terrain surface, we can compute the shortest path between pairs of POIs, i.e., perform the *POI-to-POI* (P2P) query. For earthquakes and avalanches, POIs can be villages waiting for rescuing [45], hospitals and expressway exits. For the Marsquake, POIs can be working stations of Mars rover.

3) **Oracle:** Pre-computing shortest paths on a terrain surface among POIs using an indexing technique, known as

TABLE I  
REAL EARTHQUAKE TERRAIN DATASETS

Name	Magnitude	Date
Tohoku, Japan (TJ) [6]	9.0	Mar 11, 2011
Sichuan, China (SC) [47]	8.0	May 12, 2008
Gujarat, India (GI) [5]	7.6	Jan 26, 2001
Alaska, USA (AU) [1]	7.1	Nov 30, 2018
Leogane, Haiti (LH) [44]	7.0	Jan 12, 2010
Valais, Switzerland (VS) [9]	4.1	Oct 24, 2016

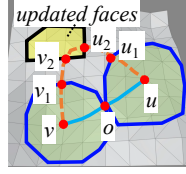


Fig. 2. An unaffected path

an oracle, can efficiently reduce the shortest path query time, especially when we need to calculate more than one shortest path with different sources and destinations (where the time taken to pre-compute the oracle is called the *oracle construction time*, the space complexity of the output oracle is called the *output size*, and the time taken to return the result is called the *shortest path query time*). We also aim to update the oracle quickly when the terrain surface changes (where the time taken to update the oracle is called the *oracle update time*). For example, if we pre-compute shortest paths (among villages, hospitals and expressway exits) using an oracle on terrain surfaces prone to earthquakes, and efficiently update the oracle after an earthquake, then we can use it to efficiently return shortest paths with different sources and destinations.

## B. Challenges

1) **Inefficiency of on-the-fly algorithms:** Consider a terrain surface  $T$  with  $N$  vertices. All existing *exact on-the-fly* shortest path algorithms [18], [31], [40], [54] on a terrain surface are slow when many shortest path queries are involved. The best-known exact algorithm [18] runs in  $O(N^2)$  time. Although *approximate* algorithms [32], [33], [36], [38] can reduce the running time, they are still not efficient enough. The best-known approximate algorithm [32] runs in  $O((N+N')\log(N+N'))$  time, where  $N'$  is the number of additional points introduced for the bound guarantee. Our experiments show that the best-known exact algorithm [18] (resp. approximate algorithm [32]) needs 11,600s  $\approx$  3.2 hours (resp. 8,600s  $\approx$  2.4 hours) to calculate 100 shortest paths on a terrain surface with 0.5M faces.

2) **Non-existence of oracles on updated terrain surfaces:** Although existing studies [29], [52], [53] can construct oracles on *static* terrain surfaces, and can then answer the P2P query efficiently, no existing study can accommodate updated terrains, where the oracle needs to be updated efficiently. When the terrain surface is updated, a straightforward adaptation of the best-known oracle [52], [53] is to re-construct the oracle. However, its oracle construction time is  $O(nN\log^2 N + cn)$ , where  $n$  is the number of POIs on  $T$  and  $c$  is a constant depending on  $T$  (note that  $c \in [35, 80]$  on average). In our experiments, its oracle construction time is 35,100s  $\approx$  9.8 hours for a terrain surface with 0.5M faces and 250 POIs, which is not acceptable.

## C. Path Oracle on Updated Terrain Surfaces

We propose an efficient  $(1 + \epsilon)$ -approximate shortest path oracle for solving the *updated terrain surfaces problem* (given

an updated terrain surface of an original terrain surface, we need to efficiently answer P2P queries on the updated terrain surface), where  $\epsilon > 0$  is the *error parameter*. We call this oracle the *Fast Update path Oracle (FU-Oracle)*. *FU-Oracle* has state-of-the-art performance in terms of the oracle construction time, oracle update time, output size and shortest path query time (compared with the best-known oracle [52], [53]) due to the concise information about pairwise shortest paths between any pair of POIs stored in the oracle.

### 1) Key ideas for achieving a short oracle update time:

Consider two terrain surfaces before and after updates, i.e.,  $T_{bef}$  and  $T_{aft}$ , respectively. The key ideas of achieving a short oracle update time of *FU-Oracle* are due to (i) a novel property, i.e., the *non-updated terrain shortest path intact* property, and (ii) the useful information on  $T_{bef}$ , i.e., the stored pairwise P2P exact shortest paths on  $T_{bef}$  when *FU-Oracle* is constructed.

#### (i) Non-updated terrain shortest path intact property:

In Figure 2, this property implies that given the light blue path between  $u$  and  $v$  on  $T_{bef}$  (with path distance  $d_1$ ), if the distances from both  $u$  and  $v$  to the updated faces are large enough (i.e., both larger than  $\frac{d_1}{2}$ ), then the path between  $u$  and  $v$  on  $T_{aft}$  remains the same and does not need to be updated.

(ii) **Necessity of storing the pairwise P2P exact shortest paths on  $T_{bef}$ :** The *exact* shortest distances are no larger than the *approximate* shortest distances. So given an exact (resp. approximate) shortest path with two endpoints  $u$  and  $v$  on  $T_{bef}$ , in the non-updated terrain shortest path intact property, it is likely (resp. unlikely) that the distances from both  $u$  and  $v$  to the updated faces are both larger than the exact (resp. approximate) length of this path, and it reduces (resp. increases) the likelihood of updating this path on  $T_{aft}$ .

### 2) Key idea for efficiently achieving a small output size:

We are not interested in returning the *pairwise* P2P exact shortest paths on  $T_{aft}$  as the oracle output.

(i) **Earthquake and avalanche:** Given three POIs  $a$ ,  $b$  and  $c$ , suppose that  $a$  is a damaged village,  $b$  and  $c$  are unaffected hospitals, the rescue teams need to transport injured citizens to the hospitals, where  $a$  is far away from  $b$  and  $c$ , but  $b$  and  $c$  are close to each other. We are not interested in using road diggers (on the ruins caused by the earthquake) to dig out two long paths (from  $a$  to  $b$  and from  $a$  to  $c$ ) and one shortest path (from  $b$  to  $c$ ) for rescuing (since it is time-consuming to dig out a rescue path in the earthquake region [27]). Rather, we only aim to dig out one long path (from  $a$  to  $b$ ) and one short path (from  $b$  to  $c$ ), so we can go from  $a$  to  $c$  by going via  $b$ . That is, given a complete graph (where the POIs are the vertices of the complete graph, and the exact shortest path between POIs are the edges of the complete graph), we hope that *FU-Oracle* can efficiently generate a sub-graph of it.

(ii) **Marsquake:** The memory size of NASA's Mars 2020 rover is 256MB [7]. Our experiments show that for a terrain surface with 2.5M faces and 250 POIs, the sub-graph output by *FU-Oracle* is 110MB, while the complete graph is 1.3GB. Thus, we can only store the sub-graph in a Mars rover.

Generating a sub-graph from a complete graph is also used in distributed systems for faster network synchroniza-

tion [16], [46] and in wireless networks for faster signal transmission [51], [49]. The best-known sub-graph generation algorithm [13], [14] runs in  $O(n^3 \log n)$  time, which is inefficient. We propose a faster algorithm called *Hierarchy Greedy Spanner* (*HieGreSpan*) that considers several vertices of the complete graph in one group. Our experiments show that when  $n = 500$ , our algorithm takes 24s, while the best-known algorithm [13], [14] takes 101s.

#### D. Contributions and Organization

We summarize our major contributions as follows.

(1) We propose the first oracle *FU-Oracle* (which is very different from the best-known oracle [52], [53]) for solving the updated terrain surfaces problem. It achieves a short oracle update time by satisfying the novel non-updated terrain shortest path intact property, and by utilizing the useful information on  $T_{bef}$  (the pairwise P2P exact shortest paths on  $T_{bef}$ ). We also propose four additional novel techniques to further reduce the oracle update time. An ablation study shows that if any one of the techniques is not satisfied, *FU-Oracle*'s oracle update time will increase very substantially. It is worth mentioning that designing an oracle on an updated terrain surface with a small oracle update time is challenging: there are no existing studies on this, and only limited information about  $T_{bef}$  can be re-used. We also develop an efficient algorithm called *HieGreSpan* to reduce the output size.

(2) We provide a thorough theoretical analysis on the oracle construction time, oracle update time, output size, shortest path query time and error bound of *FU-Oracle*.

(3) *FU-Oracle* performs much better than the best-known oracle [52], [53] in terms of the oracle construction time, oracle update time, output size and shortest path query time. Our experiments show that for a terrain surface with 0.5M faces and 250 POIs, (i) the oracle update time of *FU-Oracle* is 400s  $\approx$  7 min, while the best-known oracle needs 35,100s  $\approx$  9.8 hours, (ii) the shortest path query time for computing 100 shortest paths with different sources and destinations is 0.1s for *FU-Oracle*, while the time is 8,600s  $\approx$  2.4 hours for the best-known approximate on-the-fly algorithm [32] and 0.3s for the best-known oracle. So only *FU-Oracle* is suitable in real-world updated terrain surface applications (e.g., earthquake rescue).

The remainder of the paper is organized as follows. Section II provides the problem definition. Section III covers related work. Section IV presents *FU-Oracle*. Section V covers the empirical study, and Section VI concludes the paper.

## II. PROBLEM DEFINITION

### A. Notations and Definitions

1) **Terrain surfaces and POIs:** Consider a terrain surface  $T_{bef}$  represented as a *Triangulated Irregular Network* (TIN) [22], [38], [48], [52], [53]. Let  $V$ ,  $E$  and  $F$  be the set of vertices, edges and faces of  $T_{bef}$ , respectively. Let  $L_{max}$  be the length of the longest edge in  $E$ . Let  $N$  be the number of vertices. Each vertex  $v \in V$  has three coordinates,  $x_v$ ,  $y_v$  and  $z_v$ . If the positions of vertices in  $V$  are updated, we obtain

a new terrain surface,  $T_{aft}$ . There is no need to consider the case when  $N$  changes. This is because both the original and updated terrain surface have the same 2D grid with  $\bar{x} \times \bar{y} = N$  vertices [38], [52], [53]. Figures 1 (c) and (d) show an example of  $T_{bef}$  and  $T_{aft}$ , respectively. Let  $P$  be a set of POIs on the terrain surface and  $n$  be the size of  $P$ . We focus on the case when  $n \leq N$ . We discuss the case when  $n > N$  in the appendix.

2) **Path:** Given two points  $s$  and  $t$  in  $P$ , and a terrain surface  $T$ , we define  $\Pi(s, t|T)$  to be the exact shortest path between  $s$  and  $t$  on  $T$ , and  $|\cdot|$  to be the distance of a path (e.g.,  $|\Pi(s, t|T)|$  is the exact distance of  $\Pi(s, t|T)$  on  $T$ ).

3) **Updated and non-updated components:** Given  $T_{bef}$ ,  $T_{aft}$  and  $P$ , a set of (i) *updated vertices*, (ii) *updated edges*, (iii) *updated faces* and (iv) *updated POIs* of  $T_{bef}$  and  $T_{aft}$ , denoted by (i)  $\Delta V$ , (ii)  $\Delta E$ , (iii)  $\Delta F$  and (iv)  $\Delta P$ , is defined to be a set of (i) vertices  $\Delta V = \{v_1, v_2, \dots, v_{|\Delta V|}\}$ , where  $v_i$  is a vertex in  $V$  with coordinate values differing between  $T_{bef}$  and  $T_{aft}$ , and  $|\Delta V|$  is the number of vertices in  $\Delta V$ , (ii) edges  $\Delta E = \{e_1, e_2, \dots, e_{|\Delta E|}\}$ , where  $e_i$  is an edge in  $E$  with at least one of its two vertices' coordinate values differing between  $T_{bef}$  and  $T_{aft}$ , and  $|\Delta E|$  is the number of edges in  $\Delta E$ , (iii) faces  $\Delta F = \{f_1, f_2, \dots, f_{|\Delta F|}\}$ , where  $f_i$  is a face in  $F$  with at least one of its three vertices' coordinate values differing between  $T_{bef}$  and  $T_{aft}$ , and  $|\Delta F|$  is the number of faces in  $\Delta F$ , and (iv) POIs  $\Delta P = \{p_1, p_2, \dots, p_{|\Delta P|}\}$ , where  $p_i$  is a POI in  $P$  with coordinate values differing between  $T_{bef}$  and  $T_{aft}$ , and  $|\Delta P|$  is the number of POIs in  $\Delta P$ . It is easy to obtain  $\Delta V$ ,  $\Delta E$ ,  $\Delta F$  and  $\Delta P$  by comparing  $T_{bef}$ ,  $T_{aft}$  and  $P$ . In Figure 1 (d), the yellow area is  $\Delta F$  based on  $T_{bef}$  and  $T_{aft}$ . The vertices, edges and POIs in  $\Delta F$  are  $\Delta V$ ,  $\Delta E$  and  $\Delta P$ . In addition, there is no need to consider the case with two or more *disjoint* non-empty sets of updated faces. If this happens, we can create a larger set of faces that contains these disjoint sets. Thus, the set of updated faces that we consider is connected [43] as shown in Figure 1 (d).

4) **Three shortest path queries:** We study three shortest path queries, (i) *P2P query*, (ii) *vertex-to-vertex (V2V) query* and (iii) *arbitrary point-to-arbitrary point (A2A) query*, which returns the shortest path between pairs of (i) POIs, (ii) vertices and (iii) arbitrary points on a terrain surface. The P2P query is more general than the V2V query. By creating POIs with the same coordinate values as all vertices in  $V$ , the V2V query can be regarded as one form of the P2P query. The A2A query generalizes both the P2P query and the V2V query because it allows all possible points on a terrain surface. In the main body of this paper, we focus on the P2P query. We study the V2V query and the A2A query in the appendix. In the P2P query, there is no need to consider when  $n$  changes. When a POI is added, we create an oracle that answers the A2A query, which implies we consider all possible POIs to be added. When a POI is removed, we continue to use the original oracle. A notation table appears in the appendix.



### B. Updated terrain surfaces problem

Given  $T_{bef}$ ,  $T_{aft}$  and  $P$ , the problem is to efficiently answer P2P queries on  $T_{aft}$  (using shortest paths on  $T_{bef}$ ), such that  $|\Pi'(s, t|T_{aft})| \leq (1 + \epsilon)|\Pi(s, t|T_{aft})|$  for any  $s$  and  $t$  in  $P$ , where  $\Pi'(s, t|T_{aft})$  is the calculated shortest path between  $s$  and  $t$  on  $T_{aft}$ .

## III. RELATED WORK

We discuss the existing on-the-fly and oracle-based algorithms on terrain surfaces in Sections III-A and III-B, the subgraph generation algorithm in Section III-C, and other related studies in Section III-D.

### A. On-the-fly Algorithms on Terrain Surfaces

There are two types of algorithms for computing the shortest path on a terrain surface *on-the-fly*: (1) *exact* [18], [31], [40], [54] and (2) *approximate* [32], [33], [36], [38] algorithms.

**Exact algorithms:** The time complexities of the exact algorithms [18], [31], [40], [54] are  $O(N^2)$ ,  $O(N \log^2 N)$ ,  $O(N^2 \log N)$  and  $O(N^2 \log N)$ , respectively. They are *Single-Source All-Destination* (SSAD) algorithms, i.e., given a source, they can calculate the shortest path from it to all other vertices *simultaneously*. The best-known exact algorithm *Chen and Han on-the-Fly Algorithm* (CH-Fly-*Algo*) [18] uses a sequence tree for the shortest path query.

**Approximate algorithms:** Approximate algorithms [32], [33], [36], [38] aim at reducing the running time. The best-known approximate algorithm *Kaul on-the-Fly Algorithm* (K-Fly-*Algo*) [32] places Steiner points on edges in  $E$ , and then constructs a graph using these points and  $V$  to calculate a  $(1 + \epsilon)$ -approximate shortest path on a terrain surface. It runs in  $O(\frac{l_{max}N}{\epsilon l_{min}\sqrt{1-\cos\theta}} \log(\frac{l_{max}N}{\epsilon l_{min}\sqrt{1-\cos\theta}}))$  time, where  $l_{max}$  (resp.  $l_{min}$ ) is the length of the longest (resp. shortest) edge of  $T$ , and  $\theta$  is the minimum inner angle of any face in  $F$ .

**Drawbacks of the on-the-fly algorithms:** All exact and approximate on-the-fly algorithms are not efficient when multiple shortest path queries are involved. Our experiments show that CH-Fly-*Algo* and K-Fly-*Algo* needs 11,600s  $\approx$  3.2 hours and 8,600s  $\approx$  2.4 hours to compute 100 paths with different sources and destinations on a terrain surface with 0.5M faces, so they are not our main focus.

### B. Oracle-based Algorithms on Terrain Surfaces

Although the *Well-Separated Pair Decomposition Oracle* (WSPD-*Oracle*) [52], [53] (resp. the *Efficiently Arbitrary Pairs-to-Arbitrary Points Oracle* (EAR-*Oracle*) [29]) uses an oracle to pre-compute shortest paths on a terrain surface for answering P2P (resp. A2A) queries *approximately*, no existing oracle can accommodate updated terrains, where the oracle needs to be updated efficiently.

1) **WSPD-*Oracle*:** It uses algorithm SSAD, *compressed partition tree* [52], [53], and *well-separated node pair sets* [17] to index the  $(1 + \epsilon)$ -approximate pairwise P2P shortest paths. Its oracle construction time, output size and shortest path query time is  $O(\frac{nN \log^2 N}{\epsilon^{2\beta}} + \frac{nh}{\epsilon^{2\beta}} + nh \log n)$ ,  $O(\frac{nh}{\epsilon^{2\beta}})$  and  $O(h^2)$ , respectively, where  $h$  is the height of the compressed

partition tree and  $\beta$  is the largest capacity dimension [25], [35] ( $\beta \in [1.5, 2]$  in practice [52], [53]). It is recognized as the best-known oracle that answers the P2P query.

**Drawback of WSPD-*Oracle*:** It *only supports the static terrain surface* and does not address how to update the oracle on an *updated* terrain surface. If we use the straightforward adaptation, i.e., re-construct WSPD-*Oracle* from scratch when the terrain surface is updated, an update takes 35,100s  $\approx$  9.8 hours for a terrain dataset with 0.5M faces and 250 POIs, but the time is just 400s  $\approx$  7 min for FU-*Oracle*.

2) **WSPD-*Oracle-Adapt*:** To handle this, we employ a smart adaption by leveraging the *non-updated terrain shortest path intact* property, such that we only re-calculate the paths on  $T_{aft}$  that require updating to reduce the oracle update time. We denote it as WSPD-*Oracle-Adapt*, and its oracle update time is  $O(\mu_1 N \log^2 N + n \log^2 n)$ , where  $\mu_1$  is a data-dependent variable and  $\mu_1 \in [5, 20]$  in our experiment.

**Drawbacks of WSPD-*Oracle-Adapt*:** (i) *Not fully utilizing the non-updated terrain shortest path intact property during update:* Since WSPD-*Oracle-Adapt* only stores the pairwise P2P *approximate* shortest paths on  $T_{bef}$ , the oracle update time remains large. The oracle update time is 8,400s  $\approx$  2.4 hours on a terrain dataset with 0.5M faces and 250 POIs for WSPD-*Oracle-Adapt*, while the time is 400s  $\approx$  7 min for FU-*Oracle*. (ii) *Additional information needed during construction:* WSPD-*Oracle-Adapt* needs to calculate the shortest distance between each POI and vertex on  $T_{bef}$  when the oracle is constructed to utilize the property, which increases its oracle construction time, but FU-*Oracle* can calculate this information and the pairwise P2P exact shortest paths on  $T_{bef}$  *simultaneously*.

3) **EAR-*Oracle*:** It uses the same idea as WSPD-*Oracle*, i.e., well-separated pair decomposition. Their differences are that EAR-*Oracle* adapts WSPD-*Oracle* from the P2P query to the A2A query by using Steiner points on the terrain faces and using *highway nodes* (i.e., not POIs in WSPD-*Oracle*) for well-separated pair decomposition. Since the A2A query generalizes the P2P query, EAR-*Oracle* can also be used in the P2P query. Its oracle construction time, output size and shortest path query time is  $O(\lambda \xi m N \log^2(mN) + \frac{nN \log^2 N}{\epsilon^{2\beta}} + \frac{Nh}{\epsilon^{2\beta}} + Nh \log N)$ ,  $O(\frac{\lambda m N}{\xi} + \frac{Nh}{\epsilon^{2\beta}})$  and  $O(\lambda \xi \log(\lambda \xi))$ , respectively, where  $\lambda$  is the number of highway nodes covered by a minimum square,  $\xi$  is the square root of the number of boxes, and  $m$  is the number of Steiner points per face.

**Drawbacks of EAR-*Oracle*:** (i) *Numerous highway nodes:* In the P2P query,  $n$  is much smaller than the number of highway nodes, so the oracle construction time of EAR-*Oracle* is much larger than that of WSPD-*Oracle*. Thus, EAR-*Oracle* does not perform well in the P2P query, and it is only regarded as the best-known oracle in the A2A query. (ii) *Only supporting the static terrain surface:* EAR-*Oracle* has the same drawback as of WSPD-*Oracle*. Even for the A2A query, our experiments show that the oracle update time of EAR-*Oracle* is 710s  $\approx$  12 min, while the value is 48s for FU-*Oracle* on a terrain surface with 2k faces.

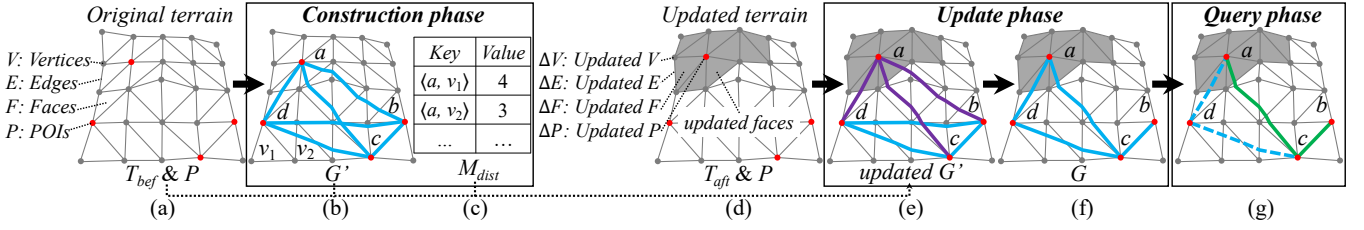


Fig. 3. Framework overview

4) **EAR-Oracle-Adapt**: We can adapt *EAR-Oracle* to *EAR-Oracle-Adapt* in the same way as of *WSPD-Oracle-Adapt*. The oracle update time of *EAR-Oracle-Adapt* is  $O(\mu_2 N \log^2 N + n \log^2 n)$ , where  $\mu_2$  is a data-dependent variable and  $\mu_2 \in [12, 45]$  in our experiment.

**Drawback of EAR-Oracle-Adapt**: *EAR-Oracle-Adapt* does not fully utilize the non-updated terrain shortest path intact property during update, i.e., it has the first drawback as of *WSPD-Oracle-Adapt*. Even in the A2A query, our experiments show that the oracle update time of *EAR-Oracle-Adapt* is 430s  $\approx$  7.2 min, while the value is 48s for *FU-Oracle* on a terrain surface with 2k faces.

#### C. Sub-graph Generation Algorithm

Algorithm *Greedy Spanner (GreSpan)* [13], [14] is the best-known algorithm for generating a sub-graph from a complete graph. However, it is very time-consuming because it does not consider using any simpler structure to approximate the sub-graph when performing Dijkstra's algorithm [23] on the sub-graph. Its time complexity is  $O(n^3 \log n)$ .

#### D. Other Related Studies

Three other studies [28], [50], [58] use indexes on updated graphs for page ranking, graph pattern matching and feature mining. Indexes on static graphs for these applications were also the subject of earlier studies [26], [30], [41], and the new parts in the three top-tier database studies relate to the updated graphs. So, the updated terrain surface problem studied in this paper is novel, and *FU-Oracle* contains a substantial departure from static oracles on terrain surfaces. In addition, updated graphs and updated terrain surfaces are very different since different data structures have different challenges, e.g., it is very challenging to update an oracle on an updated terrain surface involving many expensive path computations.

### IV. METHODOLOGY

We give an overview of *FU-Oracle* in Section III-A, and then present key ideas for achieving the shortest oracle update time and efficiently achieving the small output size of *FU-Oracle* in Sections IV-B and IV-C. We then cover the implementation details of the three phases (*construction phase*, *update phase* and *query phase*) of *FU-Oracle* in Sections IV-D, IV-E and IV-F. We offer a theoretical analysis of *FU-Oracle* in Section IV-G.

#### A. Overview of FU-Oracle

We first use an example to illustrate the framework of *FU-Oracle*. Figure 3 (a) shows an original terrain surface  $T_{bef}$  and a set of POIs  $P$ . In Figures 3 (b) and (c), for the construction phase, we store 6 pairwise P2P exact shortest paths on  $T_{bef}$ , and store the shortest distances between each POI and each vertex on  $T_{bef}$ . Figure 3 (d) shows an updated terrain surface  $T_{aft}$ . In Figures 3 (e) and (f), for the update phase, we update 6 pairwise P2P exact shortest paths (i.e., a complete graph) on  $T_{aft}$ , and we generate a sub-graph of the complete graph. In Figure 3 (g), for the update phase, we answer the shortest path between a pair of POIs. Note that in Figure 3 (e), there is no need to re-calculate all shortest paths on  $T_{aft}$ , and we use Figure 4 for better illustration. In Figures 4 (a) to (c), we use algorithm *SSAD* with  $a$ ,  $b$  and  $h$  as sources to update shortest paths on  $T_{aft}$ . But, in Figures 4 (d) and (e), due to the *non-updated terrain shortest path intact* property and the stored pairwise P2P exact shortest paths on  $T_{bef}$ , we do not need to use algorithm *SSAD* with  $f$ ,  $e$ ,  $c$ ,  $d$  and  $g$  as sources for path updating, thus saving time. Next, we introduce the four components and three phases of *FU-Oracle*.

1) **Four components of FU-Oracle**: (i) *Temporary complete graph*, (ii) *POI-to-vertex distance mapping table*, (iii) *FU-Oracle output graph* and (iv) *hierarchy graph*.

(i) **The temporary complete graph  $G$** : This is a complete graph that stores the pairwise exact shortest path between all pairs of POIs in  $P$ . Let  $G.V$  and  $G.E$  be the sets of vertices and edges of  $G$  (where each POI in  $P$  is denoted by a vertex in  $G.V$ ). Then an exact shortest path  $\Pi(u, v|T)$  between a pair of POIs  $u$  and  $v$  on  $T$  is denoted by a weighted edge  $e(u, v|T)$  in  $G.E$ , and the distance of this path  $|\Pi(u, v|T)|$  is denoted by the weight of the edge  $|e(u, v|T)|$ , where  $T$  can be  $T_{bef}$  or  $T_{aft}$ . The light blue lines in Figure 3 (b) show a complete graph  $G$  with 4 vertices and 6 edges. The light blue line between  $a$  and  $c$  is the exact shortest path  $\Pi(a, c|T_{bef})$  on  $T_{bef}$ , and also an edge  $e(a, c|T_{bef})$  in  $G$ .

(ii) **POI-to-vertex distance mapping table  $M_{dist}$** : This is a *hash table* [19] that stores the exact shortest distance from each POI in  $P$  to each vertex in  $V$  on  $T_{bef}$  (calculated when *FU-Oracle* is constructed), used for reducing the oracle update time of *FU-Oracle*. A pair of vertex  $u$  and  $v$  is stored as a key  $\langle u, v \rangle$ , and their corresponding exact shortest distance  $|\Pi(u, v|T_{bef})|$  is stored as a value.  $M_{dist}$  needs linear space in terms of the number of distances to be stored. Given a POI  $u$  and a vertex  $v$ ,  $M_{dist}$  can return the associated exact shortest

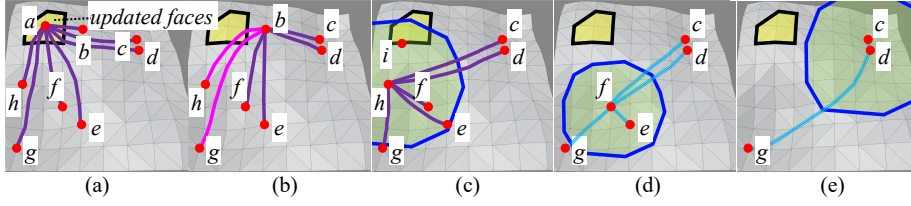


Fig. 4. In the update phase when (a) updating  $\Pi(a)$ , (b) updating  $\Pi(b)$ , (c) updating  $\Pi(f)$ , (d) no need for updating  $\Pi(c)$ , and (e) no need for updating  $\Pi(e)$

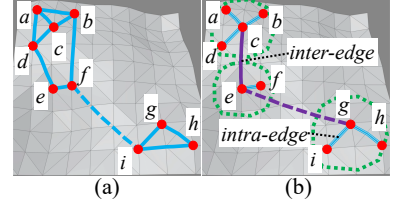


Fig. 5. (a)  $FU$ -Oracle output graph  $G'$  and (b) hierarchy graph  $H$  of  $G'$

distance  $|\Pi(u, v|T_{bef})|$  in  $O(1)$  time. In Figure 3 (c), the exact shortest distance between POI  $a$  and vertex  $v_1$  is 4.

(iii) **The  $FU$ -Oracle output graph  $G'$ :** This is a graph used for answering  $(1 + \epsilon)$ -approximate shortest path between any pair of POIs in  $P$ . The difference between  $G$  and  $G'$  is that  $G'$  is a sub-graph of  $G$  with fewer edges. Similar to  $G$ , let  $G'.V$  and  $G'.E$  be the set of vertices and edges of  $G'$ , let  $e'(u, v|T_{aft})$  be an edge between two vertices  $u$  and  $v$  in  $G'.E$ , and let  $|e'(u, v|T_{aft})|$  be the weight of this edge. Given two vertices  $s$  and  $t$  in  $G'.V$ , we define  $\Pi_{G'}(s, t|T_{aft}) = (v_1, v_2, \dots, v_l)$  to be a shortest path of  $FU$ -Oracle, such that the weighted length  $\sum_{i=1}^{l-1} |e'(v_i, v_{i+1}|T_{aft})|$  is the minimum, where  $v_1 = s$ ,  $v_l = t$ ,  $l$  is the number of vertices in this path, and for each  $i \in [1, l-1]$ ,  $(v_i, v_{i+1}) \in G'.E$ . We define  $|\Pi_{G'}(s, t|T_{aft})|$  to be the distance of  $\Pi_{G'}(s, t|T_{aft})$ . The light blue lines in Figure 3 (f) show an example of  $G'$  with 4 POIs. The light blue line between  $a$  and  $c$  is the exact shortest path  $\Pi(a, c|T_{aft})$  on  $T_{aft}$ , and also an edge  $e'(a, c|T_{aft})$  in  $G'$ . The shortest path  $\Pi_{G'}(a, b|T_{aft})$  in  $G'$  is  $(a, c, b)$  (i.e., the shortest path from POI  $a$  to POI  $c$ , and then to POI  $b$  in Figure 3 (f)), which consists of edges  $e'(a, c|T_{aft})$  and  $e'(c, b|T_{aft})$ .

(iv) **The hierarchy graph  $H$ :** This is a graph similar to  $G'$  (but has a simpler structure than  $G'$ ) used for efficiently generating a  $G'$  using  $G$ . It is maintained simultaneously with  $G'$ . We define a *group*, with *group center*  $v$  and *radius*  $r$ , to be a set of vertices  $Q_{G'} \subseteq G'.V$ , such that for every vertex  $u \in Q_{G'}$ , we have  $|\Pi_{G'}(u, v|T_{aft})| \leq r$ , where  $v \in Q_{G'}$ . A set of groups  $Q_{G'}^1, Q_{G'}^2, \dots, Q_{G'}^k$  is a *group cover* of  $G'$  if every vertex in  $G'.V$  belongs to at least one group, where  $k$  is the number of groups.  $H$  can form a set of *groups* by regarding several vertices in  $G'$  that are close to each other as one vertex. As a result, the shortest distance between  $u$  and  $v$  on  $H$  is an approximation of the shortest distance between  $u$  and  $v$  on  $G'$ . Similar to  $G'$ , let  $H.E$  be the set of edges of  $H$ . Given a group  $Q_{G'}^i$ , we define *intra-edges* to be a set of edges connecting the group center of  $Q_{G'}^i$  to all other vertices in  $Q_{G'}^i$ , and we define *inter-edges* to be a set of edges connecting two group centers.  $H$  can be constructed from a group cover by adding these two types of edges. Let  $e_H(u, v|T_{aft})$  be an (intra- or inter-) edge between two vertices  $u$  and  $v$  in  $H.E$ , and let  $|e_H(u, v|T_{aft})|$  be the weight of this edge. Given two group centers  $s$  and  $t$ , we define  $\Pi_H(s, t|T_{aft}) = (v_1, v_2, \dots, v_{l'})$  to be a shortest path of  $H$ , such that the weighted length of the inter-edges  $\sum_{i=1}^{l'-1} |e'(v_i, v_{i+1}|T_{aft})|$  is minimum, where  $v_1 = s$ ,  $v_{l'} = t$ ,  $l'$  is the number of vertices in this path, and

for each  $i \in [1, l'-1]$ ,  $v_i$  is a group center of  $H$ . Figures 5 (a) and (b) show an example of  $G'$  and the corresponding  $H$  of  $G'$ . For  $H$ , there are three groups with centers  $c$ ,  $e$  and  $g$ . The light blue lines are intra-edges and the purple lines are inter-edges. The shortest path of inter-edges  $\Pi_H(c, g|T_{aft})$  is  $(c, e, g)$  (i.e., the shortest path from POI  $c$  to POI  $e$ , and then to POI  $g$  in Figure 5 (b)).

2) **Three phases of  $FU$ -Oracle:** (i) *Construction phase*, (ii) *update phase* and (iii) *query phase*.

(i) **Construction phase:** Given  $T_{bef}$  and  $P$ , we use algorithm *SSAD* for  $n$  times to calculate the pairwise P2P exact shortest paths on  $T_{bef}$  (stored in  $G$ ) and the POI-to-vertex distance information (store in  $M_{dist}$ ).

(ii) **Update phase:** Given  $T_{bef}$ ,  $T_{aft}$ ,  $P$ ,  $G$  and  $M_{dist}$ , we efficiently update the pairwise P2P exact shortest paths on  $T_{aft}$  in  $G$  and produce  $G'$  (a sub-graph of  $G$ ) in three steps:

- **Terrain surface and POI update detection:** Given  $T_{bef}$ ,  $T_{aft}$  and  $P$ , we detect both  $\Delta F$  and  $\Delta P$ .
- **Pairwise P2P exact shortest path update:** Given  $G$ ,  $T_{aft}$ ,  $P$ ,  $M_{dist}$ ,  $\Delta F$  and  $\Delta P$ , we update the exact shortest path between all pairs of POIs in  $P$  on  $T_{aft}$  in  $G$  using algorithm *SSAD* exploiting the *non-updated terrain shortest path intact* property.
- **Sub-graph generation:** Given  $G$ , we use algorithm *HieGreSpan* to generate a sub-graph of  $G$ , i.e.,  $G'$ , for reducing the output size of  $FU$ -Oracle with the assistance of  $H$ , such that  $|\Pi_{G'}(s, t|T_{bef})| \leq (1 + \epsilon)|\Pi(s, t|T_{bef})|$  for any pair of POIs  $s$  and  $t$  in  $P$  on  $T_{aft}$ .

(iii) **Query phase:** Given two query POIs and  $G'$ , we answer the path between these two POIs on  $T_{aft}$  using  $G'$  efficiently.

## B. Key Ideas for Achieving Short Oracle Update Time

A major contribution of this paper is the short oracle update time of  $FU$ -Oracle, which is enabled by our design in the pairwise P2P exact shortest path update step of the update phase. In this step, the short oracle update time for  $FU$ -Oracle is enabled by (1) the *non-updated terrain shortest path intact* property, and (2) the stored pairwise P2P exact shortest paths on  $T_{bef}$  when  $FU$ -Oracle is constructed. We define the concept of a *disk* first. Given a point  $p$  on a terrain surface and a non-negative real number  $r$ , a disk centered at  $p$  with radius  $r$  on the terrain surface, denoted by  $D(p, r)$ , consists of all points on the terrain surface whose exact shortest distance to  $p$  is at most  $r$ . Given a face  $f_i$ , if a point  $q$  exists on  $f_i$  such that the shortest distance between  $p$  and  $q$  is at most  $r$ , then disk



$D(p, r)$  is said to be *intersect with face  $f_i$* . Figure 2 shows a disk centered at  $u$  with radius equal to the shortest distance between  $u$  and  $o$ , and it does not intersect with any updated faces.

Firstly, we give the *non-updated terrain shortest path intact* property in Property 1. **The property is satisfied in Figure 2: since disks  $D(u, \frac{|\Pi(u, v|T_{bef})|}{2})$  and  $D(v, \frac{|\Pi(u, v|T_{bef})|}{2})$  do not intersect with  $\Delta F$ , we do not need to update the light blue path  $\Pi(u, v|T_{bef})$  after the terrain surface changed.**

**Property 1 (Non-updated Terrain Shortest Path Intact Property).** *Given  $T_{bef}$ ,  $T_{aft}$  and  $\Pi(u, v|T_{bef})$ , if two disks  $D(u, \frac{|\Pi(u, v|T_{bef})|}{2})$  and  $D(v, \frac{|\Pi(u, v|T_{bef})|}{2})$  do not intersect with  $\Delta F$ , then  $\Pi(u, v|T_{aft})$  is the same as  $\Pi(u, v|T_{bef})$ .*

*Proof Sketch.* We show by contradiction that the two paths cannot be different. The detailed proofs of proof sketches in the paper appear in the appendix.  $\square$

Secondly, we illustrate the necessity of storing the pairwise P2P exact shortest paths (i.e.,  $G$ ) on  $T_{bef}$ . Let  $UR(A)$  be the *Update Ratio* of an oracle  $A$ , which is defined to be the number of POIs in  $P$  that we need to perform algorithm SSAD as source (for path updating on  $T_{aft}$ ) divided by the total number of POIs. In Figures 4 (a) to (c), we use algorithm SSAD with  $a$ ,  $b$  and  $h$  as sources to update shortest paths on  $T_{aft}$  for *FU-Oracle* and *WSPD-Oracle-Adapt*. In Figure 4 (d), *FU-Oracle* (resp. *WSPD-Oracle-Adapt*) calculates an *exact* (resp. *approximate*) path between  $c$  and  $f$  on  $T_{bef}$  with path distance  $|\Pi(c, f|T_{bef})|$  (resp.  $d_2$ ), where  $|\Pi(c, f|T_{bef})| < d_2$ . It may happen that the distance from  $f$  to  $\Delta F$  is smaller than  $\frac{d_2}{2}$ , but larger than  $\frac{|\Pi(c, f|T_{bef})|}{2}$ . That is, the disk  $D(f, \frac{|\Pi(c, f|T_{bef})|}{2})$  does not intersect (resp.  $D(f, \frac{d_2}{2})$  intersects) with  $\Delta F$ , and *FU-Oracle* does not need to (resp. *WSPD-Oracle-Adapt* needs to) use algorithm SSAD with  $f$  as source to update shortest paths on  $T_{aft}$ . The case also happens for the paths between  $c$  and  $e$ . In Figure 4 (e), the case also happens for the path between  $g$  and each POI in  $\{c, d\}$ . Thus, for *FU-Oracle* (resp. *WSPD-Oracle-Adapt*), we need to perform algorithm SSAD with 3 POIs  $a, b, h$  (resp. 7 POIs  $a, b, c, d, e, f, g$ ) as a source for path updating on  $T_{aft}$ , and there is a total of 8 POIs, so  $UR(FU-Oracle) = \frac{3}{8}$  (resp.  $UR(WSPD-Oracle-Adapt) = \frac{7}{8}$ ). The oracle update time of *WSPD-Oracle-Adapt* is 2.4 times larger than that of *FU-Oracle*. Given an oracle  $A$ , a higher  $UR(A)$  means that the oracle update time of  $A$  is larger. Lemma 1 shows the necessity of storing  $G$ .

**Lemma 1.** *Given  $T_{bef}$ ,  $T_{aft}$ ,  $P$  and an oracle  $A$  that does not store the pairwise P2P exact shortest paths on  $T_{bef}$ ,  $UR(FU-Oracle) \leq UR(A)$ .*

*Proof.* By storing  $G$ , we can minimize the likelihood of updating the paths on  $T_{aft}$ , so  $UR(FU-Oracle)$  is the smallest.  $\square$

Apart from these two ideas, we provide four additional novel techniques to further reduce the oracle update time.

1) **Novel path update sequence:** We propose a novel path update sequence before utilizing Property 1, to minimize the

oracle update time. In Figure 4 (a), we need to update shortest paths between  $a$  and two POIs in  $\{e, g\}$  on  $T_{aft}$ . By using algorithm SSAD, when we update the paths with  $a$  as the source POI, we can update these two paths simultaneously (since  $e$  and  $g$  are far away from  $\Delta F$ , we can avoid using algorithm SSAD to update the paths with  $e$  and  $g$  as the source POIs according to Property 1). But, if we first update the paths with  $e$  as the source POI, we still need to update the paths with  $g$  as the source POI, which increases the oracle update time. We say “a point (either a vertex or a POI) is in  $\Delta F$ ” if it is on a face in  $\Delta F$ , and “a path passes  $\Delta F$ ” if this path intersects with  $\Delta F$ . Then, the path update sequences that result in the smallest oracle update time are updating the paths: (i) connecting to the POIs in  $\Delta F$ , (ii) passing  $\Delta F$ , and (iii) connecting to the POIs near  $\Delta F$ . After we update all the paths belonging to one type, we process to the next type. In Figures 4 (a) to (c), (i)  $a$  is in  $\Delta F$ , (ii) one of  $b$ ’s exact shortest path  $\Pi(b, h|T_{bef})$  pass  $\Delta F$ , and (iii)  $h$  is near  $\Delta F$ , so we use  $a, b$  and  $h$  as source point in algorithm SSAD and update the paths on  $T_{aft}$  in sequence.

2) **Novel disk radius selection strategy:** We design a novel disk radius selection strategy used in Property 1 (i.e., *half* of the shortest distance between a pair of POIs as the disk radius) when updating the paths connecting to the POIs near  $\Delta F$  to minimize the likelihood of re-calculating shortest paths on  $T_{aft}$ . A naive approach is to create two disks centered at  $u$  and  $v$  with radius equal to the *full* shortest distance between  $u$  and  $v$ . It increases the likelihood of re-calculating this path on  $T_{aft}$  and increases the oracle update time.

3) **Novel distance approximation approach:** We propose a novel distance approximation approach used in Property 1, to avoid performing the expensive shortest path query algorithm on  $T_{aft}$ , for determining whether the disk intersects with  $\Delta F$  on  $T_{aft}$  (i.e., whether the minimum distances from the disk center to any point in  $\Delta F$  on  $T_{aft}$  is smaller than the disk radius), by using the POI-to-vertex distance information stored in  $M_{dist}$ . In Figure 4 (c), we do not want to perform the shortest path query algorithm between  $h$  and  $i$  on  $T_{aft}$  again, for determining whether the disk centered at  $h$  intersects with the updated faces, where  $i$  is a point belonging to the updated faces that is the closest point to  $h$  (among other points belonging to the updated faces). Instead, in Lemma 2, we show that we can use  $M_{dist}$  to obtain the lower bound of the minimum distances from the disk center (i.e., a POI) to any point in  $\Delta F$  on  $T_{aft}$ , to approximate the shortest distance on  $T_{aft}$  in  $O(1)$  time.

**Lemma 2.** *The minimum distance from a POI  $u$  to any point in  $\Delta F$  on  $T_{aft}$  is no less than  $\min_{v \in \Delta V} |\Pi(u, v|T_{bef})| - L_{max}$ .*

*Proof Sketch.* We show that the minimum distance from  $u$  to a point of  $e$  on  $T_{aft}$  is the same as on  $T_{bef}$ , where  $e$  is the edge belongs to a face in  $\Delta F$ , and the exact shortest path from  $u$  to  $\Delta F$  intersects with any point on  $e$  for the first time.  $\square$

If the lower bound is larger than the disk radius, then the minimum distances from this radius center to any point in  $\Delta F$  must be larger than the disk radius, i.e., there is no need to update the corresponding paths. In Figure 4 (c), the exact

shortest distance between  $h$  and  $i$  can be calculated in  $O(1)$  time. We can calculate  $G$  and  $M_{dist}$  simultaneously when  $FU\text{-}Oracle$  is constructed (by using algorithm *SSAD* with each POI as a source point for  $n$  times).

4) **Novel disk and updated face intersection check approach:** We design a novel disk and updated face intersection check approach, to minimize the number of intersection checks for each shortest path on  $T_{aff}$  when updating the paths connecting to the POIs near  $\Delta F$  (i.e., when checking whether (i) the disk and (ii) updated face intersects or not in Property 1). In Figure 4 (c), when checking whether we need to re-calculate the paths between  $h$  and POI  $X$  on  $T_{aff}$ , a naive approach is creating 5 disks centered at  $h$  (and another 5 disks centered at POI  $X$ ) with radius equal to half of the shortest distance between  $h$  and POI  $X$ , and check whether these 10 disks intersect with  $\Delta F$ , where  $X \in \{c, d, e, f, g\}$ . Since there are total  $O(n^2)$  paths, it needs to create  $O(n^2)$  disks. But, we just need to create *one* disk centered at  $h$  with radius equal to half of the longest distance of the paths between  $h$  and each POI in  $\{c, d, e, f, g\}$ , and check whether this disk intersects with  $\Delta F$ . Since there are total  $O(n)$  POIs, we just need to create  $O(n)$  disks. Specifically, for each POI not in  $\Delta F$  and not the endpoint of the paths pass  $\Delta F$ , we sort them from near to far according to their minimum distance to any vertex in  $\Delta V$  on  $T_{bef}$ . We then determine whether there is a need to update shortest paths using Lemma 3.

**Lemma 3.** *If the disk centered at  $u$  with radius equal to half of the longest distance of all non-updated paths adjacent to  $u$  intersects with  $\Delta F$ , we use algorithm *SSAD* to update all the non-updated paths adjacent to  $u$ . Otherwise, there is no need to update shortest paths adjacent to  $u$ .*

*Proof Sketch.* If the disk with the largest radius intersects with  $\Delta F$ , we just need to update the paths and there is no need to check other disks. If the disk with the largest radius and with the center closest to  $\Delta F$  does not intersect with  $\Delta F$ , then other disks cannot intersect with  $\Delta F$ , so there is no need to update the paths.  $\square$

(i) In Figure 4 (c), the sorted POIs are  $h, f, e, d, c, g$ . We create one disk  $D(h, \frac{|\Pi(c, h|T_{bef})|}{2})$ , since it intersects with  $\Delta F$ , we use algorithm *SSAD* to update all shortest paths adjacent to  $h$  that have not been updated. We do not need to create 10 disks, i.e., 5 disks  $D(h, \frac{|\Pi(X, h|T_{bef})|}{2})$  and 5 disks  $D(X, \frac{|\Pi(X, h|T_{bef})|}{2})$ , where  $X \in \{c, d, e, f, g\}$ .

(ii) In Figure 4 (d), the sorted POIs are  $f, e, d, c, g$ . We create one disk  $D(f, \frac{|\Pi(c, f|T_{bef})|}{2})$ , since it does not intersect with  $\Delta F$ , there is no need to update shortest paths adjacent to  $f$ . We do not need to create 8 disks, i.e., 4 disks  $D(f, \frac{|\Pi(X, f|T_{bef})|}{2})$  and 4 disks  $D(X, \frac{|\Pi(X, f|T_{bef})|}{2})$ , where  $X \in \{c, d, e, g\}$ .

### C. Key Ideas for Efficiently Achieving Small Output Size

Another major contribution of this paper is to efficiently reduce the output size of *FU-Oracle*, which comes from our design in the sub-graph generation step (using algorithm *HieGreSpan*) of the update phase. In *HieGreSpan*, unlike in

*GreSpan*, we perform Dijkstra's algorithm to calculate the shortest distance between two vertices on  $H$  (not  $G'$ ).

We first illustrate algorithm *GreSpan*. Given a complete graph  $G$ , it first sorts the edge in  $G$  based on the weight of each edge from minimum to maximum, and initializes a sub-graph  $G'$  to be empty. Then, for each sorted edge  $e(u, v) \in G$ , if  $|e(u, v)|$  is longer than  $(1 + \epsilon)$  times the distance between  $u$  and  $v$  on  $G'$  (calculated using Dijkstra's algorithm on  $G'$ ), then  $e(u, v)$  is added into  $G'$  (in Figure 5 (a), we add the dashed light blue line  $e(f, i)$  into  $G'$ ). It iterates until all the paths have been processed, and returns  $G'$  as output.

We then illustrate algorithm *HieGreSpan*. The main difference between *HieGreSpan* and *GreSpan* is the usage of  $H$ . To construct  $H$ , we first sort the edges in  $G.E$  in increasing order, and then divide them into  $\log n$  intervals, where each interval contains edges with weights in  $(\frac{2^{i-1}D}{n}, \frac{2^i D}{n}]$  for  $i \in [1, \log n]$  and  $D$  is the longest edge's weight in  $G.E$ . When processing each interval of edges, we group some vertices in  $G.V$  into one vertex (the radius of each group of vertices is  $\delta \frac{2^i D}{n}$ , where  $\delta \in (0, \frac{1}{2})$  is a small constant depending on  $\epsilon$ ), such that the shortest distance between the vertices in the same group is very small (and can be regarded as 0) compared with the current processing interval edges' weights. Thus, when checking whether  $|e(u, v)|$  is longer than  $(1 + \epsilon)$  times the distance between  $u$  and  $v$  on  $G'$ , we use Dijkstra's algorithm between the group centers of  $u$  and  $v$  on  $H$ , to approximate the distance between  $u$  and  $v$  on  $G'$ . This takes  $O(1)$  time on  $H$ , but takes  $O(n \log n)$  time on  $G'$  in algorithm *GreSpan*. When we need to process the next interval of edges with larger weight, we update  $H$  such that the radius of each group of vertices will also increase, and  $H$  is a valid approximated graph of  $G'$ . In Figure 5 (a), we add the dashed light blue line between  $f$  and  $i$  into  $G'$ . In Figure 5 (b),  $f$  belongs to  $e$  and  $i$  belongs to  $g$ , so we add the dashed purple edge between  $e$  and  $g$  into  $H$ . Our experiments show that when  $n = 500$ , algorithm *HieGreSpan* needs 24s, but algorithm *GreSpan* needs 101s. Due to algorithm *HieGreSpan*, the output size of *FU-Oracle* is only 22MB on a terrain surface with 0.5M faces and 250 POIs, but the value is 260MB for *WSPD-Oracle*.

### D. Implementation Details of the Construction Phase

We give the implementation details (with examples) of the construction phase. Given  $T_{bef}$  and  $P$ , by regarding each POI  $p_i \in P$  as a source point, we use algorithm *SSAD* to (1) calculate the exact shortest paths between  $p_i$  and other POIs in  $P$  on  $T_{bef}$ , and then store them in  $G$ , (2) calculate the exact shortest distance between  $p_i$  and each vertex in  $V$  on  $T_{bef}$ , and then store them in  $M_{dist}$ . For example, Figure 3 (a) shows  $T_{bef}$  and  $P$ . In Figures 3 (b) and (c), we first take  $a$  as a source point, and use algorithm *SSAD* to calculate the exact shortest paths between  $a$  and  $\{b, c, d\}$  (the light blue lines), and the exact shortest distance between  $a$  and all vertices. Next, we take  $b$  as a source point, and calculate the exact shortest paths between  $b$  and  $\{c, d\}$ , and the exact shortest distance between  $b$  and all vertices.



### E. Implementation Details of the Update Phase

We present the implementation details (with pseudo-code and examples) of the update phase for (1) the pairwise P2P exact shortest path update step and (2) the sub-graph generation step. For example, Figure 3 (d) shows  $T_{aft}$ . Figures 3 (e) and (f) show the output of the two steps, and Figures 4 and 5 show the detailed examples of the two steps.

1) **Pairwise P2P exact shortest path update:** Given two POIs  $u$  and  $v$  in  $P$ , after we have updated an exact shortest path  $\Pi(u, v|T_{bef})$  (stored in  $G$ ) between  $u$  and  $v$  on  $T_{bef}$ , the updated exact shortest path between  $u$  and  $v$  on  $T_{aft}$  is denoted as  $\Pi(u, v|T_{aft})$ . Let  $P_{remain} = \{p'_1, p'_2, \dots, p'_{|P_{remain}|}\}$  be a set of remaining POIs in  $P$  on  $T_{aft}$  that we have not processed, where  $|P_{remain}|$  is the number of POIs in  $P_{remain}$ .  $P_{remain}$  is initialized to be  $P$ . In each update iteration, whenever we have processed a POI, we remove this POI from  $P_{remain}$ . In Figures 4 (a) and (b),  $P_{remain} = \{b, c, d, e, f, g, h\}$  and  $P_{remain} = \{c, d, e, f, g, h\}$ , respectively. This set is different from  $\Delta P$  (which stores a set of POIs with different coordinate values between  $T_{bef}$  and  $T_{aft}$ ). For  $\Delta P$ , we use algorithm SSAD to update shortest paths on  $T_{aft}$  with the POIs in  $\Delta P$  as sources. For  $P_{remain}$ , when processing a POI  $u$ , among all the POIs in  $P_{remain}$ , we use the POI  $v$  in  $P_{remain}$  such that  $|\Pi(u, v|T_{bef})|$  is the longest, and we use  $|\Pi(u, v|T_{bef})|$  as the disk radius in our novel disk and updated face intersection check approach as mentioned in Section IV-B4. Given a POI  $u \in P_{remain}$ , we let  $\Pi(u) = \{\Pi(u, v_1|T_{bef}), \Pi(u, v_2|T_{bef}), \dots, \Pi(u, v_{|\Pi(u)|}|T_{bef})\}$  be a set of the exact shortest paths stored in  $G$  on  $T_{bef}$  with  $u$  as an endpoint and  $v_i \in P_{remain} \setminus \{u\}$ ,  $i \in \{1, l_u\}$  as the other endpoint, such that all these paths have not been updated.  $\Pi(u)$  is initialized to be all the exact shortest paths stored in  $G$  with  $u$  as an endpoint, where  $|\Pi(u)|$  is the number of paths in  $\Pi(u)$ . In Figures 4 (a) to (c), the purple and pink lines denote  $\Pi(a)$ ,  $\Pi(b)$  and  $\Pi(h)$ , respectively.

**Detail and example:** Algorithm 1 and 2 show this step. For Algorithm 1, in Figure 4 (a), we compute  $Update(a, T_{aft}, G, P_{remain} = \{b, c, d, e, f, g, h\})$ . The following illustrates Algorithm 2 with an example.

---

#### Algorithm 1 $Update(u, T_{aft}, G, P_{remain})$

---

**Input:** a POI  $u$ ,  $T_{aft}$ , temporary complete graph  $G$  and  $P_{remain}$   
**Output:** updated  $G$  and updated  $P_{remain}$   
1: use  $u$  as source point in algorithm SSAD to calculate  $\Pi(u, v|T_{aft})$  for each POI  $v \in P_{remain}$  simultaneously  
2: **for** each POI  $v \in P_{remain}$  **do**  
3:  $G.E \leftarrow G.E - \{\Pi(u, v|T_{bef})\} \cup \{\Pi(u, v|T_{aft})\}$   
4:  $\Pi(v) \leftarrow \Pi(v) - \{\Pi(u, v|T_{bef})\}$   
5:  $P_{remain} \leftarrow P_{remain} - \{u\}$   
6: **return** updated  $G$  and  $P_{remain}$

---

(i) *Path update for POI in updated face:* Lines 4-6. In Figure 4 (a),  $a \in \Delta P$ , we update the paths in purple on  $T_{aft}$ .

(ii) *Path update for path passing updated face:* Lines 7-9. In Figure 4 (b),  $b \notin \Delta P$  but one exact shortest path  $\Pi(b, h|T_{bef}) \in \Pi(u)$  passes  $\Delta F$  (the black circle), so we update the paths in purple and pink on  $T_{aft}$ .

(iii) *Path update for POI near updated face:* Lines 10-16. In lines 13-14 and Figure 4 (c), the sorted POIs are  $h, f, e, d, c, g$ ,

---

#### Algorithm 2 $PairwiseP2PUpdate(G, P, M_{dist}, \Delta F, \Delta P)$

---

**Input:**  $G$ , a set of POIs  $P$ ,  $M_{dist}$ ,  $\Delta F$  and  $\Delta P$   
**Output:** updated  $G$   
1:  $P_{remain} \leftarrow P$   
2: **for** each POI  $u \in P_{remain}$  **do**  
3:  $\Pi(u) \leftarrow$  all the exact shortest paths in  $G$  with  $u$  as an endpoint  
4: **for** each POI  $u \in P_{remain}$  **do**  
5: **if**  $u \in \Delta P$  **then**  
6:  $Update(u, T_{aft}, G, P_{remain})$   
7: **for** each POI  $u \in P_{remain}$  **do**  
8: **if**  $u \notin \Delta P$  but there exists an exact shortest path in  $\Pi(u)$  passes  $\Delta F$  **then**  
9:  $Update(u, T_{aft}, G, P_{remain})$   
10: sort each POI in  $P_{remain}$  from near to far according to their minimum distance to any vertex in  $\Delta V$  on  $T_{bef}$  using  $M_{dist}$   
11: **for** each sorted POI  $u \in P_{remain}$  **do**  
12:  $v \leftarrow$  a POI in  $P_{remain}$  such that  $|\Pi(u, v|T_{bef})|$  has the longest distance among all  $\Pi(u)$   
13: **if** disk  $D(u, \frac{|\Pi(u, v|T_{bef})|}{2})$  intersects with  $\Delta F$  **then**  
14:  $Update(u, T_{aft}, G, P_{remain})$   
15: **else**  
16:  $P_{remain} \leftarrow P_{remain} - \{u\}$   
17: **return** updated  $G$

---

the path with the longest distance is  $\Pi(c, h|T_{bef})$ . Since the disk with blue circle intersects with  $\Delta F$ , we update the paths in purple on  $T_{aft}$ . In lines 15-16 and Figure 4 (d), the sorted POIs are  $f, e, d, c, g$ , the paths with the longest distance is  $\Pi(c, f|T_{bef})$ . Since the disk with blue circle does not intersect with  $\Delta F$ , we do not need to update the paths.

2) **Sub-graph generation using algorithm HieGreSpan:** Recall that the radius of each group of vertices is  $\delta \frac{2^i D}{n}$ , we set  $\delta = \frac{1}{2}(\frac{\sqrt{\epsilon+1}-1}{\sqrt{\epsilon+1}+3})$ . Since  $\epsilon \in (0, \infty)$ , we have  $\delta \in (0, \frac{1}{2})$ .

**Detail and example:** Algorithm 3 shows *HieGreSpan*, and the following illustrates it with an example.

(i) *Edge sort, interval split, and  $G'$  initialization:* Lines 2-6.

(ii)  *$G'$  maintenance:* Lines 7-25, and Figures 5 (a) and (b).

In lines 9-15, *group construction and  $H$  intra-edge insertion:* Based on the vertices of  $G'$ , we have three groups with group center  $c, e$  and  $g$  in  $H$ . We add light blue edges  $e'(a, c|T_{aft}), \dots, e'(g, i|T_{aft})$  in  $H$ . In lines 16-19,  *$H$  first type inter-edge insertion:* We add purple edge  $e(c, e|T_{aft})$  in  $H$ . In lines 20-22,  *$H$  edge examine:* We need to examine edge  $e(f, i|T_{aft})$  on  $G'$ , the corresponding shortest path on  $H$  is  $\Pi_H(e, g|T_{aft})$  and  $|\Pi_H(e, g|T_{aft})| = \infty > (1 + \epsilon)|e(f, i|T_{aft})|$ . In lines 24,  *$G'$  edge insertion:* We add  $e(f, i|T_{aft})$  into  $G'$ . In line 25,  *$H$  second type inter-edge insertion:* We add  $e_H(e, g|T_{aft})$  with weight  $|e_H(e, f|T_{aft})| + |e(e, g|T_{aft})| + |e_H(g, i|T_{aft})|$  into  $H$ .

### F. Implementation Details of the Query Phase

We then give the implementation details (with examples) of the query phase. Given  $G'$ , and two query POIs  $s$  and  $t$  in  $P$  (i.e., two query vertices  $s$  and  $t$  in  $G'.V$ ), we use Dijkstra's algorithm [23] to find the shortest path between  $s$  and  $t$  on  $G'$ , i.e.,  $\Pi_{G'}(s, t|T_{aft})$ , which is a  $(1 + \epsilon)$ -approximate path of  $\Pi(s, t|T_{aft})$ . For example, in Figure 3 (g), given two query POIs  $a$  and  $b$ , we calculate  $\Pi_{G'}(a, b|T_{aft})$ , which consists of two green lines, i.e.,  $\Pi(a, c|T_{aft})$  and  $\Pi(c, b|T_{aft})$ .

**Algorithm 3** *HieGreSpan* ( $G, \epsilon$ )

**Input:** temporary complete graph  $G$  and error parameter  $\epsilon$   
**Output:** *FU-Oracle* output graph  $G'$  (a sub-graph of  $G$ )

- 1:  $D \leftarrow$  the weight of the longest edge in  $G.E$
- 2: **for** each edge  $e(u, v|T_{aff}) \in G.E$  **do**
- 3:   sort edge weights in increasing order
- 4:   create intervals  $I_0 = (0, \frac{D}{N}]$ ,  $I_i = (\frac{2^{i-1}D}{N}, \frac{2^i D}{N}]$  for  $i \in [1, \log n]$
- 5:    $G'.E^i \leftarrow$  sorted edges of  $G.E$  with weight in  $I_i$
- 6:    $G'.E \leftarrow G'.E^0$
- 7: **for**  $i \leftarrow 1$  to  $\log n$  **do**
- 8:    $H.E \leftarrow \emptyset$
- 9:   **for** each  $u_j \in G.V$  that has not been visited **do**
- 10:     perform Dijkstra's algorithm on  $G'$ , such that the algorithm never visits vertices further than  $\delta \frac{2^i D}{n}$  from  $u_j$
- 11:     create a group  $Q_{G'}^j \leftarrow \{u_j\}$  with group center  $u_j$ ,  $u_j \leftarrow \text{visited}$
- 12:     **for** each  $v \in G.V$  such that  $|\Pi_{G'}(u_j, v|T_{aff})| \leq \delta \frac{2^i D}{n}$  **do**
- 13:        $Q_{G'}^j \leftarrow \{v\}$ ,  $v \leftarrow \text{visited}$
- 14:        $H$  intra-edges  $\leftarrow H.E \cup \{e_H(u_j, v|T_{aff})\}$ , where  $|e_H(u_j, v|T_{aff})| = |\Pi_{G'}(u_j, v|T_{aff})|$
- 15:        $j \leftarrow j + 1$
- 16:     **for** each group center  $u_j$  **do**
- 17:       perform Dijkstra's algorithm on  $G'$ , such that the algorithm never visits vertices further than  $\frac{2^i D}{n} + 2\delta \frac{2^i D}{n}$  from  $u_j$
- 18:        $H$  inter-edges  $\leftarrow H.E \cup \{e_H(u_j, u|T_{aff})\}$ , where  $u$  is other group centers and  $|e_H(u_j, u|T_{aff})| = |\Pi_{G'}(u_j, u|T_{aff})|$
- 19:        $j \leftarrow j + 1$
- 20:     **for** each edge  $e(u, v|T_{aff}) \in G.E^i$  **do**
- 21:        $w \leftarrow$  group center of  $u$ ,  $x \leftarrow$  group center of  $v$
- 22:        $\Pi_H(w, x|T_{aff}) \leftarrow$  the shortest path between  $w$  and  $x$  calculated using Dijkstra's algorithm on  $H$
- 23:       **if**  $|\Pi_H(w, x|T_{aff})| > (1 + \epsilon)|e(u, v|T_{aff})|$  **then**
- 24:          $G'.E \leftarrow G'.E \cup \{e(u, v|T_{aff})\}$
- 25:        $H$  inter-edge  $\leftarrow H.E \cup \{e_H(w, x|T_{aff})\}$ , where  $|e_H(w, x|T_{aff})| = |e_H(w, u|T_{aff})| + |e(u, v|T_{aff})| + |e_H(v, x|T_{aff})|$
- 26: **return**  $G'$

**G. Theoretical Analysis**

Theorem 1 and 2 show the analysis of algorithm *HieGreSpan* and *FU-Oracle*, respectively.

**Theorem 1.** *The running time of HieGreSpan is  $O(n \log^2 n)$ . The output of HieGreSpan, i.e.,  $G'$ , satisfies  $|\Pi_{G'}(u, v|T_{aff})| \leq (1 + \epsilon)|\Pi(u, v|T_{aff})|$  for all pairs of vertices  $u$  and  $v$  in  $G'.V$ .*

*Proof Sketch.* The running time includes (1) the edge sort, interval split time, and  $G'$  initialization  $O(n)$  due to  $n$  vertices in  $G$ , and (2)  $G'$  maintenance time  $O(n \log^2 n)$  due to total  $\log n$  intervals and  $O(n \log n)$  time for each interval. For the error bound, we use the same notations in Algorithm 3. Since  $H$  is a valid approximation of  $G'$ , in the  $H$  edge examine step of algorithm *HieGreSpan*, when we check whether  $|\Pi_H(w, x|T)| > (1 + \epsilon)|e(u, v|T)|$ , we are checking  $|\Pi_{G'}(u, v|T)| > (1 + \epsilon)|e(u, v|T)|$ . For any edge  $e(u, v|T) \in G'.E$  that is not added to  $G'$ , we know  $|\Pi_{G'}(u, v|T)| \leq (1 + \epsilon)|e(u, v|T)|$ . Since  $|e(u, v|T)| = |\Pi(u, v|T)|$ , we have  $|\Pi_{G'}(u, v|T)| \leq (1 + \epsilon)|\Pi(u, v|T)|$ .  $\square$

**Theorem 2.** *The oracle construction time, oracle update time, output size and shortest path query time of FU-Oracle are  $O(nN \log^2 N)$ ,  $O(N \log^2 N + n \log^2 n)$ ,  $O(n)$  and  $O(\log n)$ , respectively. FU-Oracle satisfies  $|\Pi_{G'}(u, v|T)| \leq (1 + \epsilon)|\Pi(u, v|T)|$  for all pairs of POIs  $u$  and  $v$  in  $P$ .*

TABLE II  
COMPARISON OF ALGORITHMS

Algorithm	Oracle construction time	Oracle update time	Output size	Shortest path query time
<b>Oracle-based algorithm</b>				
WSPD-Oracle [52], [53]	Large	Large	Large	Small
WSPD-Oracle-Adapt [52], [53]	Large	Large	Small	Small
EAR-Oracle [29]	Large	Large	Large	Medium
EAR-Oracle-Adapt [29]	Large	Large	Small	Small
FU-Oracle (ours)	Small	Small	Small	Small
<b>On-the-fly algorithm</b>				
CH-Fly- Algo [18]	N/A	N/A	N/A	Large
K-Fly- Algo [32]	N/A	N/A	N/A	Large

*Proof Sketch.* The oracle construction time includes the pairwise P2P exact shortest paths calculation time  $O(nN \log^2 N)$  due to total  $n$  POIs and the usage of algorithm SSAD in  $O(N \log^2 N)$  time for each POI. The oracle update time includes (1) terrain surface and POI update detection time  $O(N + n)$  due to  $O(N)$  faces and  $n$  POIs, (2) the pairwise P2P exact shortest paths update time  $O(N \log^2 N)$  due to  $O(1)$  number of updated POIs and the usage of algorithm SSAD in  $O(N \log^2 N)$  time for each POI, (3) and the sub-graph generation time  $O(n \log^2 n)$  due to algorithm *HieGreSpan* in Theorem 1. The output size is  $O(n)$  due to the output graph size of algorithm *HieGreSpan*. The shortest path query time is  $O(\log n)$  due to the use of Dijkstra's algorithm on  $G'$  (in our experiment,  $G'$  has a constant number of edges and  $n$  vertices). The error bound of *FU-Oracle* is due to the error bound of algorithm *HieGreSpan*.  $\square$

**V. EMPIRICAL STUDY**

We present the experimental setup in Section V-A and the experimental results in Section V-B.

**A. Experimental Setup**

We conduct our experiments on a Linux machine with a 2.20 GHz CPU and 512GB memory. All algorithms are implemented in C++. Our experimental setup generally follows the setups in the literature [32], [33], [38], [52], [53].

1) **Datasets:** We conduct our experiment on 30 real before and after earthquake terrain datasets listed in Table I with 0.5M faces. We first obtain the earthquake terrain satellite maps with a  $5\text{km} \times 5\text{km}$  covered region from Google Earth [4] with a resolution of 10m [22], [38], [48], [52], [53], and then we use Blender [2] to generate the terrain model. To study the scalability, we follow an existing multi-resolution terrain dataset generation procedure [38], [52], [53] to obtain different resolutions of these datasets with 1M, 1.5M, 2M, 2.5M faces. This procedure appears in the appendix. We extract 500 POIs using OpenStreetMap [52], [53].

2) **Algorithms:** We include the the best-known exact on-the-fly algorithm *CH-Fly- Algo* [18], the best-known approximate on-the-fly algorithm *K-Fly- Algo* [32], the best-known oracle *WSPD-Oracle* [52], [53] that answers the P2P query, its adaption *WSPD-Oracle-Adapt*, the most recent oracle *EAR-Oracle* [29], and its adaption *EAR-Oracle-Adapt* as baselines. *WSPD-Oracle* and *WSPD-Oracle-Adapt* reveal the two major

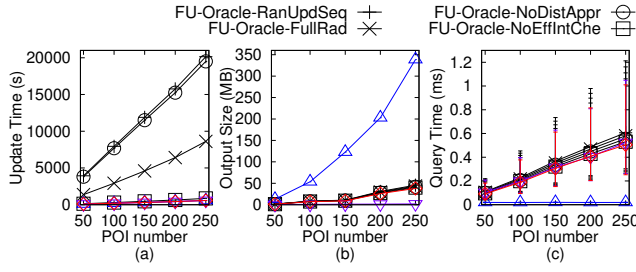


Fig. 6. Ablation study on TJ dataset with fewer POIs

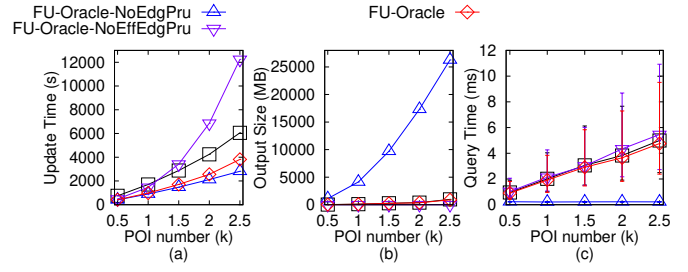


Fig. 7. Ablation study on SC dataset with more POIs

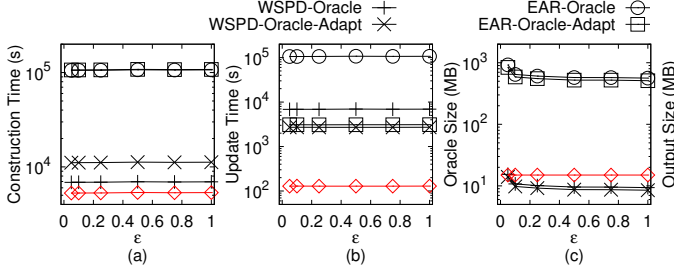


Fig. 8. Baseline comparisons (effect of  $\epsilon$  on GI dataset with fewer POIs)

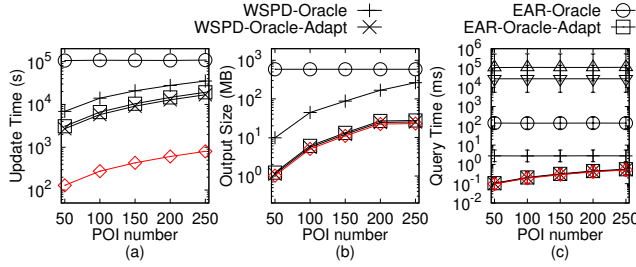


Fig. 9. Baseline comparisons (effect of  $n$  on AU dataset with fewer POIs)

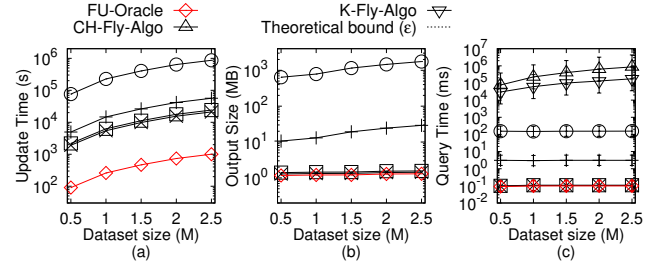


Fig. 10. Baseline comparisons (effect of  $DS$  on LH dataset with fewer POIs)

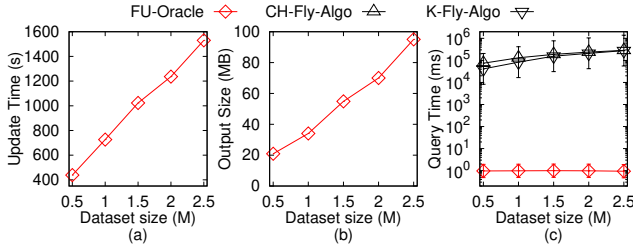


Fig. 11. Scalability test on VS dataset with more POIs

reasons for the short oracle update time of *FU-Oracle*, i.e., (i) *WSPD-Oracle* does not utilize the non-updated terrain shortest path intact property, and (ii) *WSPD-Oracle-Adapt* does not store the pairwise P2P exact shortest paths on  $T_{bef}$  when the oracle is constructed. In Table II, we compare these algorithms. The comparisons of all algorithms (with big-O notations) can be found in the appendix.

3) **Query generation:** We randomly choose pairs of POIs in  $P$  on  $T_{aft}$ , as source and destination, and we report the average, minimum, and maximum results of 100 queries.

4) **Parameters and performance metrics:** We study the effect of three parameters, namely (i)  $\epsilon$ , (ii)  $n$  and (iii) dataset size  $DS$  (i.e., the number of faces in a terrain model). We con-

sider six performance metrics, namely (i) *oracle construction time*, (ii) *oracle update time*, (iii) *oracle size* (i.e., the space consumption of  $G$ ,  $M_{dist}$  and  $H$ ), (iv) *output size* (i.e., the space consumption of  $G'$ ), (v) *shortest path query time* and (vi) *distance error* (i.e., the error of the distance returned by the algorithm compared with the exact shortest distance).

## B. Experimental Results

Our experiments show that *WSPD-Oracle*, *WSPD-Oracle-Adapt*, *EAR-Oracle* and *EAR-Oracle-Adapt* have excessive oracle update times with 500 POIs (more than 1 days), so we compare (1) all algorithms on 30 datasets with fewer POIs (50 by default), and (2) *FU-Oracle*, *CH-Fly-Algo* and *K-Fly-Algo* on 30 datasets with more POIs (500 by default). For the shortest path query time, the vertical bar and the points denote the minimum, maximum and average results.

1) **Ablation study:** We consider 6 variations of *FU-Oracle*, i.e., (i) we use a random path update sequence, instead of using our novel path update sequence, (ii) we use the full shortest distance of a shortest path as the disk radius, instead of using our novel disk radius selection strategy, (iii) we do not store the POI-to-vertex distance information and re-calculate the shortest path on  $T_{aft}$  for determining whether the disk intersects with  $\Delta F$ , instead of using our novel distance



approximation approach, (iv) we create two disks for each path when checking whether we need to re-calculate the shortest path between a pair of POIs, instead of using our novel disk and updated face intersection check approach as mentioned in Section IV-B4, (v) we remove the sub-graph generation step, i.e., algorithm *HieGreSpan* in the update phase and use a hash table to store the pairwise P2P exact shortest paths on  $T_{aff}$  in  $G$ , and (vi) we use algorithm *GreSpan* [13], [14], instead of using algorithm *HieGreSpan* in the sub-graph generation step of the update phase. We use *FU-Oracle-X* where  $X \in \{\text{RanUpdSeq}, \text{FullRad}, \text{NoDistAppr}, \text{NoEffIntChe}, \text{NoEdgPru}, \text{NoEffEdgPru}\}$  to denote these variations. The first four oracles correspond to the four techniques in Section IV-B. The last two oracles correspond to the idea covered in Section IV-C.

In Figure 6 (resp. Figure 7), we tested the 5 values of  $n$  in  $\{50, 100, 150, 200, 250\}$  on *TJ* (resp.  $\{500, 1000, 1500, 2000, 2500\}$  on *SC*) dataset while fixing  $\epsilon$  at 0.1 and  $DS$  at 0.5M (resp.  $\epsilon$  to 0.25 and  $DS$  to 0.5M) for the ablation study involving 6 variations and *FU-Oracle* (resp. *FU-Oracle-X*, where  $X \in \{\text{NoEffIntChe}, \text{NoEdgPru}, \text{NoEffEdgPru}\}$  and *FU-Oracle*, since the first 3 variations have excessive oracle update times with 500 POIs). The oracle update time for *FU-Oracle-X*, where  $X \in \{\text{RanUpdSeq}, \text{FullRad}, \text{NoDistAppr}, \text{NoEffIntChe}, \text{NoEffEdgPru}\}$  exceeds that of *FU-Oracle* due to the four techniques from Section IV-B and the use of algorithm *HieGreSpan* from Section IV-C. Although the oracle update time and the shortest path query time of *FU-Oracle-NoEdgPru* is slightly smaller than that of *FU-Oracle*, the output size for *FU-Oracle-NoEdgPru* is  $10^4$  times due to the usage of algorithm *HieGreSpan*. Thus, *FU-Oracle* is the best oracle among the variations.

2) **Baseline comparisons:** We proceed to compare different baselines with *FU-Oracle*. We study the effects of  $\epsilon$ ,  $n$  and the dataset size.

**Effect of  $\epsilon$ :** In Figure 8, we tested the 6 values of  $\epsilon$  in  $\{0.05, 0.1, 0.25, 0.5, 0.75, 1\}$  on *GI* dataset with fewer POIs while fixing  $n$  at 50 and  $DS$  at 0.5M. Although all algorithms have errors close to 0%, *FU-Oracle* offers superior performance over *WSPD-Oracle*, *WSPD-Oracle-Adapt*, *EAR-Oracle*, *EAR-Oracle-Adapt* and *CH-Fly-Algo* in terms of the oracle construction time, oracle update time, output size and shortest path query time due to the *non-updated terrain shortest path intact* property, the stored pairwise P2P exact shortest paths on  $T_{bef}$ , and the usage of algorithm *HieGreSpan* in *FU-Oracle*. Although the oracle size of *FU-Oracle* is slightly larger than that of *WSPD-Oracle* and *WSPD-Oracle-Adapt*, the oracle update time of *FU-Oracle* is 88 times and 21 times smaller than that of *WSPD-Oracle* and *WSPD-Oracle-Adapt*. Varying  $\epsilon$  has (i) no impact on the oracle construction time of *FU-Oracle* since it is independent of  $\epsilon$ , (ii) a small impact on the oracle update time of *FU-Oracle*, since when  $n$  is small, the pairwise P2P exact shortest path update step dominates the sub-graph generation step, and the former step is independent of  $\epsilon$ , and (iii) a small impact on the oracle construction time and oracle update time of other oracles since their early termination criteria of using algorithm *SSAD* are loose (i.e., they need

to use algorithm *SSAD* to cover most of the POIs or highway nodes as destinations even when  $\epsilon$  is large).

**Effect of  $n$ :** In Figure 9, we tested the 5 values of  $n$  in  $\{50, 100, 150, 200, 250\}$  on *AU* dataset while fixing  $\epsilon$  at 0.1 (we also have the results with 5 values of  $n$  in  $\{500, 1000, 1500, 2000, 2500\}$  while fixing  $\epsilon$  at 0.25 in the appendix) and  $DS$  at 0.5M. The oracle update time, output size and shortest path query time of *FU-Oracle* remain better than those of the baselines. Specifically, the oracle update time of *FU-Oracle* is 21 times and 23 times smaller than that of *WSPD-Oracle-Adapt* and *EAR-Oracle-Adapt*. Since both *WSPD-Oracle-Adapt* and *EAR-Oracle-Adapt* have the output graph  $G'$  (which is similar to *FU-Oracle*), their output size and shortest path query time are similar to that of *FU-Oracle*.

**Effect of  $DS$ :** In Figure 10, we tested the 5 values of  $LH$  in  $\{0.5M, 1M, 1.5M, 2M, 2.5M\}$  on *TJ* dataset with fewer POIs while fixing  $\epsilon$  at 0.1 and  $n$  at 50. Varying  $DS$  has a small impact on the shortest path query time of *FU-Oracle*, but has a large impact on that of *CH-Fly-Algo* and *K-Fly-Algo*. Since *FU-Oracle* is an oracle, its shortest path query time is  $10^5$  times smaller than that of *K-Fly-Algo*.

3) **Scalability test:** In Figure 11, we tested 5 values of  $DS$  in  $\{0.5M, 1M, 1.5M, 2M, 2.5M\}$  on *VS* dataset with more POIs while fixing  $\epsilon$  at 0.25 and  $n$  at 500. *FU-Oracle* can scale up to a large dataset with 2.5M points. The shortest path query time of *FU-Oracle* is much smaller than those of *CH-Fly-Algo* and *K-Fly-Algo*.

4) **Case study:** We conducted a case study on the 4.1 magnitude earthquake (which caused an avalanche) in Valais as mentioned in Section I-A. In this case study, on a terrain surface with 0.5M faces and 250 POIs, *FU-Oracle* just needs 400s  $\approx$  7 min to update the oracle, while the best-known oracle *WSPD-Oracle* needs 35,100s  $\approx$  9.8 hours.

5) **Summary:** *FU-Oracle* is up to 1.3 times, 88 times, 12 times and 3 times better than the best-known oracle *WSPD-Oracle*, in terms of the oracle construction time, oracle update time, output size and shortest path query time. For a terrain dataset with 0.5M faces and 250 POIs, *FU-Oracle*'s oracle update time is 400s  $\approx$  7 min, while *WSPD-Oracle* takes 35,100s  $\approx$  9.8 hours. When the dataset size is 0.5M and with  $\epsilon = 0.05$ , the shortest path query time for computing 100 paths is 0.1s for *FU-Oracle*, while the time is 8,600s  $\approx$  2.4 hours for *K-Fly-Algo* and 0.3s for *WSPD-Oracle*.

## VI. CONCLUSION

We propose an efficient  $(1+\epsilon)$ -approximate shortest path oracle on an updated terrain surface called *FU-Oracle*, which has state-of-the-art performance in terms of the oracle construction time, oracle update time, output size and shortest path query time compared with the best-known oracle. In future work, it is of interest to explore new pruning steps in *FU-Oracle* to further reduce the oracle update time. For example, it may be possible to reduce the likelihood of using algorithm *SSAD* when updating *FU-Oracle* by reducing the disk radius in the *non-updated terrain shortest path intact* property.

## REFERENCES

- [1] “2018 anchorage earthquake,” 2023. [Online]. Available: <https://www.usgs.gov/news/featured-story/2018-anchorage-earthquake>
- [2] “Blender,” 2023. [Online]. Available: <https://www.blender.org>
- [3] “Falcon 9,” 2023. [Online]. Available: <https://www.spacex.com/vehicles/falcon-9/>
- [4] “Google earth,” 2023. [Online]. Available: <https://earth.google.com/web>
- [5] “Gujarat earthquake, 2001,” 2023. [Online]. Available: <https://www.actionaidindia.org/emergency/gujarat-earthquake-2001/>
- [6] “Mar 11, 2011: Tohoku earthquake and tsunami,” 2023. [Online]. Available: <https://education.nationalgeographic.org/resource/tohoku-earthquake-and-tsunami/>
- [7] “Mars 2020 mission perseverance rover brains,” 2023. [Online]. Available: <https://mars.nasa.gov/mars2020/spacecraft/rover/brains/>
- [8] “Metaverse,” 2023. [Online]. Available: <https://about.facebook.com/meta>
- [9] “Moderate mag. 4.1 earthquake - 6.3 km northeast of sierre, valais, switzerland, on monday, october 24, 2016 at 16:44 gmt,” 2023. [Online]. Available: <https://www.volcanodiscovery.com/earthquakes/quake-info/1451397/mag4quake-Oct-24-2016-Leukerbad-VS.html>
- [10] “Nasa mars exploration,” 2023. [Online]. Available: <https://mars.nasa.gov>
- [11] “SpaceX,” 2023. [Online]. Available: <https://www.spacex.com>
- [12] “Turkey-syria earthquakes 2023,” 2023. [Online]. Available: <https://www.bbc.com/news/topics/cq0zxd0y39t>
- [13] I. Althöfer, G. Das, D. Dobkin, and D. Joseph, “Generating sparse spanners for weighted graphs,” in *Proceedings of the Scandinavian Workshop on Algorithm Theory*, 1990, pp. 26–37.
- [14] I. Althöfer, G. Das, D. Dobkin, D. Joseph, and J. Soares, “On sparse spanners of weighted graphs,” *Discrete & Computational Geometry*, vol. 9, no. 1, pp. 81–100, 1993.
- [15] A. Annis, F. Nardi, A. Petroselli, C. Apollonio, E. Arcangeletti, F. Tauro, C. Belli, R. Bianconi, and S. Grimaldi, “Uav-dems for small-scale flood hazard mapping,” *Water*, vol. 12, no. 6, p. 1717, 2020.
- [16] B. Awerbuch, “Communication-time trade-offs in network synchronization,” in *Proceedings of the fourth annual ACM symposium on Principles of distributed computing*, 1985, pp. 272–276.
- [17] P. B. Callahan and S. R. Kosaraju, “A decomposition of multidimensional point sets with applications to k-nearest-neighbors and n-body potential fields,” *Journal of the ACM*, vol. 42, no. 1, pp. 67–90, 1995.
- [18] J. Chen and Y. Han, “Shortest paths on a polyhedron,” in *Proceedings of the sixth annual symposium on Computational geometry*, New York, NY, USA, 1990, p. 360–369.
- [19] T. H. Cormen, C. E. Leiserson, R. L. Rivest, and C. Stein, *Introduction to algorithms*. MIT press, 2022.
- [20] G. Das and G. Narasimhan, “A fast algorithm for constructing sparse euclidean spanners,” in *Proceedings of the tenth annual symposium on Computational geometry*, 1994, pp. 132–139.
- [21] K. Deng, H. T. Shen, K. Xu, and X. Lin, “Surface k-nn query processing,” in *Proceedings of the International Conference on Data Engineering*. IEEE, 2006, pp. 78–78.
- [22] K. Deng and X. Zhou, “Expansion-based algorithms for finding single pair shortest path on surface,” in *Proceedings of the International Workshop on Web and Wireless Geographical Information Systems*, 2004, pp. 151–166.
- [23] E. W. Dijkstra, “A note on two problems in connexion with graphs,” *Numerische mathematik*, vol. 1, no. 1, pp. 269–271, 1959.
- [24] H. N. Djidjev and C. Sommer, “Approximate distance queries for weighted polyhedral surfaces,” in *Proceedings of the European Symposium on Algorithms*, 2011, pp. 579–590.
- [25] M. Fan, H. Qiao, and B. Zhang, “Intrinsic dimension estimation of manifolds by incising balls,” *Pattern Recognition*, vol. 42, no. 5, pp. 780–787, 2009.
- [26] W. Fan, X. Wang, and Y. Wu, “Diversified top-k graph pattern matching,” *Proceedings of the VLDB Endowment*, vol. 6, no. 13, pp. 1510–1521, 2013.
- [27] Y. Hong and J. Liang, “Excavators used to dig out rescue path on cliff in earthquake-hit luding of sw china’s sichuan,” *People’s Daily misc*, 2022. [Online]. Available: <http://en.people.cn/n3/2022/0909/c90000-10145381.html>
- [28] G. Hou, Q. Guo, F. Zhang, S. Wang, and Z. Wei, “Personalized pagerank on evolving graphs with an incremental index-update scheme,” *Proceedings of the 2023 ACM SIGMOD International Conference on Management of Data*, vol. 1, no. 1, pp. 1–26, 2023.
- [29] B. Huang, V. J. Wei, R. C.-W. Wong, and B. Tang, “Ear-oracle: on efficient indexing for distance queries between arbitrary points on terrain surface,” *Proceedings of the 2023 ACM SIGMOD International Conference on Management of Data*, vol. 1, no. 1, pp. 1–26, 2023.
- [30] N. Jin, C. Young, and W. Wang, “Gaia: graph classification using evolutionary computation,” in *Proceedings of the 2010 ACM SIGMOD International Conference on Management of data*, 2010, pp. 879–890.
- [31] S. Kapoor, “Efficient computation of geodesic shortest paths,” in *Proceedings of the thirty-first annual ACM symposium on Theory of computing*, 1999, pp. 770–779.
- [32] M. Kaul, R. C.-W. Wong, and C. S. Jensen, “New lower and upper bounds for shortest distance queries on terrains,” *Proceedings of the VLDB Endowment*, vol. 9, no. 3, pp. 168–179, 2015.
- [33] M. Kaul, R. C.-W. Wong, B. Yang, and C. S. Jensen, “Finding shortest paths on terrains by killing two birds with one stone,” *Proceedings of the VLDB Endowment*, vol. 7, no. 1, pp. 73–84, 2013.
- [34] T. Kawamura, J. F. Clinton, G. Zenhäusern, S. Ceylan, A. C. Horleston, N. L. Dahmen, C. Duran, D. Kim, M. Plasman, S. C. Stähler *et al.*, “S1222a—the largest marsquake detected by insight,” *Geophysical Research Letters*, vol. 50, no. 5, p. e2022GL101543, 2023.
- [35] B. Kégl, “Intrinsic dimension estimation using packing numbers,” *Advances in neural information processing systems*, vol. 15, 2002.
- [36] M. Lanthier, A. Maheshwari, and J.-R. Sack, “Approximating shortest paths on weighted polyhedral surfaces,” *Algorithmica*, vol. 30, no. 4, pp. 527–562, 2001.
- [37] H. Li and Z. Huang, “82 die in sichuan quake, rescuers race against time to save lives,” 2022. [Online]. Available: <https://www.chinadailyhk.com/article/289413#82-die-in-Sichuan-quake-rescuers-race-against-time-to-save-lives>
- [38] L. Liu and R. C.-W. Wong, “Finding shortest path on land surface,” in *Proceedings of the ACM SIGMOD International Conference on Management of data*, 2011, pp. 433–444.
- [39] N. McCarthy, “Exploring the red planet is a costly undertaking,” 2021. [Online]. Available: <https://www.statista.com/chart/24232/life-cycle-costs-of-mars-missions/>
- [40] J. S. Mitchell, D. M. Mount, and C. H. Papadimitriou, “The discrete geodesic problem,” *SIAM Journal on Computing*, vol. 16, no. 4, pp. 647–668, 1987.
- [41] D. Mo and S. Luo, “Agenda: robust personalized pageranks in evolving graphs,” in *Proceedings of the 30th ACM International Conference on Information & Knowledge Management*, 2021, pp. 1315–1324.
- [42] J. E. Nichol, A. Shaker, and M.-S. Wong, “Application of high-resolution stereo satellite images to detailed landslide hazard assessment,” *Geomorphology*, vol. 76, no. 1–2, pp. 68–75, 2006.
- [43] B. Padlewski, “Connected spaces,” *Formalized Mathematics*, vol. 1, no. 1, pp. 239–244, 1990.
- [44] R. Pallardy, “2010 haiti earthquake,” 2023. [Online]. Available: <https://www.britannica.com/event/2010-Haiti-earthquake>
- [45] S. Pan and M. Li, “Construction of earthquake rescue model based on hierarchical voronoi diagram,” *Mathematical Problems in Engineering*, vol. 2020, pp. 1–13, 2020.
- [46] D. Peleg and J. D. Ullman, “An optimal synchronizer for the hypercube,” in *Proceedings of the sixth annual ACM Symposium on Principles of distributed computing*, 1987, pp. 77–85.
- [47] K. Pletcher and J. P. Rafferty, “Sichuan earthquake of 2008,” 2023. [Online]. Available: <https://www.britannica.com/event/Sichuan-earthquake-of-2008>
- [48] C. Shahabi, L.-A. Tang, and S. Xing, “Indexing land surface for efficient knn query,” *Proceedings of the VLDB Endowment*, vol. 1, no. 1, pp. 1020–1031, 2008.
- [49] H. Shpungin and M. Segal, “Near-optimal multicriteria spanner constructions in wireless ad hoc networks,” *IEEE/ACM Transactions on Networking*, vol. 18, no. 6, pp. 1963–1976, 2010.
- [50] G. Sun, G. Liu, Y. Wang, and X. Zhou, “Updates-aware graph pattern based node matching,” in *2020 IEEE 36th International Conference on Data Engineering (ICDE)*. IEEE, 2020, pp. 697–708.
- [51] P. Von Rickenbach and R. Wattenhofer, “Gathering correlated data in sensor networks,” in *Proceedings of the joint workshop on Foundations of mobile computing*, 2004, pp. 60–66.
- [52] V. J. Wei, R. C.-W. Wong, C. Long, D. Mount, and H. Samet, “Proximity queries on terrain surface,” *ACM Transactions on Database Systems*, vol. 47, no. 4, pp. 1–59, 2022.

- [53] V. J. Wei, R. C.-W. Wong, C. Long, and D. M. Mount, “Distance oracle on terrain surface,” in *Proceedings of the 2017 ACM International Conference on Management of Data*, 2017, pp. 1211–1226.
- [54] S.-Q. Xin and G.-J. Wang, “Improving chen and han’s algorithm on the discrete geodesic problem,” *ACM Transactions on Graphics*, vol. 28, no. 4, pp. 1–8, 2009.
- [55] S. Xing, C. Shahabi, and B. Pan, “Continuous monitoring of nearest neighbors on land surface,” *Proceedings of the VLDB Endowment*, vol. 2, no. 1, pp. 1114–1125, 2009.
- [56] D. Yan, Z. Zhao, and W. Ng, “Monochromatic and bichromatic reverse nearest neighbor queries on land surfaces,” in *Proceedings of the 21st ACM international conference on Information and knowledge management*, 2012, pp. 942–951.
- [57] Y. Yan and R. C.-W. Wong, “Path advisor: a multi-functional campus map tool for shortest path,” *Proceedings of the VLDB Endowment*, vol. 14, no. 12, pp. 2683–2686, 2021.
- [58] D. Yuan, P. Mitra, H. Yu, and C. L. Giles, “Updating graph indices with a one-pass algorithm,” in *Proceedings of the 2015 ACM SIGMOD International Conference on Management of Data*, 2015, pp. 1903–1916.

## APPENDIX A SUMMARY OF FREQUENT USED NOTATIONS

Table III shows a summary of frequent used notations.

TABLE III  
SUMMARY OF FREQUENT USED NOTATIONS

Notation	Meaning
$T_{bef}/T_{aft}$	The terrain surface before / after updates
$V/E/F$	The set of vertices / edges / faces of terrain surface
$L_{max}$	The length of the longest edge in $E$ of $T_{bef}$
$N$	The number of vertices of $T$
$\Delta V$	The updated vertices of $T_{bef}$ and $T_{aft}$
$\Delta E$	The updated edges of $T_{bef}$ and $T_{aft}$
$\Delta F$	The updated faces of $T_{bef}$ and $T_{aft}$
$P$	The set of POI
$n$	The number of vertices of $P$
$\Delta P$	The updated POIs on $T_{bef}$ and $T_{aft}$
$\Pi(s, t T)$	The exact shortest path between $s$ and $t$ on the surface of $T$
$ \Pi(s, t T) $	The distance of $\Pi(s, t T)$
$G'$	The <i>FU-Oracle</i> output graph
$G'.V/G'.E$	The set of vertices / edges of $G'$
$e'(u, v T)$	An edge between $u$ and $v$ in $G'.E$
$\Pi_{G'}(s, t T)$	The shortest path between $s$ and $t$ in $G'$
$ \Pi_{G'}(s, t T) $	The distance of $\Pi_{G'}(s, t T)$
$\epsilon$	The error parameter
$G$	The temporary complete graph
$G.V/G.E$	The set of vertices / edges of $G$
$e(u, v T)$	An edge between $u$ and $v$ in $G.E$
$\Pi(u)$	A set of the exact shortest paths stored in $G$ on $T_{bef}$ with $u$ as an endpoint and $v_i \in P_{remain} \setminus u$ , $i \in \{1, l\}$ as the other endpoint, such that all these paths has not been updated
$P_{remain}$	A set of remaining POIs of $P$ on $T_{aft}$ that we have not processed
$D$	The longest edge’s weight in $G.E$
$Q_{G'}$	A group of vertices in $G'$ on $H$
$e_H(u, v T)$	An edge between $u$ and $v$ in $H$
$\Pi_H(s, t T)$	The shortest path of inter-edges between $s$ and $t$ in $H$

## APPENDIX B COMPARISON OF ALL ALGORITHMS

Table IV shows a comparison of all algorithms in terms of the oracle construction time, oracle update time, output size and shortest path query time.

## APPENDIX C V2V QUERY

Apart from the P2P query that we discussed in the main body of this paper, we also present an oracle to answer the V2V query based on our oracle *FU-Oracle*. This adapted oracle is similar to the one presented in Section IV, the only difference is that we need to create POIs which has the same coordinate values as vertices in  $V$ , then *FU-Oracle* can answer the V2V query. In this case, the number of POI becomes  $N$ . Thus, for the V2V query, the oracle construction time, oracle update time, output size and shortest path query time of *FU-Oracle* that answers the V2V query are  $O(N^2 \log^2 N)$ ,  $O(N \log^2 N)$ ,  $O(N)$  and  $O(\log N)$ , respectively. *FU-Oracle* satisfies  $|\Pi_{G'}(u, v|T)| \leq (1 + \epsilon)|\Pi(u, v|T)|$  for all pairs of vertices  $u$  and  $v$  in  $V$ .

## APPENDIX D A2A QUERY

Apart from the P2P query that we discussed in the main body of this paper, we also present an oracle to answer the A2A query based on our oracle *FU-Oracle*. This adapted oracle is similar to the one presented in Section IV, the only difference is that we need to use Steiner points as input instead of using POIs as input, where the Steiner points are introduced using the method in [24]. Specifically, work [24] places some Steiner points on the terrain surface (there are total  $O(\frac{N}{\sin \theta \sqrt{\epsilon}} \log \frac{1}{\epsilon})$  Steiner points, where  $\theta$  means the minimum inner angle of any face), and by using these Steiner points as input, we follow the construction phase and the update phase of *FU-Oracle* for oracle construction and update. For the query phase, given two arbitrary points  $u$  and  $v$ , we first find the neighborhood of  $u$  (resp.  $v$ ), denoted by  $\mathcal{N}(u)$  (resp.  $\mathcal{N}(v)$ ), which is a set of Steiner points on the same face containing  $u$  (resp.  $v$ ) and its adjacent faces [24]. Then, we return  $\Pi_{G'}(u, v|T) = \min_{p \in \mathcal{N}(u), q \in \mathcal{N}(v)} [\Pi(u, p|T) + \Pi_{G'}(p, q|T) + \Pi(q, v|T)]$ , where  $\Pi(u, p|T)$  and  $\Pi(q, v|T)$  can be calculated in  $O(1)$  time using algorithm *SSAD* and  $\Pi_{G'}(p, q|T)$  is the distance between  $p$  and  $q$  returned by *FU-Oracle*. According to work [24],  $|\mathcal{N}(u)| \cdot |\mathcal{N}(v)| = \frac{1}{\sin \theta \epsilon}$ , and if  $|\Pi_{G'}(p, q|T)| \leq (1 + \epsilon)|\Pi(p, q|T)|$ , then  $|\Pi_{G'}(u, v|T)| \leq (1 + \epsilon)|\Pi(u, v|T)|$ . Thus, for the A2A query, by setting  $n = \frac{N}{\sin \theta \sqrt{\epsilon}} \log \frac{1}{\epsilon}$  in the original *FU-Oracle* that answers the P2P query, we obtain that the oracle construction time, oracle update time, output size and shortest path query time of *FU-Oracle* that answers the A2A query are  $O(\frac{N^2 \log^2 N}{\sin \theta \sqrt{\epsilon}} \log \frac{1}{\epsilon})$ ,  $O(N \log^2 N) + \frac{N}{\sin \theta \sqrt{\epsilon}} \log \frac{1}{\epsilon} \log^2(\frac{N}{\sin \theta \sqrt{\epsilon}} \log \frac{1}{\epsilon})$ ,  $O(\frac{N}{\sin \theta \sqrt{\epsilon}} \log \frac{1}{\epsilon})$  and  $O(\log(\frac{N}{\sin \theta \sqrt{\epsilon}} \log \frac{1}{\epsilon}))$ , respectively. *FU-Oracle* satisfies  $|\Pi_{G'}(u, v|T)| \leq (1 + \epsilon)|\Pi(u, v|T)|$  for all pairs of arbitrary points  $u$  and  $v$  on  $T$ .

## APPENDIX E P2P QUERY IN THE CASE $n > N$

Apart from the P2P query when  $n \leq N$  that we discussed in the main body of this paper, we also present an oracle to



TABLE IV  
COMPARISON OF ALGORITHMS WITH DETAILS

Algorithm	Oracle construction time		Oracle update time		Output size		Shortest path query time	
<b>Oracle-based algorithm</b>								
<i>WSPD-Oracle</i> [52], [53]	$O(\frac{nN \log^2 N}{\epsilon^{2\beta}} + \frac{nh}{\epsilon^{2\beta}} + nh \log n)$	Large	$O(\frac{nN \log^2 N}{\epsilon^{2\beta}} + \frac{nh}{\epsilon^{2\beta}} + nh \log n)$	Large	$O(\frac{nh}{\epsilon^{2\beta}})$	Large	$O(h^2)$	Small
<i>WSPD-Oracle-Adapt</i> [52], [53]	$O(\frac{nN \log^2 N}{\epsilon^{2\beta}} + \frac{nh}{\epsilon^{2\beta}} + nh \log n)$	Large	$O(\mu_1 N \log^2 N + n \log^2 n)$	Large	$O(n)$	Small	$O(\log n)$	Small
<i>EAR-Oracle</i> [29]	$O(\lambda \xi m N \log^2(mN) + \frac{nN \log^2 N}{\epsilon^{2\beta}} + \frac{Nh}{\epsilon^{2\beta}} + Nh \log N)$	Large	$O(\lambda \xi m N \log^2(mN) + \frac{nN \log^2 N}{\epsilon^{2\beta}} + \frac{Nh}{\epsilon^{2\beta}} + Nh \log N)$	Large	$O(\frac{\lambda m N}{\epsilon^{2\beta}})$	Large	$O(\lambda \xi \log(\lambda \xi))$	Medium
<i>EAR-Oracle-Adapt</i> [29]	$O(\lambda \xi m N \log^2(mN) + \frac{nN \log^2 N}{\epsilon^{2\beta}} + \frac{Nh}{\epsilon^{2\beta}} + Nh \log N)$	Large	$O(\mu_2 N \log^2 N + n \log^2 n)$	Large	$O(n)$	Small	$O(\log n)$	Small
<i>FU-Oracle-RanUpdSeq</i>	$O(nN \log^2 N)$	Small	$O(nN \log^2 N + n \log^2 n)$	Large	$O(n)$	Small	$O(\log n)$	Small
<i>FU-Oracle-FullRad</i>	$O(nN \log^2 N)$	Small	$O(\mu_3 N \log^2 N + n \log^2 n)$	Medium	$O(n)$	Small	$O(\log n)$	Small
<i>FU-Oracle-NoDistAppr</i>	$O(nN \log^2 N)$	Small	$O(nN \log^2 N + n \log^2 n)$	Large	$O(n)$	Small	$O(\log n)$	Small
<i>FU-Oracle-NoEffIntChe</i>	$O(nN \log^2 N)$	Small	$O(N \log^2 N + n^2)$	Medium	$O(n)$	Small	$O(\log n)$	Small
<i>FU-Oracle-NoEdgPru</i>	$O(nN \log^2 N + n^2)$	Small	$O(N \log^2 N + n)$	Small	$O(n^2)$	Large	$O(1)$	Small
<i>FU-Oracle-NoEffEdgPru</i> [13], [14]	$O(nN \log^2 N)$	Small	$O(N \log^2 N + n^3 \log n)$	Medium	$O(n)$	Small	$O(\log n)$	Small
<b><i>FU-Oracle</i> (ours)</b>	<b><math>O(nN \log^2 N)</math></b>	<b>Small</b>	<b><math>O(N \log^2 N + n \log^2 n)</math></b>	<b>Small</b>	<b><math>O(n)</math></b>	<b>Small</b>	<b><math>O(\log n)</math></b>	<b>Small</b>
<b>On-the-fly algorithm</b>								
<i>CH-Fly-Algo</i> [18]	-	N/A	-	N/A	-	N/A	$O(N^2)$	Large
<i>K-Fly-Algo</i> [32]	-	N/A	-	N/A	-	N/A	$O(\frac{t_{\max} N}{\epsilon t_{\min} \sqrt{1 - \cos \theta}} \log(\frac{t_{\max} N}{\epsilon t_{\min} \sqrt{1 - \cos \theta}}))$	Large

Remark:  $n < N$ ,  $h$  is the height of the compressed partition tree,  $\beta$  is the largest capacity dimension [35], [25],  $\mu_1$ ,  $\mu_2$  and  $\mu_3$  are data-dependent variables,  $\mu_1 \in [5, 20]$ ,  $\mu_2 \in [12, 45]$  and  $\mu_3 \in [5, 10]$  in our experiment.

answer the P2P query in the case  $n > N$  based on our oracle *FU-Oracle*. We adopt the same oracle for answering the A2A query, which is POI-independent. This oracle can answer not only the A2A query, but also the P2P query (no matter whether  $n \leq N$  or  $n > N$ ) and the V2V query, since the A2A query generalizes both the P2P query and the V2V query.

## APPENDIX F EMPIRICAL STUDIES

### A. Experimental Results on the P2P Query

(1) Figure 12 and Figure 13 show the ablation study on *SC* dataset with fewer and more POIs, respectively. (2) Figure 14, Figure 15, and Figure 16 show the result on the *TJ* dataset (with fewer POIs) when varying  $n$ ,  $\epsilon$ , and  $DS$ , respectively. (3) Figure 17, Figure 18, and Figure 19 show the result on the *SC* dataset (with fewer POIs) when varying  $n$ ,  $\epsilon$ , and  $DS$ , respectively. (4) Figure 8, Figure 20, and Figure 21 show the result on the *GI* dataset (with fewer POIs) when varying  $n$ ,  $\epsilon$ , and  $DS$ , respectively. (5) Figure 22, Figure 23, and Figure 24 show the result on the *AU* dataset (with fewer POIs) when varying  $n$ ,  $\epsilon$ , and  $DS$ , respectively. (6) Figure 25, Figure 26, and Figure 27 show the result on the *LH* dataset (with fewer POIs) when varying  $n$ ,  $\epsilon$ , and  $DS$ , respectively. (7) Figure 28, Figure 29, and Figure 30 show the result on the *VS* dataset (with fewer POIs) when varying  $n$ ,  $\epsilon$ , and  $DS$ , respectively. (8) Figure 31, Figure 32, and Figure 33 show the result on the *TJ* dataset (with more POIs) when varying  $n$ ,  $\epsilon$ , and  $DS$  (for scalability test), respectively. (9) Figure 34, Figure 35, and Figure 36 show the result on the *SC* dataset (with more POIs) when varying  $n$ ,  $\epsilon$ , and  $DS$  (for scalability test), respectively. (10) Figure 37, Figure 38, and Figure 39 show the result on the *GI* dataset (with more POIs) when varying  $n$ ,  $\epsilon$ , and  $DS$  (for

scalability test), respectively. (11) Figure 40, Figure 41, and Figure 42 show the result on the *AU* dataset (with more POIs) when varying  $n$ ,  $\epsilon$ , and  $DS$  (for scalability test), respectively. (12) Figure 43, Figure 44, and Figure 45 show the result on the *LH* dataset (with more POIs) when varying  $n$ ,  $\epsilon$ , and  $DS$  (for scalability test), respectively. (13) Figure 46, Figure 47, and Figure 48 show the result on the *VS* dataset (with more POIs) when varying  $n$ ,  $\epsilon$ , and  $DS$  (for scalability test), respectively.

1) **Ablation study:** In Figure 12 and Figure 13, we tested the 5 values of  $n$  in  $\{50, 100, 150, 200, 250\}$  on *SC* dataset while fixing  $\epsilon$  at 0.1 and  $DS$  at 0.5M for ablation study involving 6 variations and *FU-Oracle*, and the 5 values of  $n$  in  $\{500, 1000, 1500, 2000, 2500\}$  on *SC* dataset while fixing  $\epsilon$  at 0.25 and  $DS$  at 0.5M for ablation study involving *FU-Oracle-X*, where  $X = \{NoEffIntChe, NoEdgPru, NoEffEdgPru\}$  and *FU-Oracle*, respectively. The oracle update time for *FU-Oracle-X*, where  $X = \{RanUpdSeq, FullRad, NoDistAppr, NoEffIntChe, NoEffEdgPru\}$  exceed that of *FU-Oracle*. Although the oracle update time and the shortest path query time of *FU-Oracle-NoEdgPru* is slightly smaller than that of *FU-Oracle*, the output size for *FU-Oracle-NoEdgPru* is  $10^4$  times larger than *FU-Oracle*. Thus, *FU-Oracle* is the best oracle among these variations.

2) **Baseline comparisons:** Starting from this subsection, we compare different baselines with *FU-Oracle*. We study the effect of  $\epsilon$ ,  $n$ , and the dataset size in this subsection.

**Effect of  $\epsilon$ .** In Figure 14, Figure 17, Figure 8, Figure 22, Figure 25 and Figure 28, we tested the 6 values of  $\epsilon$  in  $\{0.05, 0.1, 0.25, 0.5, 0.75, 1\}$  on *TJ*, *SC*, *GI*, *AU*, *LH* and *VS* datasets (with fewer POIs) while fixing  $n$  at 50 and  $DS$  at 0.5M. In Figure 31, Figure 34, Figure 37, Figure 40, Figure 43 and Figure 46, we tested the 6 values of  $\epsilon$  in

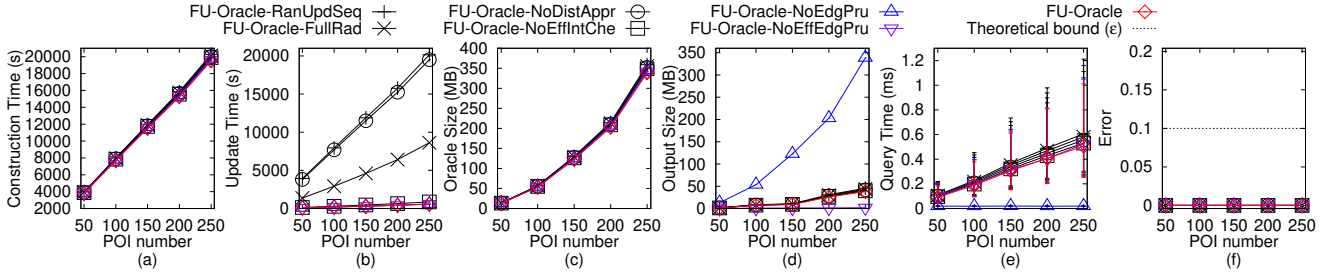


Fig. 12. Ablation study on SC dataset with fewer POIs for the P2P query

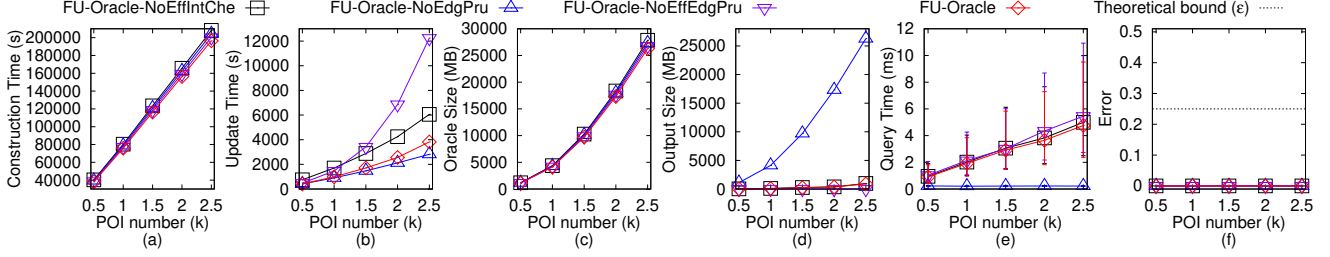


Fig. 13. Ablation study on SC dataset with more POIs for the P2P query

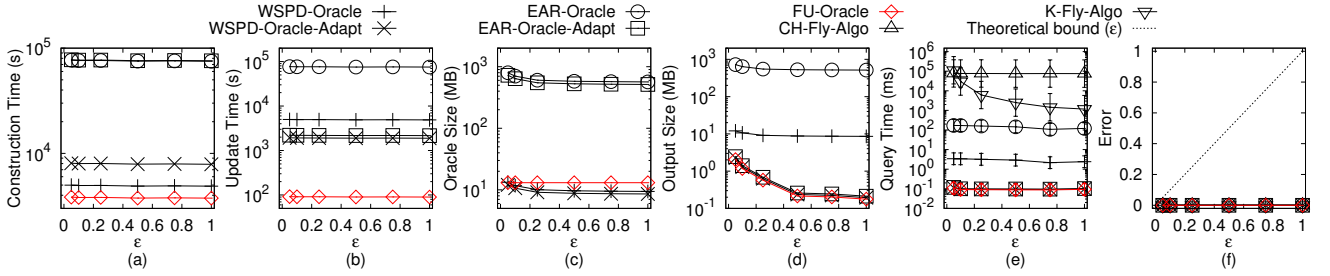


Fig. 14. Baseline comparisons (effect of  $\epsilon$  on TJ dataset with fewer POIs for the P2P query)

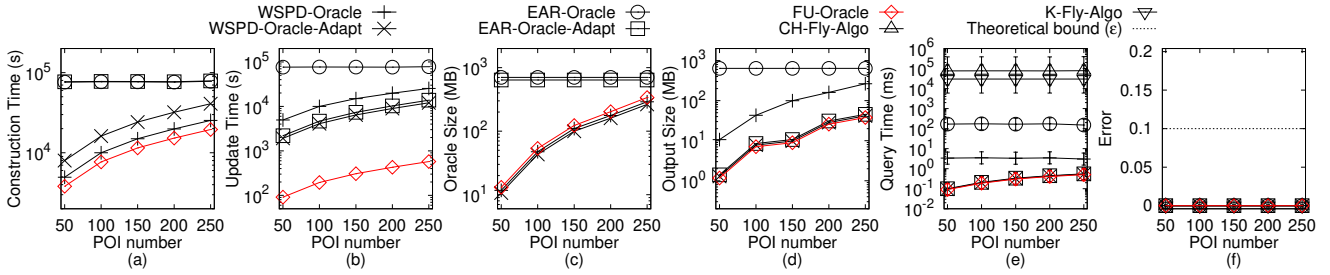


Fig. 15. Baseline comparisons (effect of  $n$  on TJ dataset with fewer POIs for the P2P query)

$\{0.05, 0.1, 0.25, 0.5, 0.75, 1\}$  on TJ, SC, GI, AU, LH and VS datasets (with fewer POIs) while fixing  $n$  at 500 and  $DS$  at 0.5M. Although *FU-Oracle* and other baselines have the similar small error (close to 0%) which are much smaller than the theoretical bound, *FU-Oracle* offers superior performance over *WSPD-Oracle*, *WSPD-Oracle-Adapt*, *EAR-Oracle*, *EAR-Oracle-Adapt*, *CH-Fly-Algo*, and *K-Fly-Algo* in terms of the oracle construction time, oracle update time, output size and shortest path query time. Although the oracle size of *FU-Oracle* is slightly larger than that of *WSPD-Oracle* and *WSPD-Oracle-Adapt*, the oracle update time of *FU-Oracle* is 88 times and 21 times smaller than that of *WSPD-Oracle* and *WSPD-Oracle-Adapt*. Varying  $\epsilon$  has a small impact on the oracle

update time, since when  $n$  is small, the pairwise P2P exact shortest path update step dominates the sub-graph generation step, and the former step is independent of  $\epsilon$ .

**Effect of  $n$ .** In Figure 15, Figure 18, Figure 20, Figure 23, Figure 26 and Figure 29, we tested the 5 values of  $n$  in  $\{50, 100, 150, 200, 250\}$  on TJ, SC, GI, AU, LH and VS dataset while fixing  $\epsilon$  at 0.1 and  $DS$  at 0.5M. In Figure 32, Figure 35, Figure 38, Figure 41, Figure 44 and Figure 47, we tested the 5 values of  $n$  in  $\{500, 1000, 1500, 2000, 2500\}$  on TJ, SC, GI, AU, LH and VS datasets while fixing  $\epsilon$  at 0.25 and  $DS$  at 0.5M. The oracle update time, output size and shortest path query time of *FU-Oracle* remain better than those of the baselines. Specifically, the oracle update time of *FU-Oracle* is 21 times

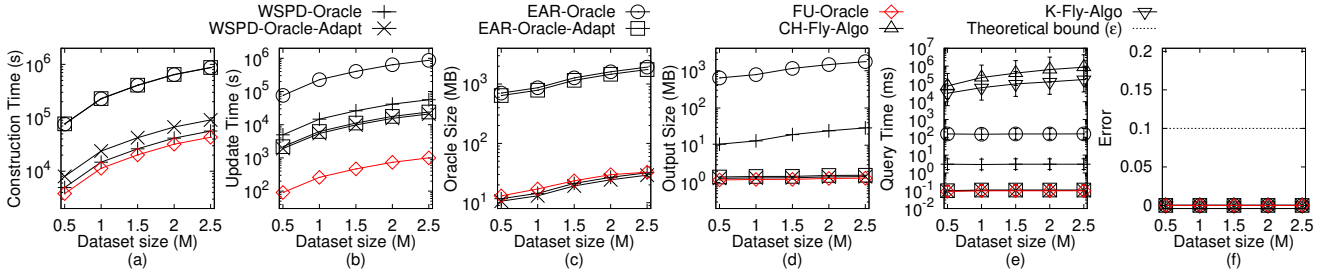


Fig. 16. Baseline comparisons (effect of  $DS$  on  $TJ$  dataset with fewer POIs for the P2P query)

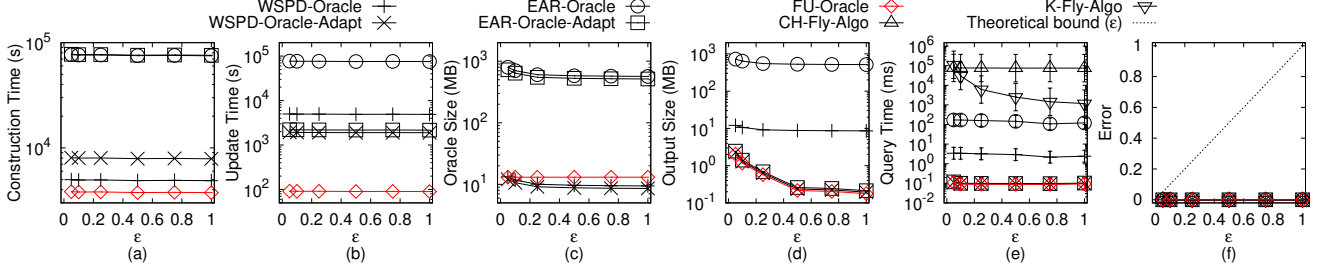


Fig. 17. Baseline comparisons (effect of  $\epsilon$  on  $SC$  dataset with fewer POIs for the P2P query)

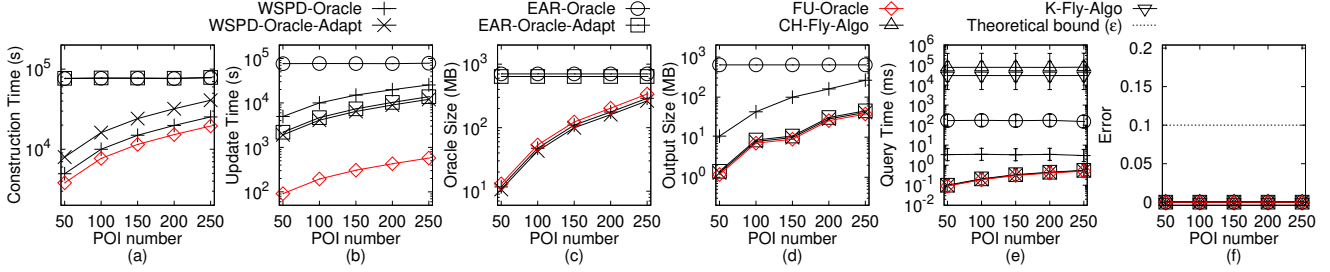


Fig. 18. Baseline comparisons (effect of  $n$  on  $SC$  dataset with fewer POIs for the P2P query)

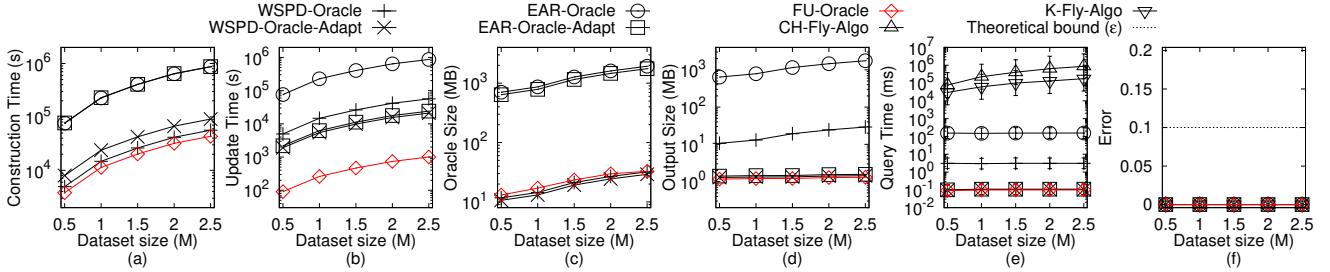


Fig. 19. Baseline comparisons (effect of  $DS$  on  $SC$  dataset with fewer POIs for the P2P query)

and 23 times smaller than that of *WSPD-Oracle-Adapt* and *EAR-Oracle-Adapt*.

**Effect of  $DS$ .** In Figure 16, Figure 19, Figure 21, Figure 24, Figure 27 and Figure 30, we tested the 5 values of  $DS$  in  $\{0.5M, 1M, 1.5M, 2M, 2.5M\}$  on  $TJ$ ,  $SC$ ,  $GI$ ,  $AU$ ,  $LH$  and  $VS$  datasets (with fewer POIs) while fixing  $\epsilon$  at 0.1 and  $n$  at 50. In Figure 33, Figure 36, Figure 39, Figure 42, Figure 45 and Figure 48, we tested 5 values of  $DS$  in  $\{0.5M, 1M, 1.5M, 2M, 2.5M\}$  on  $TJ$ ,  $SC$ ,  $GI$ ,  $AU$ ,  $LH$  and  $VS$  datasets (with more POIs) while fixing  $\epsilon$  at 0.25 and  $n$  at 500. Varying  $DS$  has a small impact on the shortest path query time of *FU-Oracle*, but has a large impact on that of *CH-Fly-Algo* and *K-Fly-Algo*. The shortest path query time of *FU-Oracle* is  $10^5$  times

smaller than that of *K-Fly-Algo*.

**3) Scalability test:** In Figure 33, Figure 36, Figure 39, Figure 42, Figure 45 and Figure 48, we tested 5 values of  $DS$  in  $\{0.5M, 1M, 1.5M, 2M, 2.5M\}$  on  $TJ$ ,  $SC$ ,  $GI$ ,  $AU$ ,  $LH$  and  $VS$  datasets (with more POIs) while fixing  $\epsilon$  at 0.25 and  $n$  at 500. The oracle update time and output size of *FU-Oracle* is scalable when  $DS$  is large. The shortest path query time of *FU-Oracle* is much smaller than that of *CH-Fly-Algo* and *K-Fly-Algo*.

### B. Experimental Results on the V2V Query

In Figure 49, we tested the V2V query by varying  $\epsilon$  from  $\{0.05, 0.1, 0.25, 0.5, 0.75, 1\}$  and fixing  $N$  at 2k on a multi-



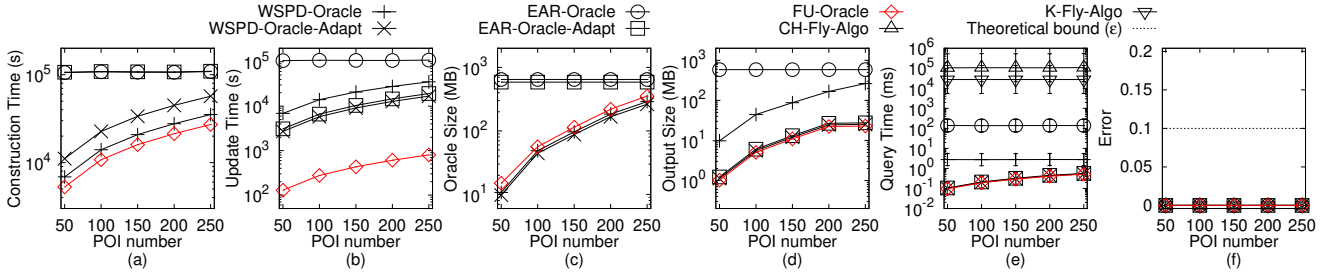


Fig. 20. Baseline comparisons (effect of  $n$  on  $GI$  dataset with fewer POIs for the P2P query)

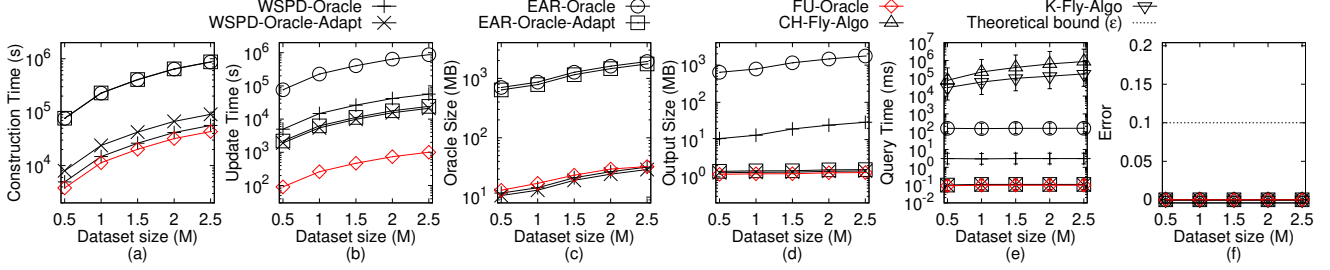


Fig. 21. Baseline comparisons (effect of  $DS$  on  $GI$  dataset with fewer POIs for the P2P query)

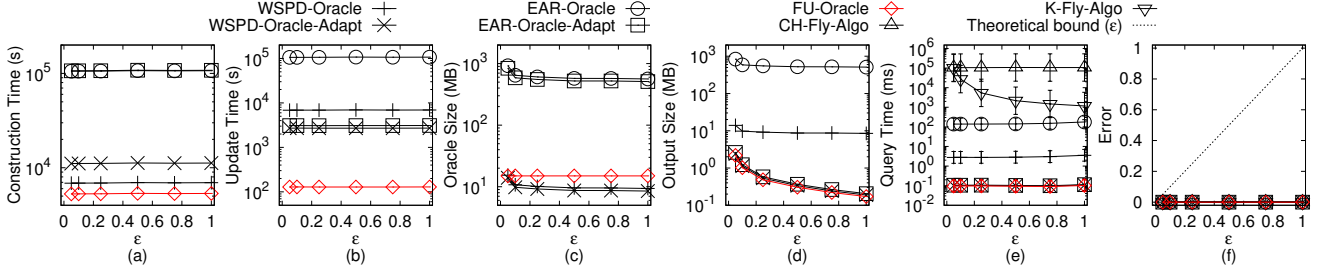


Fig. 22. Baseline comparisons (effect of  $\epsilon$  on  $AU$  dataset with fewer POIs for the P2P query)

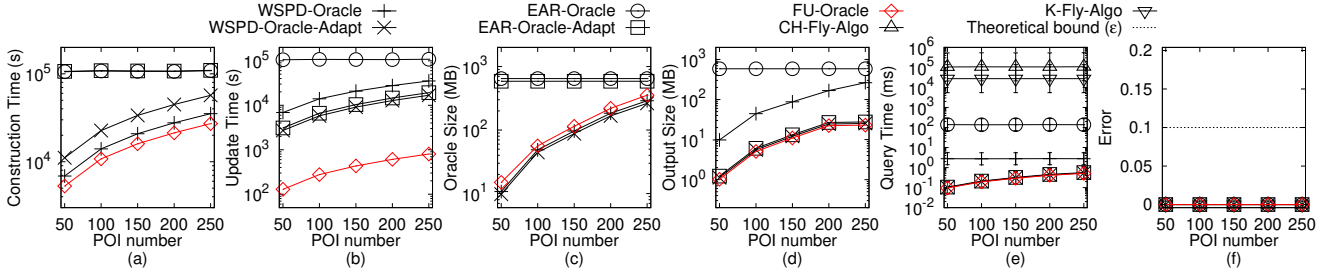


Fig. 23. Baseline comparisons (effect of  $n$  on  $AU$  dataset with fewer POIs for the P2P query)

resolution of  $SC$  dataset. It still shows that  $FU$ -Oracle superior performance of  $WSPD$ -Oracle,  $WSPD$ -Oracle-Adapt,  $EAR$ -Oracle,  $EAR$ -Oracle-Adapt,  $CH$ -Fly-Algo, and  $K$ -Fly-Algo in terms of the oracle construction time, oracle update time, output size and shortest path query time. This is because the V2V query is similar to the P2P query.

### C. Experimental Results on the P2P Query in the Case $n > N$ and the A2A Query

In Figure 50, we tested the P2P query in the case  $n > N$  and the A2A query by varying  $\epsilon$  from  $\{0.05, 0.1, 0.25, 0.5, 0.75, 1\}$  and fixing  $N$  at 2k on a multi-resolution of  $SC$  dataset. It still shows that  $FU$ -Oracle superior performance of  $WSPD$ -Oracle,

$WSPD$ -Oracle-Adapt,  $EAR$ -Oracle,  $EAR$ -Oracle-Adapt,  $CH$ -Fly-Algo, and  $K$ -Fly-Algo in terms of the oracle construction time, oracle update time, output size and shortest path query time. For  $EAR$ -Oracle and  $EAR$ -Oracle-Adapt, although their oracle construction time is slightly smaller than  $FU$ -Oracle, their oracle update time is still large. Thus,  $FU$ -Oracle is still the best oracle for the P2P query in the case  $n > N$  and the A2A query.

### D. Generating Datasets with Different Dataset Sizes

The procedure for generating the datasets with different dataset sizes is as follows. We mainly follow the procedure for generating datasets with different dataset sizes in the

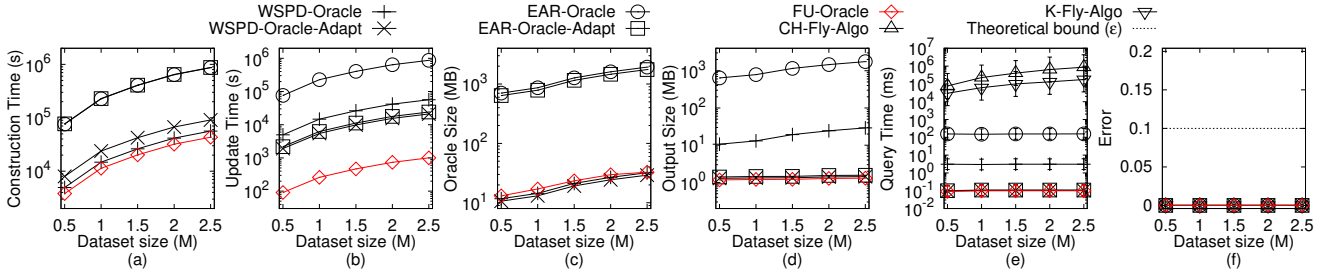


Fig. 24. Baseline comparisons (effect of  $DS$  on  $AU$  dataset with fewer POIs for the P2P query)

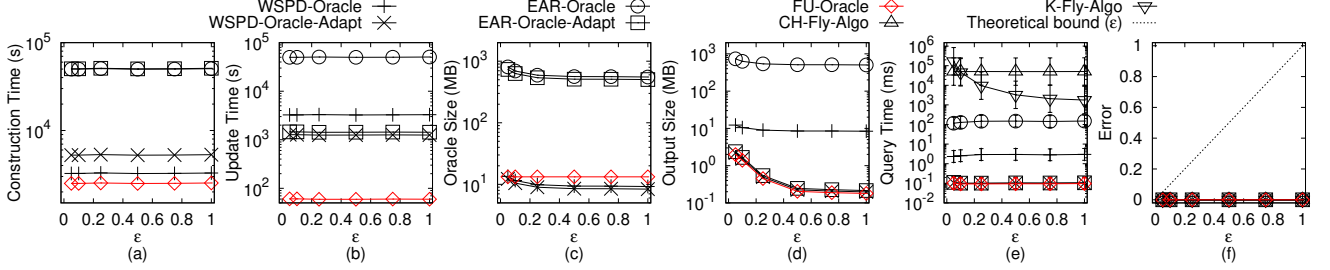


Fig. 25. Baseline comparisons (effect of  $\epsilon$  on  $LH$  dataset with fewer POIs for the P2P query)

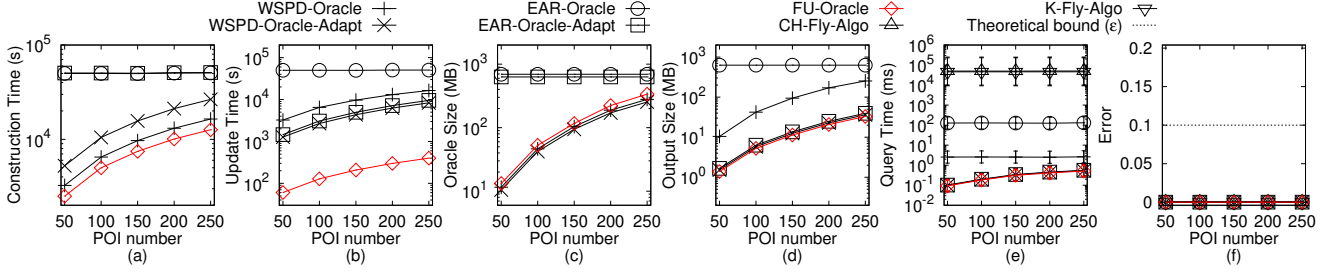


Fig. 26. Baseline comparisons (effect of  $n$  on  $LH$  dataset with fewer POIs for the P2P query)

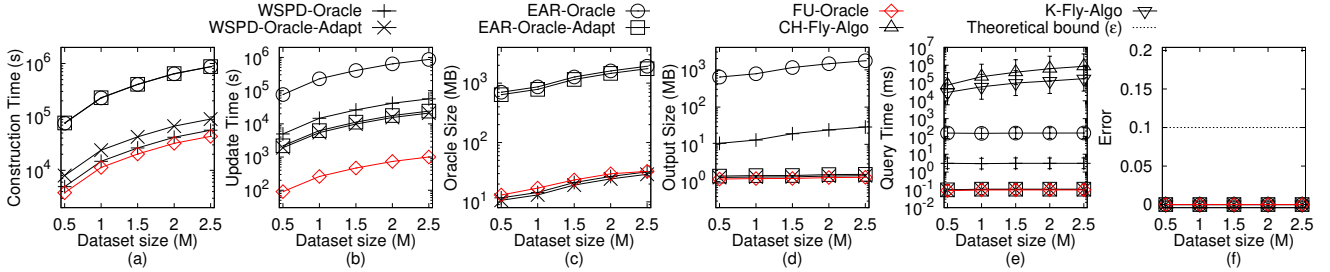


Fig. 27. Baseline comparisons (effect of  $DS$  on  $LH$  dataset with fewer POIs for the P2P query)

work [38], [52], [53]. Let  $T_t = (V_t, E_t, F_t)$  be our target terrain surface that we want to generate with  $ex_t$  edges along  $x$ -coordinate,  $ey_t$  edges along  $y$ -coordinate and dataset size of  $DS_t$ , where  $DS_t = 2 \cdot ex_t \cdot ey_t$ . Let  $T_o = (V_o, E_o, F_o)$  be the original terrain surface that we currently have with  $ex_o$  edges along  $x$ -coordinate,  $ey_o$  edges along  $y$ -coordinate and dataset size of  $DS_o$ , where  $DS_o = 2 \cdot ex_o \cdot ey_o$ . We then generate  $(ex_t + 1) \cdot (ey_t + 1)$  2D points  $(x, y)$  based on a Normal distribution  $N(\mu_N, \sigma_N^2)$ , where  $\mu_N = (\bar{x} = \frac{\sum_{v_o \in V_o} x_{v_o}}{(ex_o+1) \cdot (ey_o+1)}, \bar{y} = \frac{\sum_{v_o \in V_o} y_{v_o}}{(ex_o+1) \cdot (ey_o+1)})$  and  $\sigma_N^2 = (\frac{\sum_{v_o \in V_o} (x_{v_o} - \bar{x})^2}{(ex_o+1) \cdot (ey_o+1)}, \frac{\sum_{v_o \in V_o} (y_{v_o} - \bar{y})^2}{(ex_o+1) \cdot (ey_o+1)})$ . In the end, we project each generated point  $(x, y)$  to the surface of  $T_o$  and take the

projected point (also add edges between neighbours of two points to form edges and faces) as the newly generate  $T_t$ .

## APPENDIX G PROOF

*Proof of Property 1.* We prove by contradiction. Suppose that two disks  $D(u, \frac{|\Pi(u, v|T_{bef})|}{2})$  and  $D(v, \frac{|\Pi(u, v|T_{bef})|}{2})$  do not intersect with  $\Delta F$ , but  $\Pi(u, v|T_{aft})$  is different from  $\Pi(u, v|T_{bef})$ , and we need to update  $\Pi(u, v|T_{bef})$  to  $\Pi(u, v|T_{aft})$  due to the smaller distance of  $\Pi(u, v|T_{aft})$ , i.e.,  $|\Pi(u, v|T_{aft})| < |\Pi(u, v|T_{bef})|$ . This case will only happen when  $\Pi(u, v|T_{aft})$  passes  $\Delta F$ . We let  $u_1$  (resp.  $v_1$ ) be the point on  $\Pi(u, v|T_{aft})$  that the exact shortest distance  $\Pi(u, u_1|T)$  (resp.  $\Pi(v, v_1|T)$ )

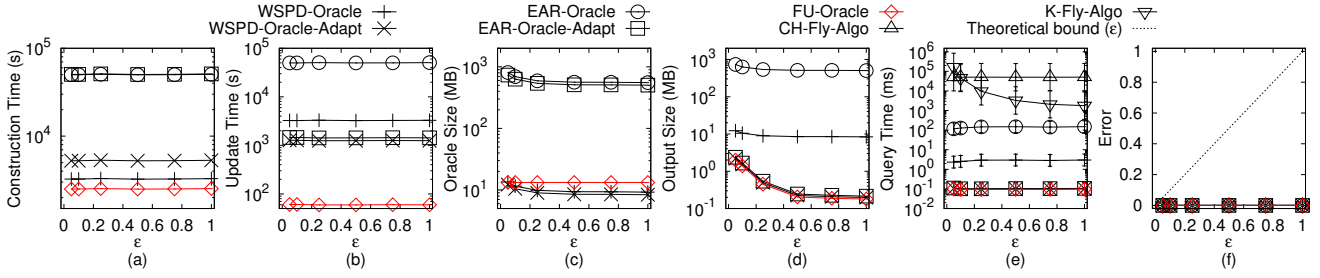


Fig. 28. Baseline comparisons (effect of  $\epsilon$  on VS dataset with fewer POIs for the P2P query)

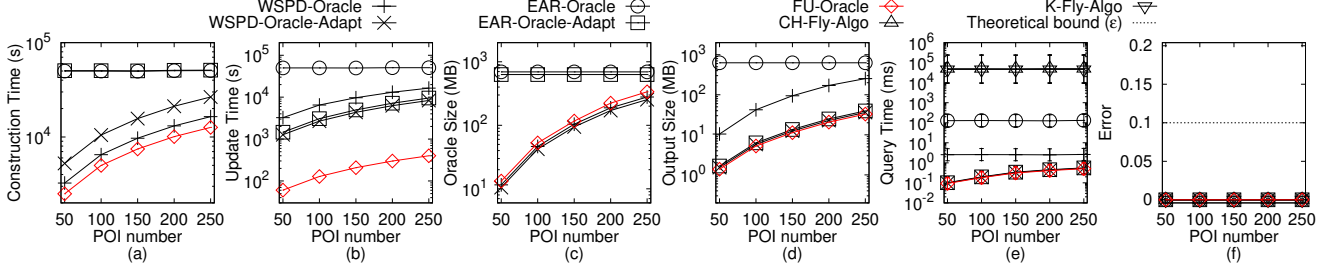


Fig. 29. Baseline comparisons (effect of  $n$  on VS dataset with fewer POIs for the P2P query)

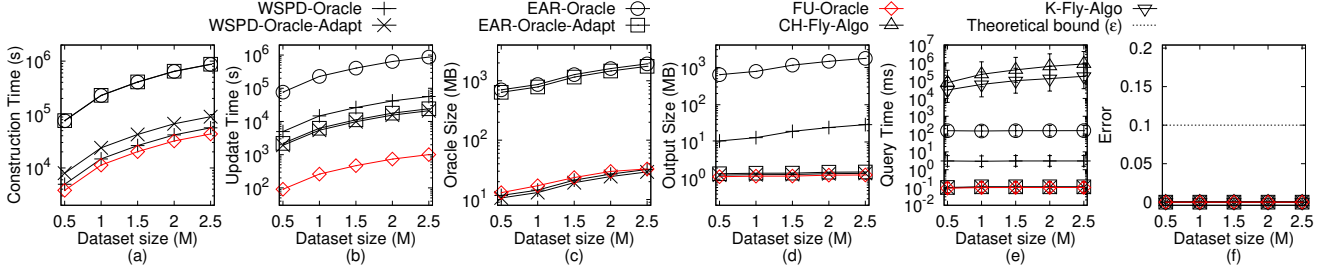


Fig. 30. Baseline comparisons (effect of  $DS$  on VS dataset with fewer POIs for the P2P query)

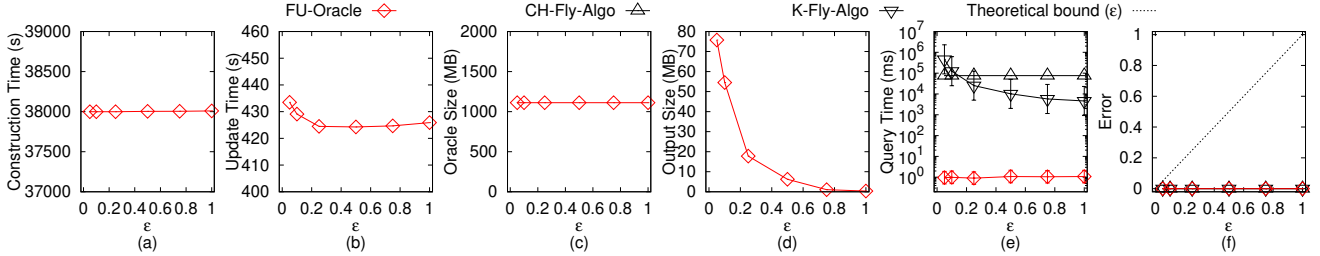


Fig. 31. Baseline comparisons (effect of  $\epsilon$  on TJ dataset with more POIs for the P2P query)

on  $T$  is the same as  $|\frac{\Pi(u,v|T_{bef})}{2}|$ . We let  $u_2$  (resp.  $v_2$ ) be the point on  $\Pi(u,v|T_{aft})$  that  $u_2$  (resp.  $v_2$ ) is a point in  $\Delta F$  and the exact shortest distance  $\Pi(u, u_2|T)$  (resp.  $\Pi(v, v_2|T)$ ) on  $T$  is the minimum one. Clearly,  $u_2$  (resp.  $v_2$ ) is the intersection point between  $\Pi(u,v|T_{aft})$  and  $\Delta F$ , such that the exact shortest distance  $\Pi(u, u_2|T)$  (resp.  $\Pi(v, v_2|T)$ ) on  $T$  is the minimum one. Note that a point is said to be in  $\Delta F$  if this point is on a face in  $\Delta F$ . We let  $o$  be the midpoint on  $\Pi(u,v|T_{bef})$ , clearly we have  $|\Pi(u, o|T)| = |\Pi(v, o|T)| = |\frac{\Pi(u,v|T_{bef})}{2}|$ . We also know that  $|\Pi(u, u_1|T)| = |\Pi(u, o|T)| = |\Pi(v, v_1|T)| = |\Pi(v, o|T)| = |\frac{\Pi(u,v|T_{bef})}{2}|$ . Figure 2 shows an example of these notations. The light blue line is  $\Pi(u, v|T_{bef})$  and the yellow line is  $\Pi(u, v|T_{aft})$ . Since the minimum distance

from both  $u$  and  $v$  to the updated faces  $\Delta F$  is no smaller than  $|\frac{\Pi(u,v|T_{bef})}{2}|$ , we know  $|\Pi(u, o|T)| = |\Pi(u, u_1|T)| \leq |\Pi(u, u_2|T)|$  and  $|\Pi(v, o|T)| = |\Pi(v, v_1|T)| \leq |\Pi(v, v_2|T)|$ . Since  $\Pi(u, v|T_{aft})$  passes  $\Delta F$ ,  $|\Pi(u_2, v_2|T_{aft})| \geq 0$ . Thus, we have  $|\Pi(u, u_2|T)| + |\Pi(v, v_2|T)| + |\Pi(u_2, v_2|T_{aft})| = |\Pi(u, v|T_{aft})| \geq |\Pi(u, v|T_{bef})| = |\Pi(u, o|T)| + |\Pi(v, o|T)|$ , which is a contradiction of our assumption  $|\Pi(u, v|T_{aft})| < |\Pi(u, v|T_{bef})|$ . Thus, we finish the proof.  $\square$

*Proof of Lemma 2.* According to [52], [53], since the exact shortest distance on a terrain surface is a metric, and therefore it satisfies the triangle inequality. Given an edge  $e$  which belongs to a face in  $\Delta F$  with two endpoints  $u_1$  and  $u_2$ ,



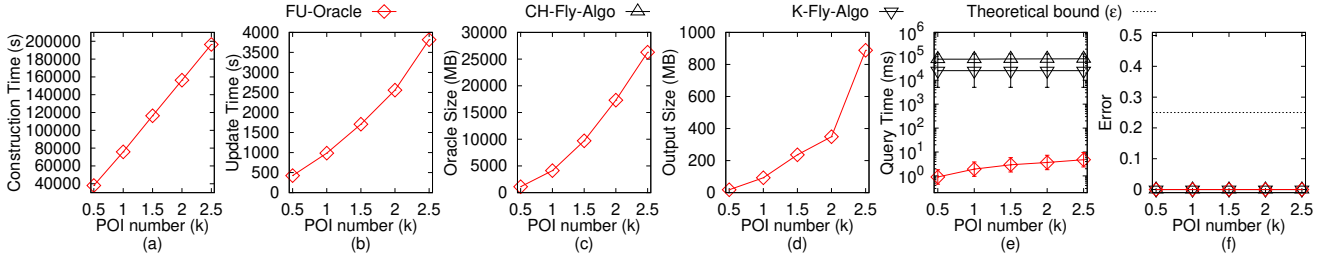


Fig. 32. Baseline comparisons (effect of  $n$  on  $TJ$  dataset with more POIs for the P2P query)

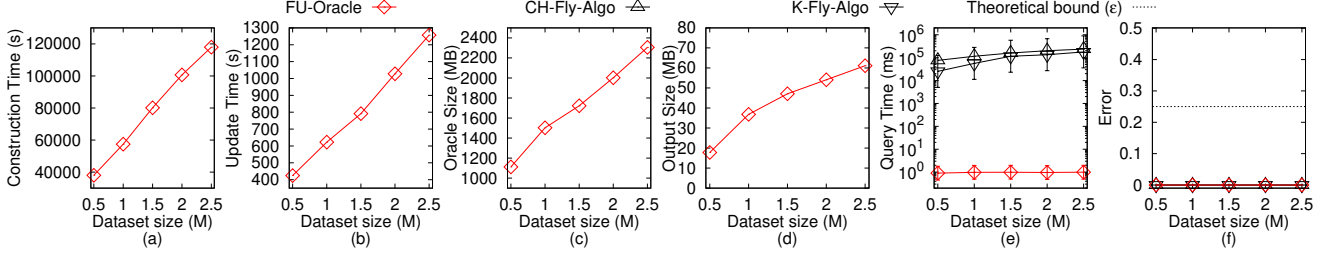


Fig. 33. Baseline comparisons (effect of  $DS$  on  $TJ$  dataset with more POIs for the P2P query) and scalability test on  $TJ$  dataset with more POIs for the P2P query

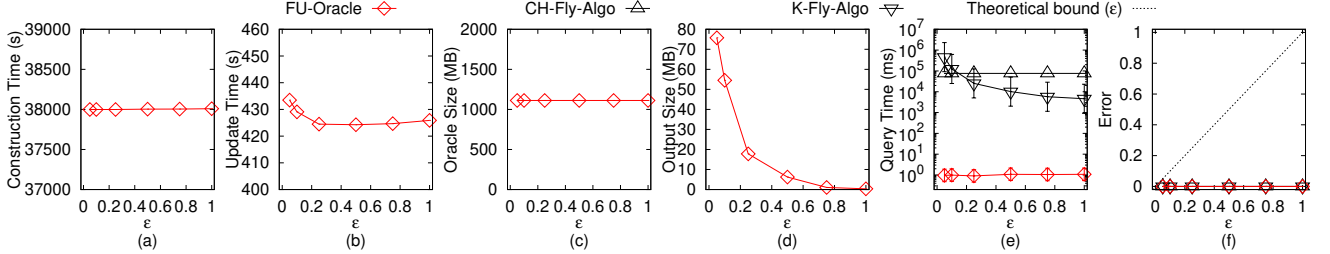


Fig. 34. Baseline comparisons (effect of  $\epsilon$  on  $SC$  dataset with more POIs for the P2P query)

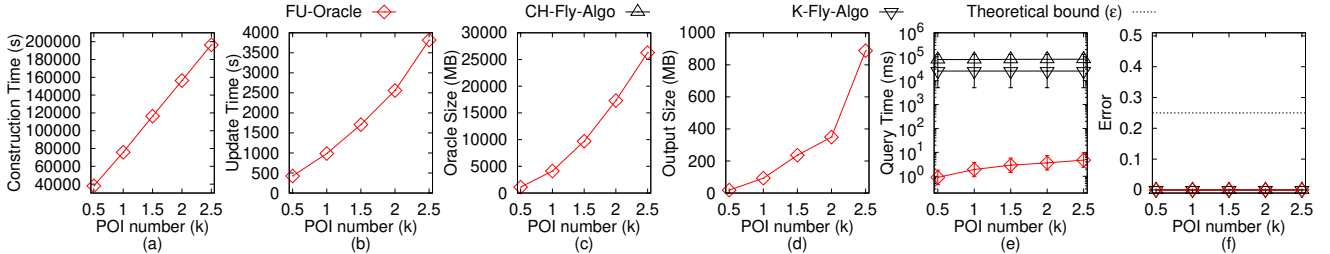


Fig. 35. Baseline comparisons (effect of  $n$  on  $SC$  dataset with more POIs for the P2P query)

suppose that the exact shortest path from  $u$  to  $\Delta F$  intersects with any point on  $e$  for the first time. There are two cases:

- If the intersection point is one of the two endpoints of  $e$  (e.g.,  $u_1$  without loss of generality), since  $u_1$  is a vertex of a face in  $\Delta F$ , so the minimum distance from  $u$  to  $\Delta F$  in non-updated faces of  $T_{aft}$  is the same as the exact shortest distance from  $u$  to  $u_1$  on  $T_{bef}$ . Since the exact shortest distance from  $u$  to  $u_1$  on  $T_{bef}$  is at least the minimum distance from  $u$  to any vertex in  $\Delta V$  on  $T_{bef}$ , we obtain that the minimum distance from  $u$  to  $\Delta F$  in non-updated faces of  $T_{aft}$  is at least the minimum distance from  $u$  to any vertex in  $\Delta V$  on  $T_{bef}$ .
- If the intersection point is on  $e$ , we denote this intersection point as  $u_3$ . Without loss of generality, suppose that the

exact shortest distance from  $u$  to  $u_1$  on  $T_{bef}$  minus  $|u_1u_3|$  is smaller than the exact shortest distance from  $u$  to  $u_2$  on  $T_{bef}$  minus  $|u_2u_3|$ , where  $|u_1u_3|$  (resp.  $|u_2u_3|$ ) is the length of the segment between  $u_1$  and  $u_3$  (resp. between  $u_2$  and  $u_3$ ) on edge  $e$ . According to triangle inequality, the minimum distance from  $u$  to  $\Delta F$  in non-updated faces of  $T_{aft}$  is at least the exact shortest distance from  $u$  to  $u_1$  on  $T_{aft}$  minus  $|u_1u_3|$ . Since we only care about the minimum distance, so the exact shortest distance from  $u$  to  $u_1$  on  $T_{aft}$  is the same as the exact shortest distance from  $u$  to  $u_1$  on  $T_{bef}$ . Since the exact shortest distance from  $u$  to  $u_1$  on  $T_{bef}$  is at least the minimum distance from  $u$  to any vertex in  $\Delta V$  on  $T_{bef}$  and  $|u_1u_3|$  is at most  $L_{max}$ , we obtain that the minimum distance from  $u$  to  $\Delta F$  in non-updated faces of  $T_{aft}$  is at

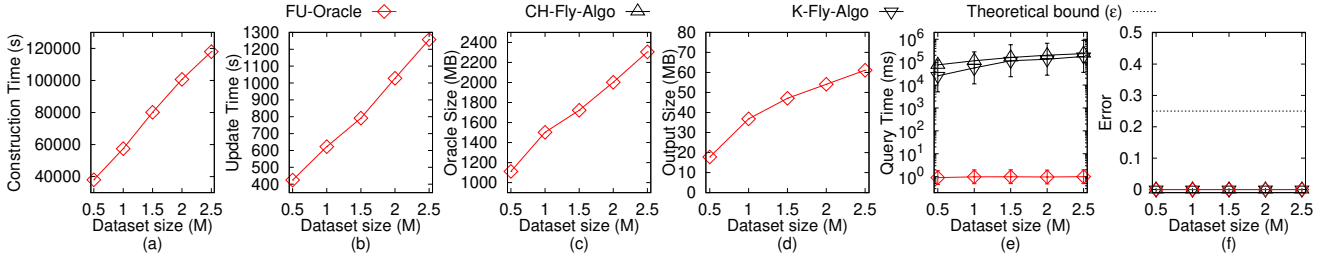


Fig. 36. Baseline comparisons (effect of  $DS$  on  $SC$  dataset with more POIs for the P2P query) and scalability test on  $SC$  dataset with more POIs for the P2P query

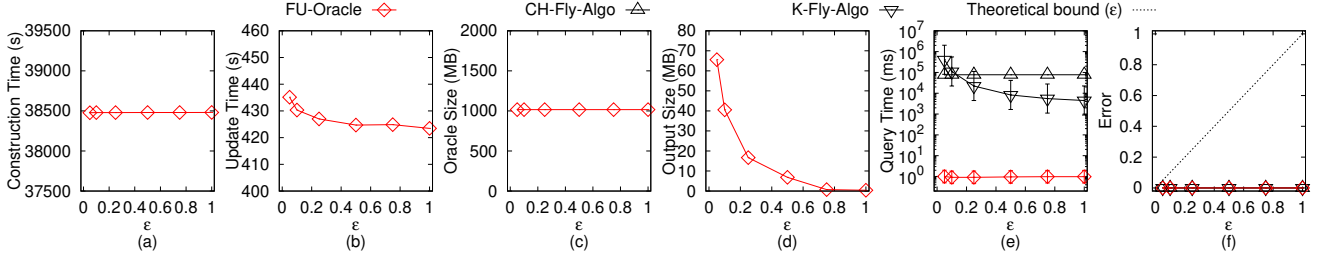


Fig. 37. Baseline comparisons (effect of  $\epsilon$  on  $GI$  dataset with more POIs for the P2P query)

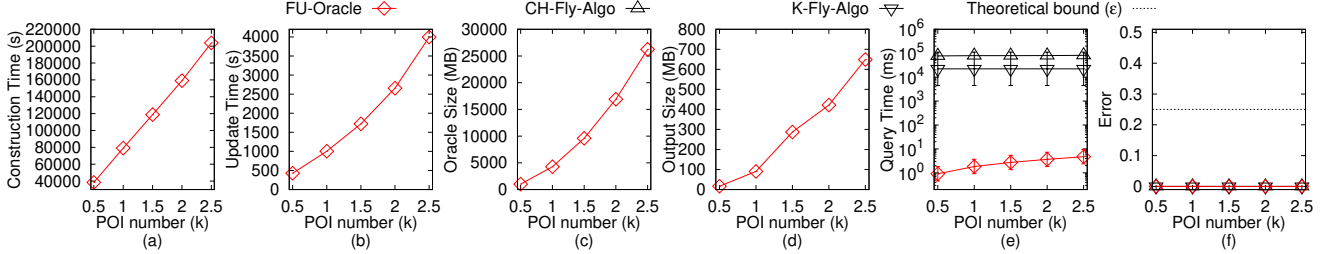


Fig. 38. Baseline comparisons (effect of  $n$  on  $GI$  dataset with more POIs for the P2P query)

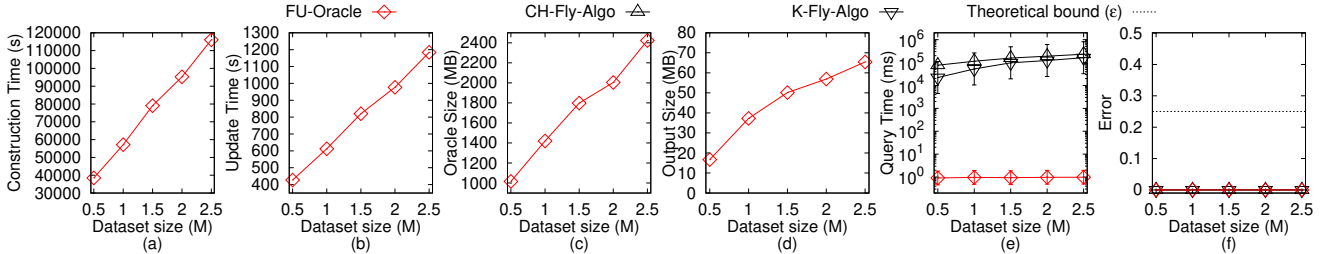


Fig. 39. Baseline comparisons (effect of  $DS$  on  $GI$  dataset with more POIs for the P2P query) and scalability test on  $GI$  dataset with more POIs for the P2P query

least the minimum distance from  $u$  to any vertex in  $\Delta V$  on  $T_{bef}$  minus  $L_{max}$ .

□

*Proof of Lemma 3.* If the disk with the largest radius intersects with  $\Delta F$ , we just need to update the paths and there is no need to check other disks. In Figure 4 (c), the sorted POIs are  $h, f, e, d, c, g$ . We create one disk  $D(h, \frac{|\Pi(c, h|T_{bef})|}{2})$ , since it intersects with  $\Delta F$ , we use algorithm SSAD to update all shortest paths adjacent to  $h$  that have not been updated. We do not need to create ten disks, i.e., five disks  $D(h, \frac{|\Pi(X, h|T_{bef})|}{2})$  and five disks  $D(X, \frac{|\Pi(X, f|T_{bef})|}{2})$ , where  $X = \{c, d, e, f, g, h\}$ . Since the disk  $D(h, \frac{|\Pi(c, h|T_{bef})|}{2})$  with the largest radius already

intersects with  $\Delta F$ , so there is no need to check other disks.

If the disk with the largest radius and with the center closest to  $\Delta F$  does not intersect with  $\Delta F$ , then other disks cannot intersect with  $\Delta F$ , so there is no need to update the paths. In Figure 4 (d), the sorted POIs are  $f, e, d, c, g$ . We create one disk  $D(f, \frac{|\Pi(c, f|T_{bef})|}{2})$ , since it does not intersect with  $\Delta F$ , there is no need to update shortest paths adjacent to  $f$ . We do not need to create eight disks, i.e., four disks  $D(f, \frac{|\Pi(X, f|T_{bef})|}{2})$  and four disks  $D(X, \frac{|\Pi(X, f|T_{bef})|}{2})$ , where  $X = \{c, d, e, f, g\}$ . Since the disk  $D(f, \frac{|\Pi(c, f|T_{bef})|}{2})$  with the largest radius does not intersect with  $\Delta F$ , so the disks  $D(f, \frac{|\Pi(X, f|T_{bef})|}{2})$  with smaller radius and the disks  $D(X, \frac{|\Pi(X, f|T_{bef})|}{2})$  with centers further away from  $\Delta F$  com-

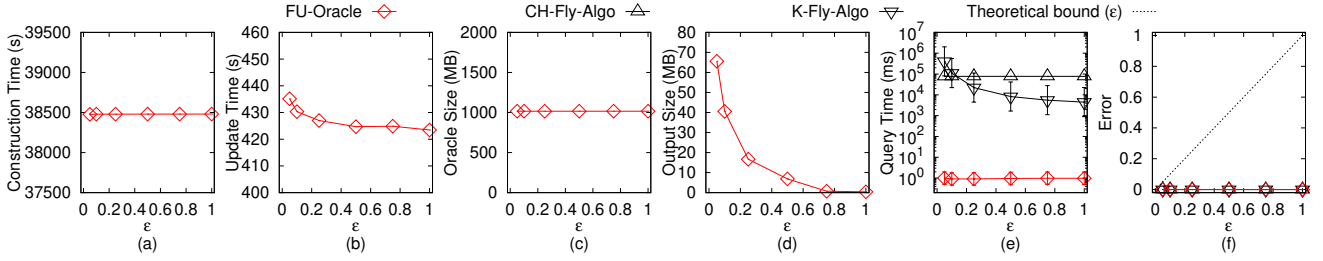


Fig. 40. Baseline comparisons (effect of  $\epsilon$  on AU dataset with more POIs for the P2P query)

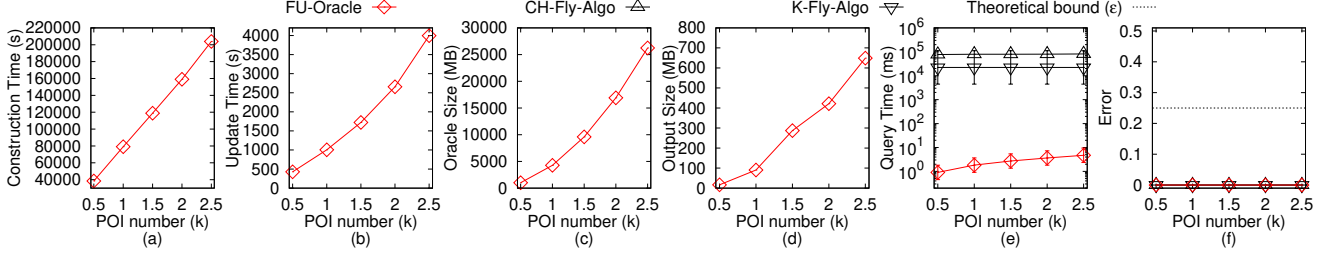


Fig. 41. Baseline comparisons (effect of  $n$  on AU dataset with more POIs for the P2P query)

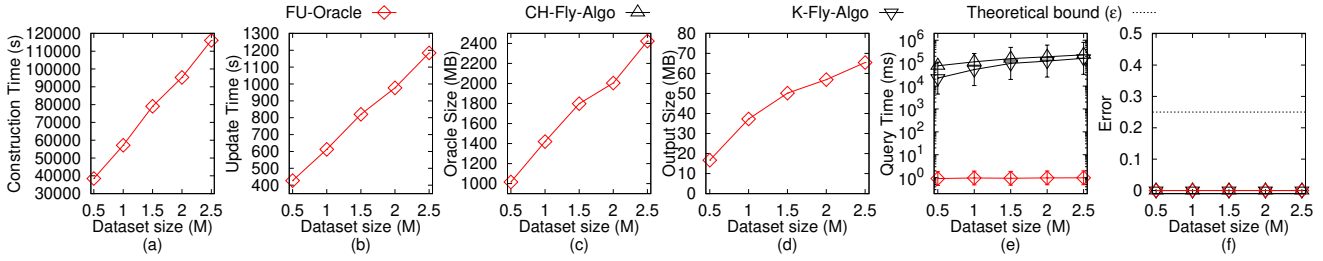


Fig. 42. Baseline comparisons (effect of  $DS$  on AU dataset with more POIs for the P2P query) and scalability test on AU dataset with more POIs for the P2P query

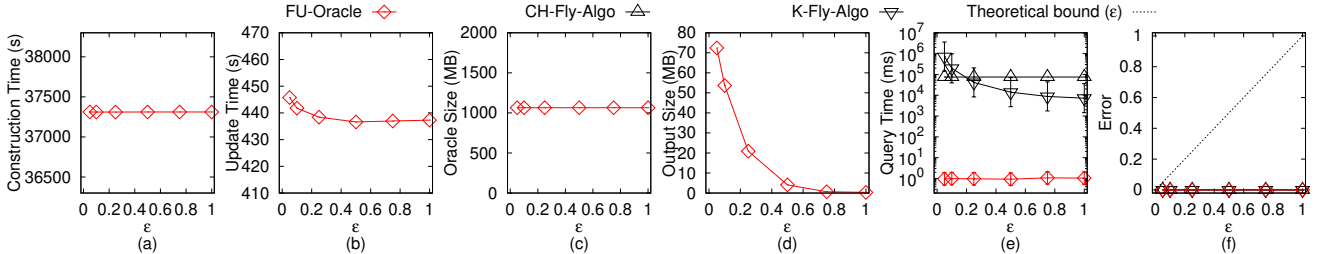


Fig. 43. Baseline comparisons (effect of  $\epsilon$  on LH dataset with more POIs for the P2P query)

pared with  $f$  cannot intersect with  $\Delta F$ . Recall that given a POI  $u$ , we use  $\min_{v \in \Delta V} |\Pi(u, v|T_{bef})| - L_{max}$  as the lower bound of the minimum distance from  $u$  to any point in  $\Delta F$  on  $T_{aft}$ . If  $D(f, \frac{|\Pi(c, f|T_{bef})|}{2})$  does not intersect with  $\Delta F$ , then  $\min_{v \in \Delta V} |\Pi(c, v|T_{bef})| - L_{max} > \frac{|\Pi(c, f|T_{bef})|}{2}$ , then  $\min_{v \in \Delta V} |\Pi(X, v|T_{bef})| - L_{max} > \frac{|\Pi(c, f|T_{bef})|}{2}$  (since we sort  $X$  from near to far according to their minimum distance to any vertex in  $\Delta V$  on  $T_{bef}$ ), and then  $\min_{v \in \Delta V} |\Pi(X, v|T_{bef})| - L_{max} > \frac{|\Pi(X, f|T_{bef})|}{2}$  (since  $|\Pi(c, f|T_{bef})| \geq |\Pi(X, f|T_{bef})|$ ), i.e., the disks  $D(X, \frac{|\Pi(X, f|T_{bef})|}{2})$  cannot intersect with  $\Delta F$ , where  $X = \{c, d, e, f, g\}$ .  $\square$

**Lemma 4.** After the pairwise P2P exact shortest path update step in the update phase of FU-Oracle,  $G$  stores the

correct exact shortest path between all pairs of POIs in  $P$  on  $T_{aft}$ .

*Proof of Lemma 4.* After the pairwise P2P exact shortest path update step, there are two types of pairwise P2P exact shortest paths stored in  $G$ , i.e., (1) the updated exact shortest paths calculated on  $T_{aft}$ , and (2) the non-updated exact shortest paths calculated on  $T_{bef}$ . Due to Property 1, we know that the non-updated exact shortest paths calculated on  $T_{bef}$  is exactly the same as the exact shortest path on  $T_{aft}$ . Thus, after the pairwise P2P exact shortest path update step in the update phase of FU-Oracle,  $G$  stores the correct exact shortest path between all pairs of POIs in  $P$  on  $T_{aft}$ .  $\square$

*Proof of Theorem 1.* Firstly, we prove the running time of



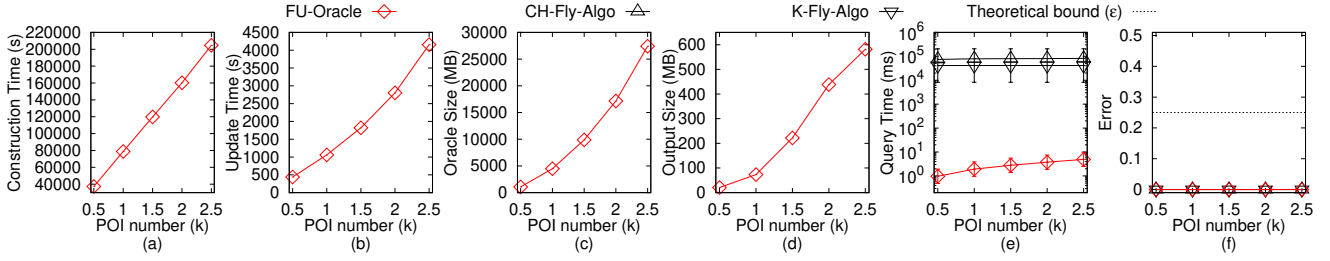


Fig. 44. Baseline comparisons (effect of  $n$  on  $LH$  dataset with more POIs for the P2P query)

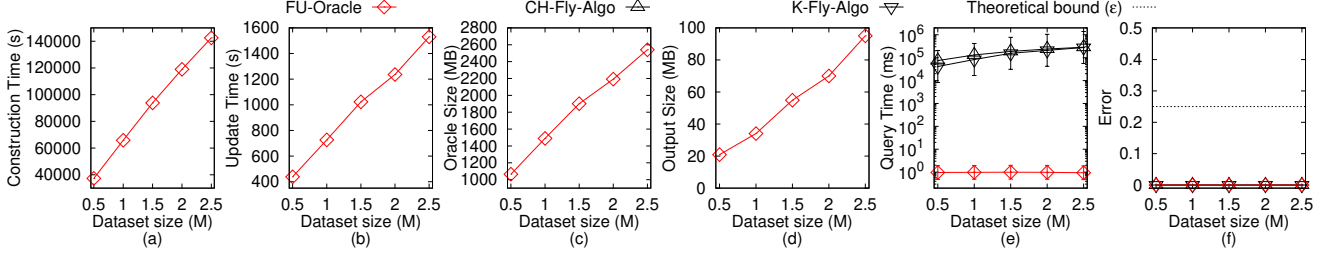


Fig. 45. Baseline comparisons (effect of  $DS$  on  $LH$  dataset with more POIs for the P2P query) and scalability test on  $LH$  dataset with more POIs for the P2P query

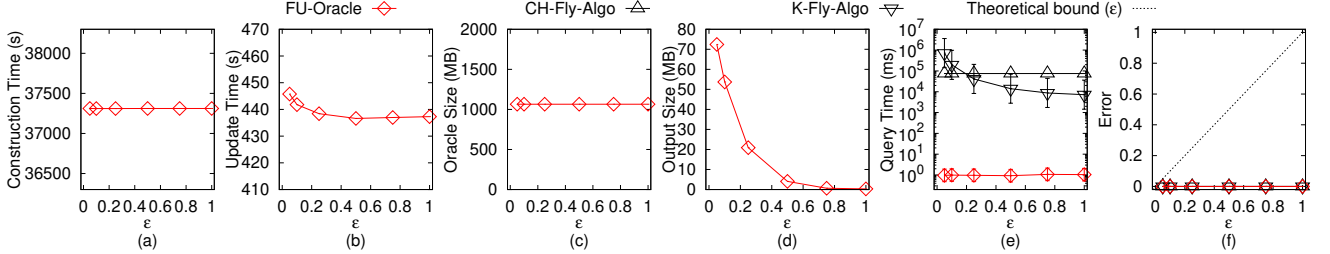


Fig. 46. Baseline comparisons (effect of  $\epsilon$  on  $VS$  dataset with more POIs for the P2P query)

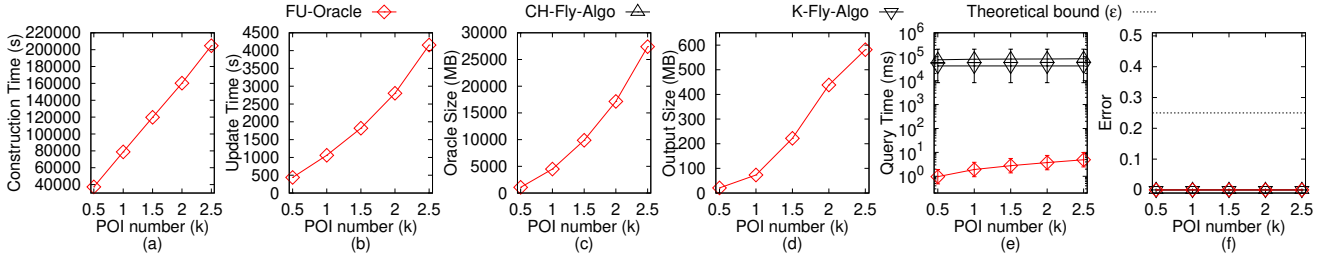


Fig. 47. Baseline comparisons (effect of  $n$  on  $VS$  dataset with more POIs for the P2P query)

algorithm *HieGreSpan*.

- In the edge sort, interval split, and  $G'$  initialization step, it needs  $O(n)$  time. Since we perform algorithm *SSAD* for each POI to generate  $G'$ , so given a POI, the distances between this POI and other POIs have already been sorted. Since there are  $n$  vertices in  $G$ , so this step needs  $O(n)$  time.
- In the  $G'$  maintenance step, for each edge interval, it needs  $O(n \log n + n) = O(n \log n)$  time (shown as follows). Since there are total  $\log n$  intervals, it needs  $O(n \log^2 n)$  time.
  - In the group construction and  $H$  intra-edge insertion step, it needs  $O(n \log n)$  time. This is because according to Lemma 6 in [20], we know that a vertex in  $H$  belongs to at most  $O(1)$  groups (i.e., there are at most  $O(1)$  group

centers in  $H$ ), so we just need to run  $O(n \log n)$  Dijkstra's algorithm on  $G'$  for  $O(1)$  times in order to calculate intra-edges for  $H$ .

- In the  $H$  first type inter-edge insertion step, it needs  $O(n \log n)$  time. This is still because there are at most  $O(1)$  group centers in  $H$ , so we just need to run  $O(n \log n)$  Dijkstra's algorithm on  $G'$  for  $O(1)$  times in order to calculate inter-edges for  $H$ .
- In the  $H$  edge examine step, it needs  $O(n)$  time. According to [20], there are  $O(n)$  edges in each interval. Since there are at most  $O(1)$  group centers in  $H$ , so answering the shortest path query using Dijkstra's algorithm on  $H$  needs  $O(1)$  time. So, in order to examine  $O(n)$  edges, this step needs  $O(1)$  Dijkstra's algorithm on  $H$  for  $O(n)$

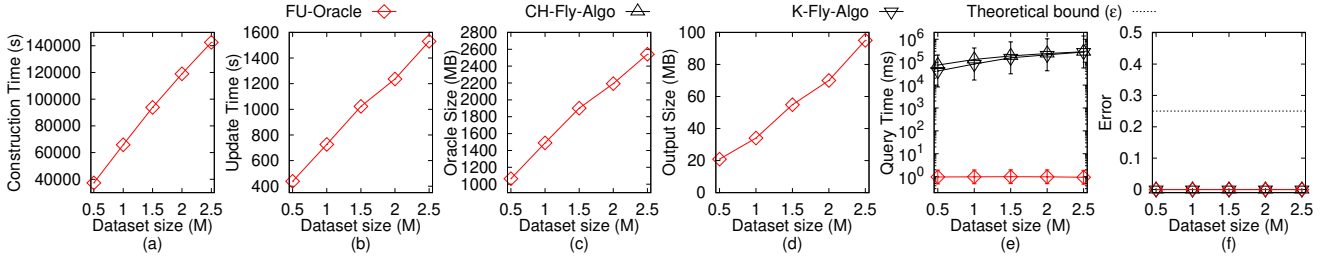


Fig. 48. Baseline comparisons (effect of  $DS$  on VS dataset with more POIs for the P2P query) and scalability test on VS dataset with more POIs for the P2P query

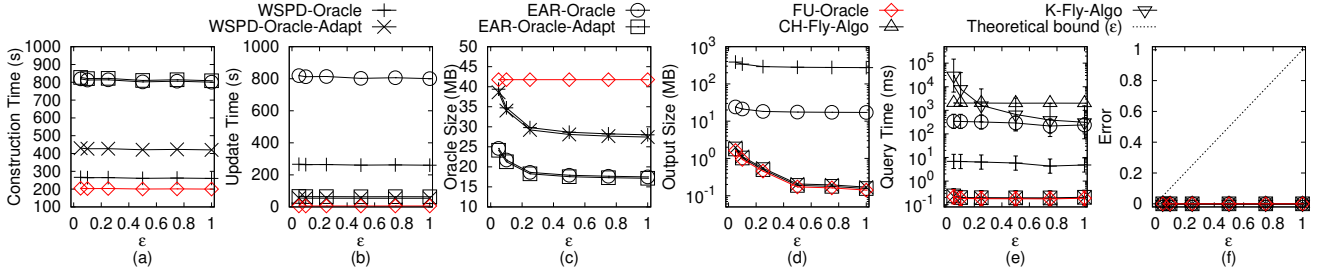


Fig. 49. V2V query on SC dataset

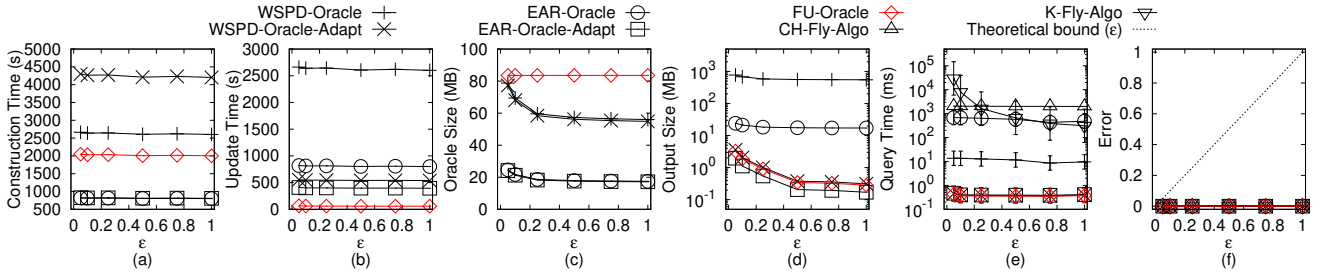


Fig. 50. P2P query in the case  $n > N$  and A2A query on SC dataset

times, and the total running time is  $O(n)$ .

In general, the running time for algorithm *HieGreSpan* is  $O(n) + O(n \log^2 n) = O(n \log^2 n)$ , and we finish the proof.

Secondly, we prove the *error bound* of algorithm *HieGreSpan*. According to Lemma 8 in [20], we know that in algorithm *HieGreSpan*, during the processing of any group of edges  $G'.E^i$ , the hierarchy graph  $H$  is always a valid approximation of  $G'$ . Thus, in the  $H$  edge examine step of algorithm *HieGreSpan*, for each edge  $e(u, v|T) \in G'.E^i$  between two vertices  $u$  and  $v$ , when we need to check whether  $|\Pi_H(w, x|T)| > (1 + \epsilon)|e(u, v|T)|$ , where  $\Pi_H(w, x|T)$  is the shortest path of group centers calculated using Dijkstra's algorithm on  $H$ ,  $w$  and  $x$  are two group centers, such that,  $u$  is in  $w$ 's group, and  $v$  is in  $x$ 's group,  $\Pi_H(w, x|T)$  is a valid approximation of  $\Pi_{G'}(u, v|T)$ . In other words, we are actually checking whether  $|\Pi_{G'}(u, v|T)| > (1 + \epsilon)|e(u, v|T)|$  or not. Consider any edge  $e(u, v|T) \in G'.E$  between two vertices  $u$  and  $v$  which is not added to  $G'$  by algorithm *HieGreSpan*. Since  $e(u, v|T)$  is discarded, it implies that  $|\Pi_{G'}(u, v|T)| \leq (1 + \epsilon)|e(u, v|T)|$ . Since  $|e(u, v|T)| = |\Pi(u, v|T)|$ , so on the output graph of algorithm *HieGreSpan*, i.e.,  $G'$ , we always have  $|\Pi_{G'}(u, v|T)| \leq (1 + \epsilon)|\Pi(u, v|T)|$  for all pairs of vertices  $u$  and  $v$  in  $G'.V$ . We finish the proof.  $\square$

*Proof of Theorem 2.* Firstly, we prove the *oracle construction time* of *FU-Oracle*. When calculating the pairwise P2P exact shortest paths, it needs  $O(nN \log^2 N)$  time, since there are  $n$  POIs, and each POI needs  $O(N \log^2 N)$  time using algorithm *SSAD* for calculating the exact shortest path from this POI to other POI on  $T_{bef}$ . So the oracle construction time of *FU-Oracle* is  $O(nN \log^2 N)$ .

Secondly, we prove the *oracle update time* of *FU-Oracle*.

- In the terrain surface and POI update detection step, it needs  $O(N + n)$  time. Since we just need to iterate each face in  $T_{aft}$  and  $T_{bef}$ , and iterate each POI in  $P$ . Since the number of faces in  $T_{aft}$  and  $T_{bef}$  is  $O(N)$ , and the number of POIs in  $P$  is  $n$ , so it needs  $O(N + n)$  time.
- In the pairwise P2P exact shortest path update step, it needs  $O(N \log^2 N)$  time. Since we just need to update a constant number of POIs (which is shown by our experimental result) using algorithm *SSAD* for calculating the exact shortest path from this POI to other POI on  $T_{aft}$ , and each algorithm *SSAD* needs  $O(N \log^2 N)$  time, so it needs  $O(N \log^2 N)$  time in total.
- In the sub-graph generation step, it needs  $O(n \log^2 n)$  time. Since this step is using algorithm *HieGreSpan*, and algorithm *HieGreSpan* runs in  $O(n \log^2 n)$  time as stated

in Theorem 1.

In general, the oracle update time of *FU-Oracle* is  $O(N \log^2 N + n \log^2 n)$ .

Thirdly, we prove the *output size* of *FU-Oracle*. According to [20], we know that the output graph of algorithm *HieGreSpan*, i.e.,  $G'$ , has  $O(n)$  edges. So, the output size of *FU-Oracle* is  $O(n)$ .

Fourthly, we prove the *shortest path query time* of *FU-Oracle*. Since we need to perform Dijkstra's algorithm on  $G'$ , and in our experiment,  $G'$  has a constant number of edges and  $n$  vertices, so using a Fibonacci heap in Dijkstra's algorithm, the shortest path query time of *FU-Oracle* is  $O(\log n)$ .

Fifthly, we prove the *error bound* of *FU-Oracle*. The error bound of *FU-Oracle* is due to the error bound of algorithm *HieGreSpan*. As stated in Theorem 1, on the output graph of algorithm *HieGreSpan*, i.e.,  $G'$ , we always have  $|\Pi_{G'}(u, v|T)| \leq (1 + \epsilon)|\Pi(u, v|T)|$  for all pairs of vertices  $u$  and  $v$  in  $G'.V$ . Thus, we have the error bound of *FU-Oracle*, i.e., *FU-Oracle* satisfies  $|\Pi_{G'}(u, v|T)| \leq (1 + \epsilon)|\Pi(u, v|T)|$  for all pairs of POIs  $u$  and  $v$  in  $P$ .

In general, we finish the proof of the oracle construction time, oracle update time, output size, shortest path query time and error bound of *FU-Oracle*.  $\square$

**Theorem 3.** *The oracle construction time, oracle update time, output size and shortest path query time of WSPD-Oracle [52], [53] are  $O(\frac{nN \log^2 N}{\epsilon^{2\beta}} + \frac{nh}{\epsilon^{2\beta}} + nh \log n)$ ,  $O(\frac{nN \log^2 N}{\epsilon^{2\beta}} + \frac{nh}{\epsilon^{2\beta}} + nh \log n)$ ,  $O(\frac{nh}{\epsilon^{2\beta}})$  and  $O(h^2)$ , respectively. WSPD-Oracle has  $(1 - \epsilon)|\Pi(u, v|T)| \leq |\Pi_{WSPD-Oracle}(u, v|T)| \leq (1 + \epsilon)|\Pi(u, v|T)|$  for all pairs of POIs  $u$  and  $v$  in  $P$ , where  $\Pi_{WSPD-Oracle}(u, v|T)$  is the shortest path of WSPD-Oracle between  $u$  and  $v$ .*

*Proof.* The proof of the oracle construction time, output size and error bound of *WSPD-Oracle* is in [52], [53].

For the *oracle update time*, since *WSPD-Oracle* does not support the updated terrain surface setting, so the oracle update time is the same as the oracle construction time.

For the *shortest path query time*, suppose that we need to query the shortest path between two POIs  $a$  and  $b$ ,  $a$  belongs to a disk with  $c$  as center,  $b$  belongs to a disk with  $d$  as center, and *WSPD-Oracle* stores the exact shortest path between  $c$  and  $d$ . In order to find the shortest path between  $a$  and  $b$ , we also need to find the shortest path between  $a$  and  $c$ ,  $c$  and  $b$ , then connect the shortest path between  $a$  and  $c$ ,  $c$  and  $d$ ,  $d$  and  $b$ , to form the shortest path between  $a$  and  $b$ . It takes  $O(h^2)$  time to query the shortest path between  $a$  and  $c$ ,  $c$  and  $d$ ,  $d$  and  $b$ , respectively, since the shortest path query time of *WSPD-Oracle* is  $O(h^2)$  in [52], [53]. Thus, the shortest path query time of *WSPD-Oracle* should be  $O(3h^2) = O(h^2)$ .  $\square$

**Theorem 4.** *The oracle construction time, oracle update time, output size and shortest path query time of WSPD-Oracle-Adapt [52], [53] are  $O(\frac{nN \log^2 N}{\epsilon^{2\beta}} + \frac{nh}{\epsilon^{2\beta}} + nh \log n)$ ,  $O(\mu_1 N \log^2 N + n \log^2 n)$ ,  $O(n)$  and  $O(\log n)$ , respectively, where  $\mu_1$  is a data-dependent variable, and  $\mu_1 \in [5, 20]$  in our experiment. WSPD-Oracle-Adapt satisfies*

$|\Pi_{WSPD-Oracle-Adapt}(u, v|T)| \leq (1 + \epsilon)|\Pi(u, v|T)|$  for all pairs of POIs  $u$  and  $v$  in  $P$ , where  $\Pi_{WSPD-Oracle-Adapt}(u, v|T)$  is the shortest path of WSPD-Oracle-Adapt between  $u$  and  $v$ .

*Proof.* The proof of the output size, shortest path query time and error bound of *WSPD-Oracle-Adapt* is similar in *FU-Oracle*.

For the *oracle construction time*, *WSPD-Oracle-Adapt* first needs  $O(\frac{nN \log^2 N}{\epsilon^{2\beta}} + \frac{nh}{\epsilon^{2\beta}} + nh \log n)$  for oracle construction, which is the same as *WSPD-Oracle*. It then needs  $O(nN \log^2 N)$  for computing the distance from each POI to each vertex in  $V$  on  $T_{bef}$ . So the oracle construction time is  $O(\frac{nN \log^2 N}{\epsilon^{2\beta}} + \frac{nh}{\epsilon^{2\beta}} + nh \log n)$ .

For the *oracle update time*, since *WSPD-Oracle-Adapt* uses the update phase of *FU-Oracle*, so it first needs  $O(N + n)$  time for terrain surface and POI update detection, then needs to update  $\mu_1$  number of POIs (which is shown by our experimental result) using algorithm *SSAD* for calculating the exact shortest path from this POI to other POI on  $T_{aft}$ , where each algorithm *SSAD* needs  $O(N \log^2 N)$  time, and then needs  $O(n \log^2 n)$  time for sub-graph generation. So the oracle update time of *WSPD-Oracle-Adapt* is  $O(\mu_1 N \log^2 N + n \log^2 n)$ .  $\square$

**Theorem 5.** *The oracle construction time, oracle update time, output size and shortest path query time of EAR-Oracle [29] are  $O(\lambda \xi m N \log^2(mN) + \frac{nN \log^2 N}{\epsilon^{2\beta}} + \frac{Nh}{\epsilon^{2\beta}} + Nh \log N)$ ,  $O(\lambda \xi m N \log^2(mN) + \frac{nN \log^2 N}{\epsilon^{2\beta}} + \frac{Nh}{\epsilon^{2\beta}} + Nh \log N)$ ,  $O(\frac{\lambda m N}{\epsilon} + \frac{Nh}{\epsilon^{2\beta}})$  and  $O(\lambda \xi \log(\lambda \xi))$ , respectively. EAR-Oracle has  $|\Pi_{EAR-Oracle}(u, v|T)| \leq (1 + \epsilon)|\Pi(u, v|T)| + 2\delta$  for all pairs of POIs  $u$  and  $v$  in  $P$ , where  $\Pi_{EAR-Oracle}(u, v|T)$  is the shortest path of EAR-Oracle between  $u$  and  $v$  and  $\delta$  is an error parameter [29].*

*Proof.* The proof of the oracle construction time, output size, shortest path query time and error bound of *EAR-Oracle* is in [29].

For the *oracle update time*, since *EAR-Oracle* does not support the updated terrain surface setting, so the oracle update time is the same as the oracle construction time.  $\square$

**Theorem 6.** *The oracle construction time, oracle update time, output size and shortest path query time of EAR-Oracle-Adapt [29] are  $O(\lambda \xi m N \log^2(mN) + \frac{nN \log^2 N}{\epsilon^{2\beta}} + \frac{Nh}{\epsilon^{2\beta}} + Nh \log N)$ ,  $O(\mu_2 N \log^2 N + n \log^2 n)$ ,  $O(n)$  and  $O(\log n)$ , respectively, where  $\mu_2$  is a data-dependent variable, and  $\mu_1 \in [12, 45]$  in our experiment. EAR-Oracle-Adapt satisfies  $|\Pi_{EAR-Oracle-Adapt}(u, v|T)| \leq (1 + \epsilon)|\Pi(u, v|T)|$  for all pairs of POIs  $u$  and  $v$  in  $P$ , where  $\Pi_{EAR-Oracle-Adapt}(u, v|T)$  is the shortest path of EAR-Oracle-Adapt between  $u$  and  $v$ .*

*Proof.* The proof of the oracle construction time of *EAR-Oracle-Adapt* is similar in *EAR-Oracle*. The proof of the output size, shortest path query time and error bound of *EAR-Oracle-Adapt* is similar in *FU-Oracle*.

For the *oracle update time*, since *EAR-Oracle-Adapt* uses the update phase of *FU-Oracle*, so it first needs  $O(N + n)$  time for terrain surface and POI update detection, then needs to update  $\mu_2$  number of POIs (which is shown by our experimental

result) using algorithm SSAD for calculating the exact shortest path from this POI to other POI on  $T_{aft}$ , where each algorithm SSAD needs  $O(N \log^2 N)$  time, and then needs  $O(n \log^2 n)$  time for sub-graph generation. So the oracle update time of *EAR-Oracle-Adapt* is  $O(\mu_2 N \log^2 N + n \log^2 n)$ .  $\square$

**Theorem 7.** *The oracle construction time, oracle update time, output size and shortest path query time of *FU-Oracle-RanUpdSeq* are  $O(nN \log^2 N)$ ,  $O(nN \log^2 N + n \log^2 n)$ ,  $O(n)$  and  $O(\log n)$ , respectively. *FU-Oracle-RanUpdSeq* satisfies  $|\Pi_{FU-Oracle-NoEffEdgPru}(u, v|T)| \leq (1+\epsilon)|\Pi(u, v|T)|$  for all pairs of POIs  $u$  and  $v$  in  $P$ , where  $\Pi_{FU-Oracle-RanUpdSeq}(u, v|T)$  is the shortest path of *FU-Oracle-RanUpdSeq* between  $u$  and  $v$ .*

*Proof.* The proof of the oracle construction time, output size, shortest path query time and error bound of *FU-Oracle-RanUpdSeq* is similar in *FU-Oracle*.

For the oracle update time, the only difference between *FU-Oracle* and *FU-Oracle-RanUpdSeq* is that the latter one uses the random path update sequence before utilizing the non-updated terrain shortest path intact property, so it cannot fully utilize this property, and in the pairwise P2P exact shortest path update step, it needs to use algorithm SSAD for all POIs for  $n$  times. The other oracle update time is the same as the *FU-Oracle*. So the oracle update time of *FU-Oracle-RanUpdSeq* is  $O(nN \log^2 N + n \log^2 n)$ .  $\square$

**Theorem 8.** *The oracle construction time, oracle update time, output size and shortest path query time of *FU-Oracle-FullRad* are  $O(nN \log^2 N)$ ,  $O(\mu_3 N \log^2 N + n \log^2 n)$ ,  $O(n)$  and  $O(\log n)$ , respectively, where  $\mu_3$  is a data-dependent variable, and  $\mu_3 \in [5, 10]$  in our experiment. *FU-Oracle-FullRad* satisfies  $|\Pi_{FU-Oracle-NoEffEdgPru}(u, v|T)| \leq (1+\epsilon)|\Pi(u, v|T)|$  for all pairs of POIs  $u$  and  $v$  in  $P$ , where  $\Pi_{FU-Oracle-FullRad}(u, v|T)$  is the shortest path of *FU-Oracle-FullRad* between  $u$  and  $v$ .*

*Proof.* The proof of the oracle construction time, output size, shortest path query time and error bound of *FU-Oracle-FullRad* is similar in *FU-Oracle*.

For the oracle update time, the only difference between *FU-Oracle* and *FU-Oracle-FullRad* is that the latter one uses the full shortest distance of a shortest path as the disk radius. In the pairwise P2P exact shortest path update step, it needs to use algorithm SSAD for  $\mu_3$  number of POIs (which is shown by our experimental result). The other oracle update time is the same as the *FU-Oracle*. So the oracle update time of *FU-Oracle-FullRad* is  $O(\mu_3 N \log^2 N + n \log^2 n)$ .  $\square$

**Theorem 9.** *The oracle construction time, oracle update time, output size and shortest path query time of *FU-Oracle-NoDistAppr* are  $O(nN \log^2 N)$ ,  $O(nN \log^2 N + n \log^2 n)$ ,  $O(n)$  and  $O(\log n)$ , respectively. *FU-Oracle-NoDistAppr* satisfies  $|\Pi_{FU-Oracle-NoEffEdgPru}(u, v|T)| \leq (1+\epsilon)|\Pi(u, v|T)|$  for all pairs of POIs  $u$  and  $v$  in  $P$ , where  $\Pi_{FU-Oracle-NoDistAppr}(u, v|T)$  is the shortest path of *FU-Oracle-NoDistAppr* between  $u$  and  $v$ .*

*Proof.* The proof of the oracle construction time, output size, shortest path query time and error bound of *FU-Oracle-NoDistAppr* is similar in *FU-Oracle*.

For the oracle update time, the only difference between *FU-Oracle* and *FU-Oracle-NoDistAppr* is that the latter one does not store the POI-to-vertex distance information and needs to calculate the shortest path on  $T_{aft}$  again for determining whether the disk intersects with the updated faces on  $T_{aft}$ . It needs to perform such shortest path queries for each POI, so we can regard it re-calculate the pairwise P2P exact shortest paths  $T_{aft}$ , that is, it needs to use algorithm SSAD for all POIs for  $n$  times. The other oracle update time is the same as the *FU-Oracle*. So the oracle update time of *FU-Oracle-NoDistAppr* is  $O(nN \log^2 N + n \log^2 n)$ .  $\square$

**Theorem 10.** *The oracle construction time, oracle update time, output size and shortest path query time of *FU-Oracle-NoEffIntChe* are  $O(nN \log^2 N)$ ,  $O(nN \log^2 N + n \log^2 n)$ ,  $O(n)$  and  $O(\log n)$ , respectively. *FU-Oracle-NoEffIntChe* satisfies  $|\Pi_{FU-Oracle-NoEffEdgPru}(u, v|T)| \leq (1+\epsilon)|\Pi(u, v|T)|$  for all pairs of POIs  $u$  and  $v$  in  $P$ , where  $\Pi_{FU-Oracle-NoEffIntChe}(u, v|T)$  is the shortest path of *FU-Oracle-NoEffIntChe* between  $u$  and  $v$ .*

*Proof.* The proof of the oracle construction time, output size, shortest path query time and error bound of *FU-Oracle-NoEffIntChe* is similar in *FU-Oracle*.

For the oracle update time, the only difference between *FU-Oracle* and *FU-Oracle-NoEffIntChe* is that the latter one creates two disks for each path when checking whether we need to re-calculate the shortest path between a pair of POIs. In the pairwise P2P exact shortest path update step, since there are total  $O(n^2)$  pairwise P2P exact shortest paths, it needs to create  $O(n^2)$  disks. The other oracle update time is the same as the *FU-Oracle*. So the oracle update time of *FU-Oracle-NoEffIntChe* is  $O(nN \log^2 N + n \log^2 n)$ .  $\square$

**Theorem 11.** *The oracle construction time, oracle update time, output size and shortest path query time of *FU-Oracle-NoEdgPru* are  $O(nN \log^2 N + n^2)$ ,  $O(N \log^2 N + n)$ ,  $O(n^2)$  and  $O(1)$ , respectively. *FU-Oracle-NoEdgPru* satisfies  $|\Pi_{FU-Oracle-NoEdgPru}(u, v|T)| = |\Pi(u, v|T)|$  for all pairs of POIs  $u$  and  $v$  in  $P$ , where  $\Pi_{FU-Oracle-NoEdgPru}(u, v|T)$  is the shortest path of *FU-Oracle-NoEdgPru* between  $u$  and  $v$ .*

*Proof.* Firstly, we prove the oracle construction time of *FU-Oracle-NoEdgPru*. The oracle construction of *FU-Oracle-NoEdgPru* is similar in *FU-Oracle*. But, it also needs to store the pairwise P2P exact shortest paths on  $T_{bef}$  into a hash table in  $O(n^2)$  time. So the oracle construction time of *FU-Oracle-NoEdgPru* is  $O(nN \log^2 N + n^2)$ .

Secondly, we prove the oracle update time of *FU-Oracle-NoEdgPru*. For the oracle update time, the only difference between *FU-Oracle* and *FU-Oracle-NoEdgPru* is that the latter one does not use any sub-graph generation algorithm to prune out the edges. So there is no sub-graph generation step. But after The pairwise P2P exact shortest path update step, it needs to update a constant number of POIs using algorithm



SSAD for calculating the exact shortest path from this POI to other  $n$  POI on  $T_{\text{aft}}$ , and update them in the hash table takes  $O(n)$  time. So the oracle update time of *FU-Oracle-NoEdgPru* is  $O(N \log^2 N + n)$ .

Thirdly, we prove the *output size* of *FU-Oracle-NoEdgPru*. Since there are  $O(n^2)$  edges in *FU-Oracle-NoEdgPru*, so the output size of *FU-Oracle-NoEdgPru* is  $O(n)$ .

Fourthly, we prove the *shortest path query time* of *FU-Oracle-NoEdgPru*. Since we have a hash table to store the pairwise P2P exact shortest paths of *FU-Oracle-NoEdgPru*, and the hash table technique needs  $O(1)$  time to return the value with the given key, the shortest path query time of *FU-Oracle-NoEdgPru* is  $O(1)$ .

Fifthly, we prove the *error bound* of *FU-Oracle-NoEdgPru*. Since *FU-Oracle-NoEdgPru* stores the pairwise P2P exact shortest paths, so there is no error in *FU-Oracle-NoEdgPru*, i.e., *FU-Oracle-NoEdgPru* satisfies  $|\Pi_{\text{FU-Oracle-NoEdgPru}}(u, v|T)| = |\Pi(u, v|T)|$  for all pairs of POIs  $u$  and  $v$  in  $P$ .

In general, we finish the proof of the oracle construction time, oracle update time, output size, shortest path query time and error bound of *FU-Oracle-NoEdgPru*.  $\square$

**Theorem 12.** *The oracle construction time, oracle update time, output size and shortest path query time of *FU-Oracle-NoEffEdgPru* are  $O(nN \log^2 N)$ ,  $O(N \log^2 N + n^3 \log n)$ ,  $O(n)$  and  $O(\log n)$ , respectively. *FU-Oracle-NoEffEdgPru* satisfies  $|\Pi_{\text{FU-Oracle-NoEffEdgPru}}(u, v|T)| \leq (1 + \epsilon)|\Pi(u, v|T)|$  for all pairs of POIs  $u$  and  $v$  in  $P$ , where  $\Pi_{\text{FU-Oracle-NoEffEdgPru}}(u, v|T)$  is the shortest path of *FU-Oracle-NoEffEdgPru* between  $u$  and  $v$ .*

*Proof.* Firstly, we prove the *oracle construction time* of *FU-Oracle-NoEffEdgPru*. The oracle construction of *FU-Oracle-NoEffEdgPru* is similar in *FU-Oracle*. So the oracle construction time of *FU-Oracle-NoEffEdgPru* is  $O(nN \log^2 N)$ .

Secondly, we prove the *oracle update time* of *FU-Oracle-NoEffEdgPru*. For the oracle update time, the only difference between *FU-Oracle* and *FU-Oracle-NoEffEdgPru* is that the latter one uses algorithm *GreSpan* for the sub-graph generation step. In the sub-graph generation step, since there are  $n$  vertices in *FU-Oracle-NoEffEdgPru*, so answering the shortest path query using Dijkstra's algorithm on *FU-Oracle-NoEffEdgPru* needs  $O(n \log n)$  time. Since we need to examine total  $O(n^2)$  edges in  $G$ , so the total running time of algorithm *GreSpan* is  $O(n^3 \log n)$ . So the oracle update time of *FU-Oracle-NoEffEdgPru* is  $O(N \log^2 N + n^3 \log n)$ .

Thirdly, we prove the *output size* of *FU-Oracle-NoEffEdgPru*. According to [20], we know that the output graph of algorithm *GreSpan*, i.e., *FU-Oracle-NoEffEdgPru*, has  $O(n)$  edges. So, the output size of *FU-Oracle-NoEffEdgPru* is  $O(n)$ .

Fourthly, we prove the *shortest path query time* of *FU-Oracle-NoEffEdgPru*. Since we need to perform Dijkstra's algorithm on  $G'$ , and in our experiment,  $G'$  has a constant number of edges and  $n$  vertices, so using a Fibonacci heap

in Dijkstra's algorithm, the shortest path query time of *FU-Oracle-NoEffEdgPru* is  $O(\log n)$ .

Fifthly, we prove the *error bound* of *FU-Oracle-NoEffEdgPru*. The error bound of *FU-Oracle-NoEffEdgPru* is due to the error bound of algorithm *GreSpan*. Let  $V_{\text{FU-Oracle-NoEffEdgPru}}$  and  $E_{\text{FU-Oracle-NoEffEdgPru}}$  be the set of vertices and edges of *FU-Oracle-NoEffEdgPru*. In algorithm *GreSpan*, consider any edge  $e_{\text{FU-Oracle-NoEffEdgPru}}(u, v|T) \in G'.E$  between two vertices  $u$  and  $v$  which is not added to *FU-Oracle-NoEffEdgPru*. Since  $e_{\text{FU-Oracle-NoEffEdgPru}}(u, v|T)$  is discarded, it implies that  $|\Pi_{\text{FU-Oracle-NoEffEdgPru}}(u, v|T)| \leq (1 + \epsilon)|\Pi(u, v|T)|$ . Since  $|\Pi(u, v|T)| = |\Pi(u, v|T)|$ , so on the output graph of algorithm *GreSpan*, i.e., *FU-Oracle-NoEffEdgPru*, we always have  $|\Pi_{\text{FU-Oracle-NoEffEdgPru}}(u, v|T)| \leq (1 + \epsilon)|\Pi(u, v|T)|$  for all pairs of vertices  $u$  and  $v$  in  $V_{\text{FU-Oracle-NoEffEdgPru}}$ . Thus, we have the error bound of *FU-Oracle-NoEffEdgPru*, i.e., *FU-Oracle-NoEffEdgPru* satisfies  $|\Pi_{\text{FU-Oracle-NoEffEdgPru}}(u, v|T)| \leq (1 + \epsilon)|\Pi(u, v|T)|$  for all pairs of POIs  $u$  and  $v$  in  $P$ .

In general, we finish the proof of the oracle construction time, oracle update time, output size, shortest path query time and error bound of *FU-Oracle-NoEffEdgPru*.  $\square$

**Theorem 13.** *The shortest path query time of *CH-Fly-Algo* [18] is  $O(N^2)$ . *CH-Fly-Algo* returns the exact shortest path for all pairs of POIs  $u$  and  $v$  in  $P$ .*

*Proof.* The proof can be found in the work [18].  $\square$

**Theorem 14.** *The shortest path query time of *K-Fly-Algo* [32] is  $O(\frac{l_{\max} N}{\epsilon l_{\min} \sqrt{1 - \cos \theta}} \log(\frac{l_{\max} N}{\epsilon l_{\min} \sqrt{1 - \cos \theta}}))$ . *K-Fly-Algo* satisfies  $|\Pi_{\text{K-Fly-Algo}}(u, v|T)| \leq (1 + \epsilon)|\Pi(u, v|T)|$  for all pairs of POIs  $u$  and  $v$  in  $P$ , where  $\Pi_{\text{K-Fly-Algo}}(u, v|T)$  is the shortest path of *K-Fly-Algo* between  $u$  and  $v$ .*

*Proof.* The proof of the *shortest path query time* and *error bound* of *K-Fly-Algo* is in [32]. Note that in Section 4.2 of [32], the shortest path query time of *K-Fly-Algo* is  $O((N + N')(\log(N + N') + (\frac{l_{\max} K}{l_{\min} \sqrt{1 - \cos \theta}})^2))$ , where  $N' = O(\frac{l_{\max} K}{l_{\min} \sqrt{1 - \cos \theta}} N)$  and  $K$  is a parameter which is a positive number at least 1. By Theorem 1 of [32], we obtain that its error bound  $\epsilon$  is equal to  $\frac{1}{K-1}$ . Thus, we can derive that the shortest path query time of *K-Fly-Algo* is  $O(\frac{l_{\max} N}{\epsilon l_{\min} \sqrt{1 - \cos \theta}} \log(\frac{l_{\max} N}{\epsilon l_{\min} \sqrt{1 - \cos \theta}}) + \frac{l_{\max}^2}{(\epsilon l_{\min} \sqrt{1 - \cos \theta})^2})$ . Since for  $N$ , the first term is larger than the second term, so we obtain the shortest path query time of *K-Fly-Algo* is  $O(\frac{l_{\max} N}{\epsilon l_{\min} \sqrt{1 - \cos \theta}} \log(\frac{l_{\max} N}{\epsilon l_{\min} \sqrt{1 - \cos \theta}}))$ .  $\square$